TRANSITIONING BETWEEN PREPARATORY AND PRECISELY SEQUENCED NEURONAL ACTIVITY IN PRODUCTION OF A SKILLED MOTOR BEHAVIOR

APPROVED BY SUPERVISORY COMMITTEE

NOTE: The top line is for the Supervising Professor's name. There should be as many lines as there are members of the committee. All signatures must be original and in ink. Adjust "Approved by Supervisory Committee" line upward if the committee list is very large.

First Name Last Name, credentials

_____

_____

_____

_____

_____

_____

DEDICATION

I would like to thank the members of my Graduate Committee, specifically Dr. Todd Roberts for his mentorship and for giving me the confidence to pursue a difficult project. I would specifically like to thank Jennifer Holdway and Andrea Guerrero for their laboratory support and animal husbandry, and without whom the laboratory would fall into complete disarray. I'm grateful for my lab colleagues who made it easier to get through the sting of failed experiments. In addition, I could not have completed this journey without the unconditional support of my family and my friends, who had to put up with my endless string of terrible jokes. Lastly, I would like to thank Dr. Sarah Rosen, who, despite being thousands of miles away, always felt nearby.

TRANSITIONING BETWEEEN PREPARATORY ACTIVITY AND PRECISELY SEQUENCED NEURONAL ACTIVITY IN PRODUCTION OF A SKILLED MOTOR BEHAVIOR

by

VAMSI KRISHNA DALIPARTHI

DISSERTATION / THESIS

Presented to the Faculty of the Graduate School of Biomedical Sciences

The University of Texas Southwestern Medical Center at Dallas

In Partial Fulfillment of the Requirements

For the Degree of

DOCTOR OF PHILOSOPHY

The University of Texas Southwestern Medical Center at Dallas

Dallas, Texas

August 9, 2019

TRANSITIONING BETWEEN PREPARATORY AND PRECISELY SEQUENCED NEURONAL ACTIVITY IN PRODUCTION OF A SKILLED MOTOR BEHAVIOR

Publication No. 3

Vamsi Krishna Daliparthi, Ph.D.

The University of Texas Southwestern Medical Center at Dallas, 2019

Supervising Professor: Todd Freeman Roberts, Ph.D.

Precise neural sequences are associated with the production of well-learned skilled behaviors. Yet, how neural sequences arise in the brain remains unclear. In songbirds, premotor projection neurons in the cortical song nucleus HVC are necessary for producing learned song and exhibit precise sequential activity during singing. Using cell-type specific calcium imaging we identify populations of HVC premotor neurons associated with the beginning and ending of singing-related neural sequences. We characterize neurons that bookend singing-related sequences and neuronal populations that transition from sparse preparatory activity prior to song to precise neural sequences during singing. Recordings from downstream premotor neurons or the respiratory system suggest that pre-song activity may be involved in motor preparation to sing. These findings reveal population mechanisms associated with moving from non-vocal to vocal behavioral states and suggest that precise neural sequences begin and end as part of orchestrated activity across functionally diverse populations of cortical premotor neurons.

TABLE OF CONTENTS

PRIOR PUBLICATIONS

Liu, P., Lu, H., Filbey, F.M., Pinkham, A.E., McAdams, C.J., Adinoff, B., Daliparthi, V. and Cao, Y., 2014. Automatic and reproducible positioning of phase-contrast MRI for the quantification of global cerebral blood flow. *PloS one*, *9*(5), p.e95721.

Winter, A.N., Ross, E.K., Daliparthi, V., Sumner, W.A., Kirchhof, D.M., Manning, E., Wilkins, H.M. and Linseman, D.A., 2017. A Cystine-Rich Whey Supplement (Immunocal®) Provides Neuroprotection from Diverse Oxidative Stress-Inducing Agents In Vitro by Preserving Cellular Glutathione. *Oxidative medicine and cellular longevity*, *2017*.

Daliparthi, V.K., Tachibana, R.O., Cooper, B.G., Hahnloser, R.H.R., Kojima, S., Sober, S.J., and Roberts, T.F., 2019. Transitioning between preparatory and precisely sequenced neuronal activity in production of a skilled motor behavior. *eLife 2019*, 8: e43732.

LIST OF FIGURES

LIST OF TABLES

CHAPTER 1

Introduction

In the acclaimed documentary, *Free Solo*, professional rock climber Alex Honnold attempted to climb 900 meters up a massive rock formation called El Capitan unassisted and without any safety equipment. Any minor mishap along the climbing route would result in certain death. To prepare for his climb, Honnold rehearsed and memorized the sequence of movements up the rock wall for several years, going so far as to build facsimiles of particularly tricky parts of the climb to ensure that he had the skill and technique necessary to successfully traverse those sections. His preparation for the climb was not without mistakes, but after aborted attempts and following years of dedicated practice he managed to complete the climb in June 2017, after 3 hours and 56 minutes of harrowing climbing.

The ability to produce complex motor tasks in a sequential manner provides a great advantage to a wide range of species. Breaking down the production of complicated behaviors into precise sequential movements that can be reproduced in a stereotyped fashion enables robust functional chunking of a wide range of behaviors. Tasks ranging from brushing our teeth to playing a musical experiment (or scaling natural rock formations!) require the reproduction of several complex motor movements in a sequential order to belie meaningful functional significance. When we perform motor tasks, such as typing on a keyboard or playing a musical instrument we rely on a temporally structured motor program that reflects purposeful motor movements. In 1951, Karl Lashley called the problem of coordinating individual movements into temporally structured patterns the "action syntax" problem (Lashley 1951, Tanji 2001). As fundamental as these types of

complex behaviors are relatively little is know about how these behaviors are encoded across populations of neurons in the brain and how action information is retrieved for future performances.

I will begin this chapter by introducing the topic of neural sequences and the potential importance of preparing for impending motor behaviors. I will then discuss the strengths of the songbird model in explicating these basic neuroscience questions and what we already know about how song is encoded in the avian brain as well as the function of peripheral mechanisms for song generation. Next, I will present what is still unclear in the neural processes underlying song production and end the chapter with an outline of this thesis.

Neural representations of temporally structured behaviors

Despite the ubiquity of complex sequential motor tasks the neural representation of these behaviors across large networks of neurons remains unclear. One proposed mechanism by which the brain may encode these types of temporally structured motor tasks is through sequential neuronal activity. The sequential activation of neurons is implicated in a wide variety of behaviors ranging from episodic memory encoding and sensory processing to the voluntary production of skilled motor behaviors (Fee et al., 2004; Fiete et al., 2010; Hahnloser et al., 2002; Li et al., 2015; Lynch et al., 2016; Markowitz et al., 2015; Okubo et al., 2015; Peters et al., 2014; Rajan et al., 2016; Svoboda and Li, 2017). Neural sequences develop through experience and have been described in several brain areas, including the motor cortex, hippocampus, cerebellum, and the basal ganglia (Barnes et al., 2005; Dragoi and Buzsaki, 2006; Foster and Wilson, 2006; Harvey et al., 2012; Jin et

al., 2009; Li et al., 2015; Luczak et al., 2007; Mauk and Buonomano, 2004; Peters et al., 2014; Pfeiffer and Foster, 2013, 2015; Schwartz and Moran, 1999). Recordings in the sensorimotor striatum of rats performing a T-maze task revealed neural sequences tiling the entire duration of the task as well as distinct moments within the task (i.e. task start, onset of auditory cue, goal, etc.) (Barnes et al 2005, Jog et al 1999). Similarly, spontaneous activity in layer V of the neocortex of rats suggests that stereotyped sequential activity is an emergent property of cortical networks and may play a critical role in information flow across networks of neurons (Luczak et al 2007). Neural sequences are not unique to procedural tasks – hippocampal activation during spatial navigation tasks is often accompanied by sequential neuronal activity that encodes past, present, and future locations and is thought to be important for integrating sequential information in space and time (Dragoi & Buzsaki 2006). In addition, feed-forward networks in the posterior parietal cortex are hypothesized to play a role in tasks that require perceptual decision-making and spatial navigation (Harvey et al 2012).

Synfire chains and propagation of neural activity

Although there is a wealth of evidence suggesting neural sequences are correlated with complex sequential behaviors, how this activity propagates through neuronal circuits remains unclear. The most prominent theoretical model for how sequences of synchronous activity are encoded in neural ensembles is the “synfire chain” theory (Abeles 1982, Abeles 1991). In this model, anatomically interconnected neurons form a complete transmission line through which temporally precise sequential activity can be generated. Different pools of neurons form different layers of activity that are presumably wired together with stable

synaptic connections. However, to date, there remains insufficient data to confirm that this is indeed the physiological method by which sequential activity is encoded in populations of neurons. In part, this is due to the difficulty in verifying the presence of a stable transmission line. To provide concrete evidence of synfire chains in the brain, an experimenter would have to record from as many of the individual neurons thought to participate in temporal sequences and show that stimulating only the first layers of the neuronal chain could reliably drive activity in subsequent layers with the same temporal precision as the naturally occurring structure. While these exact experiments have yet to be successfully performed, systematic intracellular recordings and population-level functional imaging have revealed the existence of stereotyped activity flow through chains of synchronized activity. *In vivo* recordings from cat primary visual cortex and slice recordings from mouse primary visual cortex were some of the first to reveal the existence of robust patterns of activity along with evidence for structured spatial organization of the neurons that generated chain-like activity (Ikegaya et al 2004). Interestingly, however, more recent work suggests that minimal spatial structure in a complex neural circuit is actually required to produce the sequential activity observed during various behavioral tasks (Rajan et al 2016). Instead, new evidence suggests that neural sequences are emergent properties of complex interactions between external (primarily excitatory) inputs and recurrent connections within the circuitry (Rajan et al 2016). This is in stark contrast to previous models that have attempted to build structured synaptic connectivity from an initially randomly structured network to determine the plausibility of the canonical synfire chain hypothesis (Fiete et al 2010).

Computational models of sequential activity

Computational models have attempted to elucidate the types of networks that support robust sequential activation along with the cellular components that enable initiation and propagation of neuronal circuits (Churchland et al 2010, Fiete et al 2004, Fiete et al 2010, Haga & Fukai 2018, Harvey et al 2012, Kumar et al 2010, Rajan et al 2016). Feed forward sequences of activity are thought to play a crucial role in encoding temporally structured behaviors but how these networks are built from initially stochastic ensembles of neurons is a key question in computational neuroscience. Despite the ubiquity of sequential spiking propagation across different behavioral tasks, brain regions, and species, the plasticity rules and network structures that govern these types of neural circuits remains unclear. Moreover, reliable and redundant propagation of sequential activity is likely to be essential for robust production of temporally structured behaviors yet synchronous activity is reliant on the probabilistic and unreliable nature of synaptic release. Synfire chains are the most prominent model for transmission of neural activity through populations of neurons and require stable, unidirectional flow of activity through the circuit. Hypothetically, synfire chains would have both forward and backward directionality along the plane of neuronal network; however, unidirectional flow is likely important to ensure proper representation of temporally structured behaviors.

Several computational studies have examined the ability of spike-timing dependent plasticity (STDP) to build synchronous chains of activity. STDP rules asymmetrically increase synaptic strength; if neuron B fires after neuron A synaptic strength is increased in the forward direction (neuron B is more likely to fire after neuron A) and weakened in the reverse direction (neuron A is less likely to fire after neuron B). However, network models

relying solely on STDP to build long chains of sequential activity have failed because it tends to focus activity to a handful of cells creating temporal and spatial bunching in which single cells are driving bursts of activity through large populations of neurons rather than building structured chains. To circumvent this tendency, models have incorporated preformed seed-chains or discrete synaptic rules that may or may not be physiologically relevant. Although computational models have provided tests of neuron parameters required for robust propagation of activity much of this information has come from simplified networks only containing a fraction of the neuronal compartments found in nature. Take, for example, neural sequences underlying the production of song in zebra finches; computational models for this system have typically only examined the role of single classes of neurons within region of the brain associated with the behavior (Table 1). Moreover, computational models of sequential activity have almost exclusively relied on single structured inputs to drive chains of activity, which is inconsistent with observations of pre-movement activity prior to trained motor tasks. This raises a crucial question in the context of this thesis, how does a network of neurons go from an initially quiescent and inactive state to robustly propagating synchronous neuronal activity? Prior computational modeling would suggest that a simple ping of the network is sufficient to drive hypothetical synfire chains related to the behavior. However, this hypothesis has not been tested in the framework of a naturally occurring temporally structured behavior, and theories related to the pre-movement activity have proposed more complex network-level requirements for initiating neural sequences in the brain.

Learned vocalizations as complex motor tasks

Amongst the wide spectrum of behaviors produced by animals, one of the most complex, at least in terms of motor coordination, is the production of species-specific vocalizations. Although many species produce vocalizations, only a select few follow a prolonged process of vocal learning to generate these complex motor programs, namely select species of cetaceans, elephants, bats, songbirds, and humans. Language production in humans requires the coordination of hundreds of different muscle groups in a precise temporal order for accurate and meaningful sounds to be produced. Although, some vocalizations produced by humans are innate, such as crying and laughing, most require distinct phases of sensory and sensorimotor learning to develop comprehensible human language. Human infants listen to their adult caretakers during a developmental sensory window and through a process of vocal exploration and auditory-feedback dependent learning go through stages of vocal "babbling" to more robust and complex vocalizations, eventually building a full linguistic repertoire. Likewise, species of juvenile songbirds listen to the courtship song of their adult male caretaker during a developmental critical period (~ 25 to 60 days post hatch, dph) and form a memory of this adult song. This is followed by an overlapping period of sensorimotor learning during which juvenile songbirds use auditory-feedback to guide the production of their vocalizations to produce a near identical copy of their adult "tutor's" song. The courtship song produced by adult zebra finches is highly stereotyped and quantifiable, lending this complex natural occurring motor behavior a strong degree of experimental tractability. The courtship song produced by zebra finches is composed of spectrally complex sounds or "syllables" that are separated by silent gaps. Typically, 3 to 7 syllables with silent gaps in between are strung together to create a "motif" that can range in duration from 0.5 to 1s in length; this motif is the largest

stereotyped repeated structure in the birds vocalizations. A variable number of motifs can be repeated to create a song bout, and multiple bouts are combined to create the complex structure underlying a typical courtship song directed by a male towards a female.

Brain regions involved in human speech production

Vocal motor circuits in the brain involved in the production and control of self-generated vocalizations are hierarchically organized in humans and songbirds. At the top of the hierarchy in humans within the cortex sit the anterior cingulate cortex, perisylvian cortical area, and the posterior parieto-temporal cortex are all thought to play a critical role in vocal motor control and speech learning. Most prominently, Broca's area (located in the posterior frontal inferior cortex) and Wernicke's area (in the posterior temporal lobe) are necessary for speech production and comprehension, respectively. A variety of functional imaging techniques in humans have observed activation in all of the above areas during speech generation. These brain regions via direct and indirect pathways project into the midbrain containing the periaqueductal gray (PAG) and parabrachial tegmentum. The PAG is thought to be important for the production of innate vocalizations and is also thought to be involved in the initiation of vocalizations; stimulating the PAG in non-human primates evokes vocalizations though often without a significant degree of complexity. The midbrain in humans then sends projections to the nucleus ambiguous and cranial motor nuclei that control respiratory movements and the muscles of the vocal tract. Human speech requires the coordination of the mouth, tongue, teeth and lips to manipulate the air during expiration to finally generate the acoustic structures underlying speech and other vocalizations.

Brain regions involved in zebra finch courtship song production

In stark contrast to humans and other mammals, the songbird brain does not have a neocortex and instead is organized into discrete nuclei, similar to the striatum in humans. Although, recent evidence suggests that the avian pallium (analogous to mammalian cortex) has similar neuronal projections and genetically identifiable neuronal subsets to the canonical neocortical circuit (Calabrese and Woolley, 2015). Analogous to the premotor cortex (with some evidence to suggest tangential homology to Broca's Area, see Pfenning et al. 2014), HVC sits atop the vocal motor control hierarchy in zebra finches. Populations of neurons within HVC send direct projections downstream to RA (robust nucleus of the arcopallium, akin to the laryngeal motor cortex in mammals). Neurons in the dorsal third of RA project down to medullary nuclei that control song-related respiratory patterns; the nucleus retroambigualis (RAm) and nucleus paraambigualis (PAm) control expiration and inspiration, respectively. The ventral two-thirds of RA connect directly to the vocal motor neurons in the tracheosyringeal portion of the hypoglossal nucleus (nXIIts) that innervate the muscles controlling the syrinx, the avian vocal organ. Importantly, there are indirect and direct connections between RAm, PAm, RA, the dorsomedial intercollicular nucleus (DM), and nXIIts, combining to create a complex network underlying the song generation. In addition, PAm and DM are know to send ascending projections to nucleus uvaeformis (UVA, a thalamic nucleus) which eventually synapses back into HVC through direct and indirect (via nucleus interfacialis, NIF) pathways suggesting an important role in providing song-related motor feedback to HVC.

Populations of neurons within HVC also send projections to Area X a region homologous to the mammalian basal ganglia circuitry. Neurons within Area X send projections to the lateral magnocellular nucleus of the anterior neostriatum (LMAN). LMAN is the primary output nucleus of the songbird basal ganglia circuitry and neurons within LMAN project back into the song motor pathway (HVC-RA-Brainstem Regions) at the level of RA.

Organization of the HVC microcircuit

The premotor nucleus HVC is known to contain at least three populations of projection neurons and one pool of local interneurons(Mooney & Prather 2005). Sequential recordings from neurons in slice preparations of HVC have revealed a complex local microcircuitry with the four populations of HVC neurons showing heavy interconnectivity(Mooney & Prather 2005, Prather & Mooney 2003). One class of HVC projection neurons (HVC-X) project to a striatal and basal ganglia homologue of the avian brain called Area X that is necessary for vocal plasticity and song learning(Mooney & Prather 2005). The second class of HVC projection neurons (HVC-RA neurons) sends direct projections to the downstream motor nucleus RA and is of particular interest to this thesis(Mooney 1992). A third recently identified population (HVC-Av) projects to a subregion of the brain analogous to the secondary auditory cortex(Roberts et al 2017). Evidence suggests that HVC-RA, HVC-X, and interneurons all send local collaterals within HVC, whereas HVC-Av seem to project directly to Avalanche (Av). HVC-RA neurons synapse onto local interneurons and other HVC-RA neurons; they may also directly innervate HVC-X neurons. Likewise, HVC-X neurons synapse onto local interneurons and other HVC-X

neurons. Interneurons within the circuit are a source of feedback and feed forward inhibition. HVC-Av neurons are thought to receive direct synaptic connections from HVC-RA neurons suggesting a pathway for motor information to enter auditory regions of the brain(Roberts et al 2017).

Representation of courtship song timing within HVC and RA

The song premotor nucleus HVC is required for the production of song in adult male zebra finches, HVC lesions occlude the production of all learned components of song(Nottebohm et al 1976). In addition, a large body of literature, primarily using single-cell and multiunit recordings of neurons within HVC, indicate that the nucleus contains essential timing information for the production of song(Amador et al 2013, Fee et al 2004, Hahnloser et al 2002, Kozhevnikov & Fee 2007, Lynch et al 2016, Markowitz et al 2015, Picardo et al 2016). Multi-unit recordings in HVC have revealed significant increases in activity compared to baseline during production of individual motifs and during the introductory notes leading up to song. Closer examination of HVC activity revealed strong modulation of neuronal activity during singing suggesting finer temporal scale encoding of song behavior within the neuronal circuit. Indeed, single-unit recordings of neurons in HVC showed distinct classes of functional activity. First, interneurons are tonically active in non-singing birds firing on average about 8Hz; during song they dramatically increase firing rates up to 95Hz on average(Fee et al 2004). The singing related modulation of interneuron activity is time-locked to the silent gaps between syllables and are not typically continuously active during song as originally thought(Cannon et al 2015, Kosche et al 2015). Pharmacological inactivation of interneurons with gabazine resulted in severe

degradation of the song motif in adult zebra finches suggesting that local inhibitory circuits are crucial for the accurate production of song and that structured inhibitory tone may be important for the sequential activation of neurons(Kosche et al 2015).

Next, HVC-RA and HVC-X neurons are know to fire sparse and temporally precise bursts of action potentials within an individual motif. HVC-X neurons have low levels of spontaneous activity (less than 1Hz) and have been shown to burst up to 5 times within a single motif(Fee et al 2004). HVC-RA neurons are generally quiescent (rarely do they have spontaneous activity outside of song) and typically only exhibit 1 burst of action potentials time-locked to a single point within the birds' motif(Fee et al 2004, Hahnloser et al 2002). There are occasionally HVC-RA neurons that have been shown to fire up to two bursts during a motif. HVC-RA neurons show a remarkable level of precision from motif to motif showing less than a 1ms of temporal jitter of bursts from trial to trial(Hahnloser et al 2002). Several studies now point to a sparse and sequential representation of individual motifs in populations of neurons in HVC. Two models have been proposed for how motifs are included in the brain: 1) the gestural extrema model (GTE model) and 2) the synfire chain hypothesis(Amador et al 2013, Fee et al 2004).

The gestural extrema model relies on dimensionality reduction of song into movement gestures related to the peripheral generation of vocalizations using biomechanical models of respiratory patterns, muscle tension in the syrinx, and filtering in the vocal tract. Activity during singing and during song playback in sleeping birds was then compared to the timing of motor gestures within song suggesting that motor trajectories relevant to vocalization are encoded in HVC neurons, specifically, unidentified HVC projection neurons were show to be time-locked to the onset of gestural extrema while

interneurons displayed suppressed activity near the onset of motor gestures(Amador et al 2013). A surprising and unresolved observing from the GTE model was that HVC projection neuron bursting was synchronized to onset of peripheral gesture times implying a near-zero time lag for activity to influence behavior(Amador et al 2013). This observation would imply negligible synaptic delay between HVC activity and song vocalization, which might downplay the importance of HVC for singing behavior contrasting the conclusions of previous literature. The near-zero time lag observed in the GTE model has to yet be thoroughly explicated.

The most strongly supported model for how neurons in HVC encode song is the synfire chain hypothesis. The synfire chain hypothesis states that neurons in HVC form a continuous physiological transmission line that forms a temporally continuous representation of song(Fee et al 2004). Evidence for this type of neural network underling song generation emerged following sequential recordings of neurons in HVC and in RA. In contrast to the GTE model, this hypothesis predicts that neurons in HVC encode each time point with the song motor sequence rather than putative motor trajectories within the motif. Most evidence suggests that neurons in HVC and particularly HVC-RA neurons fire precise high-frequency bursts (600 to 800Hz) at time-locked moments within the song motifs(Hahnloser et al 2002, Kozhevnikov & Fee 2007). In addition, large datasets of HVC projection neuron activity in singing birds suggests that song-activity within HVC is uniformly distributed (Lynch et al 2016, Picardo et al 2016). Lynch et al. examined a data set of 450 HVC neurons, 384 of which were putative or identified projection neurons, and found that distribution of song-related burst times to be most consistent with a continuous time-model and not with the gestural extrema model(Lynch et al 2016). HVC projection

neurons were identified antidromically by placing bipolar stimulating electrodes in RA or Area X; a single biphasic stimulation lasting 0.2 ms was sufficient to evoke spikes with a latency on average of 2-8 ms for HVC-RA neurons and 2-11 ms for HVC-X neurons, both classes of neurons exhibited stimulus evoked spike jitter of less than 50 microseconds(Lynch et al 2016).

Optical imaging experiments have also lent insight into how populations of HVC neurons encode song behavior and have similarly concluded uniform distribution of HVC projection neurons activity during singing(Picardo et al 2016). Picardo et al. developed a novel imaging paradigm in which head-fixed adult male zebra finches were trained to sing to a female; males were rewarded with water on successful trials. HVC neurons expressing GCaMP6 provided readout of network level activity during singing behavior. Head-fixed functional imaging revealed that neurons in HVC were encoding elapsed time within the song and are not reflecting on-going kinematics underlying song vocalization. Importantly, this paper developed a computational algorithm to infer spike timing from low temporal resolution calcium transients from GCaMP6(Picardo et al 2016). This provided the ability to record relatively fine temporal resolution of spike activity from populations of HVC neurons for the first time with GCaMP6. This technical advance enabled the verification of uniformly distributed HVC projection neuron activity during zebra finch song motifs.

Given that HVC-RA neurons typically have a single high frequency burst of action potentials lasting ~6 to 10 ms its hypothesized that there are 200 coactive HVC-RA neurons at any time during the birds' song (assuming a 600ms motif length)(Fee et al 2004). This activity has been shown to drive stereotyped bursts in RA neurons during song. Unlike HVC-RA neurons, each RA neurons fire between 10 to 12 high frequency bursts of

action potentials with millisecond precision(Yu & Margoliash 1996). Current models suggest that ~12% of RA neurons are active at any given point in the birds' motif(Fee et al 2004). RA neurons then drive activity in motor neurons in the brain stem controlling respiratory muscles and the muscles of the Syrinx.

In this wide body of literature examining song-related activity in HVC neurons, people have reported that about half of HVC-RA neurons don't seem to be active during the song motif leaving the role of much of the direct song-motor pathway unclear.

Formation and stability of song-related neural sequences

The song learning process in zebra finches and other songbirds lends itself to addressing questions about how neural sequences underlying the production of stereotyped complex sequential behaviors develop. Computational and electrophysiological studies in singing birds have provided insight into how neural sequences underlying song production develop. Okubo et al. is the foremost study to examine song-related neural sequences in the HVC of developing songbirds(Okubo et al 2015). Using sequential *in vivo* electrophysiological recordings from mostly unidentified HVC projection neurons, they found that initially rhythmic, imprecise bursts of activity during the subsong stage of song learning transitions to sparse precise bursts of activity time-locked to specific moments within the motif. In addition, they found proto-neural sequences that are shared between underdeveloped song syllables split into syllable-specific neural sequences as the song imitation improves. Neural sequences observed before or after the production of the motif were thought to serve as seed sequences for the final chain of motif-relevant activity; that this sequences occurring outside of song

production are thought to be a computational network strategy to develop the actual sequences necessary for song vocalization. These seed sequences are hypothesized to become less important or disappear entirely once a stable adult song chain has formed(Okubo et al 2015).

Song-related neural sequences are thought to form temporally precise chains of activity, but the stability of the timing of individual projection neurons from trial-to-trial and day-to-day remains a contentious topic. Population-level functional imaging of HVC projection neurons using a head-mountable miniaturized fluorescent microscope has revealed temporal drift of activity over the course of multiple song renditions over the course of several days(Liberti et al 2016). While head-fixed functional imaging with the higher spatial resolution of two-photon microscopy of the same neurons over several days to weeks has revealed stable motif-related patterns of activity(Katlowitz et al 2018). The authors of the head-fixed imaging protocol argue that the low spatial resolution of miniscope imaging does not lend itself for stably monitoring neuron activity over the course of different day and suggest that precise song timing is maintained at level of single neurons within HVC.

Neural correlates of anticipatory and preparatory activity

Electroencephalographic (EEG) recordings of humans voluntarily producing motor tasks were the first to show anticipatory activity leading up to the onset of movement. In these recordings, increased activity termed “bereitshaftspotential” or “readiness potential” beginning 2s prior to movement onset was observed in the supplementary motor area followed by subsequent activation of the nearby premotor and primary motor cortices(Kornhuber & Deecke 2016). These were some of the first studies to provide

evidence for the existence of brain activity preceding the initiation of spontaneous and voluntary movement. Since these seminal findings, anticipatory or preparatory activity has been observed across a wide range of species performing a variety of motor tasks. Preparatory activity needs to fit three criteria: 1) it must occur prior to movement onset; 2) it needs to show some specificity to the movement; and 3) it must be able to predict subsequent movement(Svoboda & Li 2017). The significance of pre-movement activity remains unclear, although prior research has indicated that the absence or suppression of neural activity prior to movement onset is associated with reduced accuracy, greater variability of movement parameters, and increased reaction time(Churchland et al 2010, Svoboda & Li 2017). These observations suggest that preparatory activity is important for robust production of trained motor behaviors. In contrast to the precisely structured activity observed during movement itself, preparatory activity is typically more variable from trial to trial perhaps reflecting stochastic network-level or movement decision-related activity(Churchland et al 2010, Kaufman et al 2014, Svoboda & Li 2017). In addition, although preparatory activity is associated with improved motor production, how it actually influences motor generation has been hard to pinpoint(Churchland et al 2006a, Churchland et al 2006b). The complexity of preparatory activity has led to the development of several theories. Perhaps the simplest theory is that the observed pre-movement activity is just subthreshold activity of the same neurons underlying the generation of the movement(Churchland et al 2010). This stems from the idea that movement-related neurons might be more likely to fire precisely assuming the subthreshold activity gets them closer to some arbitrary threshold important for movement generation. Although there is some evidence that this might be true, the subthreshold activity seen prior to movement

seems to have little to no correlation between movement parameters themselves and lacks the temporal structure seen during movement. Indeed, recent evidence suggest that although preparatory activity might have subthreshold components that resemble suprathreshold activity during movement, the tight relationship between movement parameters and the presence of anticipatory activity suggest that there may be an alternative mechanistic role for this activity. The variability and complexity of preparatory activity has been difficult to explain. While some neurons recorded in the non-human primate active prior to movement onset showed tuning to movement speed and timing, most neurons don't seem to be coded to any particular movement parameter at all. In other words, at the population level preparatory activity is variable but tightens movement accuracy and timing, but at the individual neuron level may not have any relationship to the movement itself other than predicting the onset(Churchland et al 2010, Svoboda & Li 2017). This contradiction has led to the development of hypothesis from the perspective of dynamical systems theory(Churchland et al 2010, Shenoy et al 2013). A dynamical system has a future state that is a product of the current state, a perturbation, and system noise. This theory (not new to the field of neuroscience and in fact has been applied to other aspects of the nervous system) interprets preparatory activity as a reflection of decision-making or internal network processes that are not necessarily well described by the subsequent movement but are still necessary for movement generation. Dimensionality reduction of population-level neuronal activity in non-human primates has revealed that preparatory activity occupies a low-dimensional subspace(Churchland et al 2010, Kaufman et al 2014, Shenoy et al 2013, Svoboda & Li 2017). Further analysis of preparatory activity within the confines of the low-dimensional subspace revealed that pre-movement activity

converges to a specific threshold within the subspace and that on trials where the activity falls outside of the subspace subsequent movements tend to be slower and less stereotyped(Churchland et al 2010, Kaufman et al 2014, Shenoy et al 2013). Experiments that enable manipulation of the initial conditions of intact neural networks will be required to better understand the role of preparatory activity in guiding subsequent motor movements, this is an ongoing area of research and is likely to provide a more comprehensive understanding of how populations drive and represent complex behaviors. The presence of preparatory activity suggests that the nervous is more likely to use dynamical representations of behavior rather than clearly defined discrete computational principles but further research is required to really understand these network level processes that break down at the individual neuron level.

Pre-song activity in the songbird brain

Neural activity that might be associated with motor planning and preparation has been described in HVC neurons and in other regions of the songbird brain. In fact, the earliest know description of pre-song activity was described in 1987 with recordings in singing mockingbirds showing anticipatory activity. Previous work in zebra finches has identified preparatory activity on the order of hundreds of milliseconds prior to song onset in a variety of different songbird brain regions and cell-types: HVC-X and interneurons (~217-775 ms before song onset; Rajan 2018), subpopulations of Area-X neurons projecting to DLM (~0.56 s before song onset; Goldberg et al., 2010), LMAN neurons during undirected song (~600 to 100 ms before song onset; Kao et al., 2008), multi-unit HVC activity in juveniles with immature song (no clear time scale, Day et al., 2009), and putative projection

neurons in HVC of juveniles with immature songs (~0 to 300 ms before and after song onset, Okubo et al., 2015). These previous findings are summarized in Table 2. However, no prior study has examined preparatory activity exclusively in populations of HVC-RA neurons; evidence for preparatory activity in HVC-RA neurons might provide a model for better understanding how sequential activity directly related (and essential) to the production of temporally structured motor behavior is initiated by the brain. Moreover, as stated above half of all recorded HVC-RA neurons don't seem to have any active during the motif, suggesting that they may instead play a role in planning and preparation of courtship song. In addition, although preparatory activity has been reported in the neurons and regions listed above and in Table 2, lesions or inactivation's in Area X and LMAN suggest that they are not crucial for the production of song in zebra finches. This suggests that perhaps HVC-RA neurons are coordinating preparatory activity in other regions of the songbird brain and that preparatory activity within HVC-RA neurons may play or more direct role in song generation than in the areas described in previous research. Preparatory activity in the mammalian system has also been shown in multiple different brain regions, but the complexity of the mammalian nervous system and the lack of specificity of the neurons studied with respect to the behavior make exact interpretations of the role of preparatory activity difficult. In contrast, if HVC-RA neurons have preparatory activity (as shown later in this thesis), this would provide the most reduced circuit to date of motor-related sequential activity and the role of pre-movement activity in ensuring robust production of a complex sequential motor task.

Peripheral mechanisms of song vocalization in zebra finches

Song vocalization in zebra finches is primarily a respiratory behavior, in the sense that song is a result of the careful modulation of expiration and inspiration, with sound generated by rapid expiratory pulses. Birds' lungs consist of rigid tubes and air is moved through them with several interconnected air sacs, expiratory and inspiratory muscles adjacent to the air sac compress or expand the volume to move air in a circular fashion through the birds' respiratory system. The level of fine respiratory control of song is unknown, for example, it is not clear whether the respiratory system simply provides a pressure bulkhead that is then modulated by the vocal tract or if air sacs are themselves capable of introducing fine pressure modulations. Regardless of the level of control, respiratory recordings with pressure sensors implanted in the thoracic air sacs have revealed high stereotypy of respiratory pressures underlying the production of motifs. During song, birds alternate between long expirations and short silent inspirations (or minibreaths); the amplitude of air sac pressure increase dramatically compared to baseline respiration with expiration amplitude increasing by factors of 6 to 20 and inspiration amplitude increasing by 4 to 10. Recordings from respiratory muscles show that expiratory and inspiratory muscles alternate during song and do not seem to have antagonistic activity. Interestingly, previous research has observed increases in respiratory rate and increased oxygen consumption prior to song onset in the presence of a female, following song offset there is a marked period of apnea, where oxygen consumption in some cases dropped down to zero. This period of apnea following singing was directly related to song duration, suggesting that this plays a mechanistic role in expelling carbon dioxide and returning the bird to normal baseline respiration.

The syrinx is the second system that modulates song vocalization. The syrinx is composed of twelve muscles, six on each side that independently control two sound sources. Sound generation is a nonlinear process and involves complex physical forces. The medial and lateral labia vibrate within the synrix and are thought to be the main sound-generating devices in zebra finches. Complex interactions between the labia and syringeal valve are thought to control the spectral features of song vocalization. Vocalization requires strict coordination between respiratory patterns, syringeal muscles, and the upper vocal tract, which is composed of the beak, tongue, larynx, and trachea, all of which are capable of introducing acoustic filtering to the final output sound. How all of these different complex systems interact on short timescales combined with input from motor neurons in the brainstem and neurons in HVC is not fully understood, but provide a well-delineated model to explore the complex phenomena underlying sequential motor actions.

The probabilistic courtship song of Bengalese finches

Most of the research into song behavior has been done in zebra finches, but a similar species with identical brain circuitry provides another testing ground that incorporates a slightly more complex courtship song than zebra finches. Bengalese finches have the same song-related brain regions and peripheral physiology but produce a song that is probabilistic in nature. Zebra finch courtship song is defined as linear in which there is a fixed order of notes or syllables, while Bengalese finches are described as having a non-deterministic song in which there may be a finite number of song syllables but the specific order of those syllables varies from song rendition. Bengalese finches have transition probabilities that vary based on the previous syllable that was sung and therefore may

have more complex sequential representation of this behavior in HVC, although the types of electrophysiological recordings done in singing zebra finches have yet to be conducted in Bengalese finches. This species, therefore, provides another experimental model to test how song is initiated in a more complex song phenotype. One question that we attempt to address in this thesis is if preparatory activity is present in the HVC of Bengalese finches and whether it displays similar characteristics to that of zebra finches. A related and perhaps more interesting question that remains unresolved is how the kinetics of preparatory activity changes given increasingly complex neural sequences and motor behavior.

Summary

Although much is already known about zebra finch behavior and the neural circuitry underlying production of song, the exact computations the brain needs to perform to robustly produce this complex stereotyped behavior is yet to be fully understood. Moreover, our understanding of song vocalization is still somewhat compartmentalized in the sense that we know the components involved in generating courtship song but have yet to develop a unified understanding of how complex neural sequences are initiated, propagated to downstream neural circuits, transformed into physical manipulation of respiration and muscle groups, and then the subsequent termination of neural sequences. We attempt to better understand these processes by performing population-level functional recordings of HVC-RA neurons, and the downstream respiratory patterns. We also examine multi-unit activity in HVC and single-unit recordings in RA of singing Bengalese finches to verify the conservation of preparatory activity in different species of

songbird and whether this activity is likely to influence preparatory activity in downstream brain regions. The results presented in this thesis are a product of fruitful scientific collaboration that provides better mechanistic insight of the interplay between neural sequences, preparatory activity, and peripheral dynamics associated with the production of a complex motor behavior.

Chapter 2

I will begin by discussing technical advances that were required to address these questions in zebra finches. Specifically, explaining the challenges I encountered with viral transfection, cranial windowing, head-mounted imaging, and calcium data analysis.

Chapter 3

This chapter presents the bulk of the results of my graduate research work, presenting the findings of preparatory activity in HVC-RA neurons and our interpretation that anticipatory activity functions to set up the initial conditions for sequential neural activity and prepares the downstream periphery for accurate production of the complex motor task. Combined with complementary data from Bengalese finches showing the conservation of preparatory activity and the propagation of this activity to the downstream region RA.

Chapter 4

This chapter provides a discussion and interpretation of the implications of our findings and future work that will be needed to better understand these behaviors and their neural underpinnings.

Table 1

Reference	Cell Type	Computational Model	Sequence Initiation
Fiete et al., 2010	HVC-RA neurons and a global inhibitory unit representing the pool of HVC interneurons	Heterosynaptic competition combined with spike-time-dependent plasticity	Random barrage of external input
Li and Greenside, 2006	Either Leaky integrate-and-fire (LIF) neurons or single-compartment conductance based (HH, for Hodgkin-Huxley like) neurons.	1-dimensional, homogenous, excitatory chain of nonbursting neurons	A brief high-frequency burst.
Gibb, Gentner, and Abarbanel 2009	HVC-RA and HVC interneurons using single compartment Hodgkin-Huxley neurons.	Chain of bistable clusters	Burst was initiated with a 3-4ms DC current pulse into 50% of HVC-RA neurons.

Jin and Ramazanoğlu, 2007	HVC-RA neurons	Two-compartment model of HVC-RA neurons, minimal conductance-based model	Burst propagation was initiated by stimulating eight spikes in neurons in the first group of the chain, via current injection lasting 10ms.

Table 2

Reference	Cell Type	Description of Activity	Timing
Okubo et al. 2015	Putative HVC projection neurons: N= 285; 137/285 bout onset neurons; 98/285 bout offset neurons; 50/285 active both before and after bouts. 1 identified HVC-RA neuron firing at the end of bouts. At least 3 identified HVC-X neurons (2 bout onset, 1 bout offset).	Significant pre and post-bout activity in the 300ms window before and after bouts. Both pre and post-bout peaks occurred between 0 to 100 ms before or after bout onset or offset, respectively.	Activity hundreds of milliseconds before or after song vocalizations in mixed populations of neurons.
Kao et al., 2008	LMAN neurons: N= 18; elevated activity before undirected song onset. N=16; decreased activity following cessation of undirected song.	In 18 neurons, "firing rate in a 500ms interval from 600 to 100ms before undirected song was greater than the average spontaneous firing rate". In 16 neurons, firing rate "was lower than the	Activity in LMAN neurons hundreds of milliseconds before or after song vocalization, but only in undirected social context.

		average level of spontaneous activity" following song offset.	
Goldberg et al., 2010	Area X-DLM neurons (HF-2 neurons): N=37 neurons	In HF-2 neurons, "firing rate gradually increased before singing (0.56 ± 0.22s), and slowly returned to baseline following singing (1.64 ± 1.2s)."	Activity in AreaX-DLM neurons exhibited pre-song activity hundreds of milliseconds before song onset, and seconds after song offset.
Day et al., 2009	Multiunit activity in HVC	Elevated activity in juvenile birds before and after song vocalization.	Unclear
Rajan and Doupe, 2013	HVC-X neurons: N= 30; 12 antidromically identified, 18 putative. Putative Interneurons: N= 16	Activity of putative interneurons and HVC-X neurons shown to be correlated with onset times of introductory notes.	Activity time-locked to introductory note vocalization.
Vyssotski et al 2016	NIF neurons projecting to HVC	16 Nif-HVC neurons fire on average above baseline levels 70 ms prior to song onset and it decays to baseline about 30 ms prior to song offset.	Activity is time locked to introductory note type. Authors did not look beyond 500 or 1000 ms before song onset.
Rajan 2018	HVC-X neurons: N=39; 13 antidromically identified, 26 putative. Putative interneurons: N=17	4 HVC-X neurons increased their activity (-928 ms to -129ms prior to song bout onset). 3 HVC-X neurons decreased activity -528ms to -47ms). 13 interneurons increased activity (~-674ms to -117ms).	Activity before any vocalization including introductory notes.

CHAPTER 2

Research Approach

The experiments conducted during the course of my graduate training required several technically challenging and novel methodologies that were not previously performed in the songbird species. Specifically, population level imaging of identified projection neuron cell-types in freely behaving zebra finches. At the start of the project, there were no published or anecdotal protocols for expressing the novel calcium sensor GCaMP6 in zebra finches and a verification of viral efficacy, although more traditional calcium buffers had been used and kinetics verified with simultaneous electrophysiology recordings. The usability of a head-mountable miniaturized fluorescent microscope in zebra finches was also unclear, and the practicality was doubtful because the miniscope weighs ~2 grams which amounts to 20% of the average body weight of a zebra finch.

When I first joined the lab, I intended to develop techniques for functional imaging in the HVC of juvenile songbirds as they first listen to a tutor and in the initial stages of vocal learning. The idea was to examine how or whether initial sensory experiences activate HVC projection neurons and how song-related neural sequences develop early in development. However, there were some immediate technical hurdles that prevented these experiments from moving forward. First, expression of GCaMP6 was exceedingly low and inconsistent, moreover, viral injections and expression in juveniles had to occur within the limited time frame of the critical period. Performing HVC injections too early in development made it more difficult to find HVC, while waiting later in development did not seem to provide enough time for viral expression prior to closing of the critical window for song sensory experience and learning. Next, juvenile birds are slightly smaller and weaker

than adult zebra finches, therefore carrying the miniscope was made more impractical for juvenile zebra finches and in the handful of attempts where expression was present it was not obvious whether there was any activity or if the bird was attending to the tutor. I switched to adult birds in an attempt to troubleshoot viral expression and the counterbalancing necessary for zebra finches to comfortably carry the miniscope. This proved to be technically more feasible, and within a few weeks of attempting to image adult zebra finches with direct injections of GCaMP6s into HVC, I collected my first dataset with song-related activity. Intriguingly, although we only had 12 neurons labeled, we observed a wide range of activity occurring before and after song on multiple trials. This serendipitous finding led to a shift in focus to song-related activity in adult zebra finches, with a specific focus on the role of HVC-RA neurons in the behavioral epochs before and after song vocalizations.

Viral Vectors

Initial viral injection protocols involved injecting an AAV9-CAG-GCaMP6s construct directly into HVC. However this was accompanied with two problems: 1) direct injection of GCaMP6 into HVC did not enable cell-type specific labeling of HVC projection neurons (i.e. we could not easily distinguish HVC-X from HVC-RA neurons) and 2) direct injections seem to only label neurons in proximity to the injection tract and did not uniformly label neurons within HVC. Although there may be a significant number of neurons labeled with GCaMP6, the one-photon imaging of the miniscope limits the focal plane to superficial layers of HVC rendering neurons labeled deeper in the brain inaccessible. In order to gain cell-type specificity within HVC, I injected the same AAV9-CAG-GCaMP6s construct into RA; the

AAV9 viral serotype is known to travel retrogradely in zebra finches. Although, this enabled cell-type specific labeling of HVC-RA neurons, the transfection rate was low and needed greater than 6 weeks to see any labeling within HVC, this essentially made the procedure invalid for functional imaging in juveniles. This led us to shift toward a transactional viral labeling strategy, in which we injected an AAV9-Cre into RA and cre-dependent expression of GCaMP6 in HVC. This enabled cell-type specific imaging with more uniform labeling throughout HVC, and provided more robust expression in the cells that were labeled. The results detailed in chapter 3 are from an injection protocol using 3 injections and 3 separate sites in HVC. The center of HVC was first identified with extracellular recordings then 2 additional sites 150 microns rostral and caudal to the center of HVC were mapped. Three injections of 500 nL were made in the 3 locations in HVC, and 1 injection of 350 nL of cre were injected into RA. However, although this surgery protocol was successful, it was not consistent and most birds did not show robust neuronal labeling (collected behavioral data from 6 birds out of >140 surgery attempts). More recent injection protocols have moved towards a single injection of 1500 nL into the center of HVC, with a few modifications. First, the most inferior and superior edges of HVC are identified, then injections (15 nL per injection, 5nL/s rate of injection, 30s between injections) start at the inferior edge with 2 injections, then the pipette is moved up 25 microns and another 2 injections are performed; this is repeated all the way to the middle where 800-1000nL are injected and then pipette is moved up all the way to the top in 25 micron increments. The slow rate of injection combined with the high volume of virus seems to produce more consistent labeling from bird to bird. The following adeno-associated viral vectors were used in these experiments: AAV2/9.CAG.Flex.GCaMP6s.WPRE.SV40 (University of

Pennsylvania Vetor Core; Addgene Catalog #: 100842-AAV9), AAV2/9.CMV.EGFP.Cre.WPRE.SV40 (University of Pennsylvania Vector Core; Addgene Catalog #: 105545-AAV9) and AAV2/9.CAG.GCaMP6s.WPRE.SV40 (University of Pennsylvania Vector Core; Addgene Catalog #: 100844-AAV9). All viral vectors were aliquoted and stored at -80°C until use.

Imaging Equipment

Head-mounted miniaturized fluorescent microscopy in freely behaving singing birds was conducted with an nVista system (Inscopix). Two-photon microscopy was conducted with a commercial microscope (Ultima IV, Bruker) running Prairie View software using a 20x (1.0 NA) objective (Zeiss) with excitation at 920 nm (Mai Tai HP DS, Newport). Two-photon and initial single photon imaging was conducted in lightly anesthetized head-fixed animals. Two-photon and single-photon images of HVC were acquired through the cranial window using an sCMOS camera (QImaging, optiMOS) and these images were used to guide placement of the baseplate for the miniaturized single-photon microscope (Inscopix). CAD files for head holders and stereotaxic devices are available upon request.

Stereotaxic Surgery

All surgical procedures were performed under aseptic conditions. Birds were anesthetized using isoflurane inhalation (~1.5-2%) and placed in a stereotaxic apparatus. Viral injections were performed using previously described procedures (Roberts et al., 2012, 2017) at the following approximate stereotaxic coordinates relative to interaural zero and the brain surface (rostral, lateral, depth, in mm): HVC (0, 2.4, 0.1-0.6); and RA (-1.0, 2.4, 1.7-

2.4). The centers of HVC and RA were identified with electrophysiology. For calcium imaging experiments, 1.0 – 1.5 μL of Cre-dependent GCaMP6s was injected at 3 different sites into HVC and 350 nL of Cre was injected into RA. Viruses were allowed to express for a minimum of 6 weeks before a cranial window over HVC was made.

Cranial Windowing, Imaging and Baseplate Implantation

Briefly, a unilateral square craniotomy (~3.5 x 3.5 mm) was created over HVC and the dura was removed. A glass coverslip was cut to match the dimensions of the craniotomy and held in place with a stereotaxic arm as Kwik Sil was applied to the edges of the cranial window. Dental acrylic was applied over the Kwik Sil and allowed to slightly overlap with the glass coverslip to ensure the window would not move and would apply the appropriate amount of pressure to the brain. An aluminum head post was affixed to the front of the bird's head to enable head-fixed imaging under the 2-photon microscope and to enable head-fixation for baseplate implantation. Following verification of labeling, identification of HVC boundaries, and high-resolution images of neurons under the 2-photon microscope, the bird was lightly anesthetized with isoflurane and the miniaturized fluorescent microscope (Inscopix) was placed over the cranial window. The field of view that matched the 2-photon images was identified and the focal plane that enabled the largest number of neurons to be in focus was selected. Dental acrylic was used to fix the baseplate in the desired position and any exposed skull was covered with dental acrylic. Once the dental acrylic dried, the microscope was removed from the baseplate and the bird was allowed to recover overnight. About 30 minutes before the birds' subjective daytime, the microscope was attached to the counterbalance (Instech) with enough cable to allow the bird to move

freely throughout the cage. The microscope was then secured to the baseplate with a setscrew. The bird was allowed to wake up and accommodate to the weight of the microscope over the next 2-3 days. After the end of imaging experiments, the baseplate was removed and stereotactic injections of AlexFluor 594 were made into Area X. After 1 week, birds were given an overdose of Euthasol, perfused and tissue was sectioned.

GCaMP6s Imaging Using a Miniaturized Fluorescent Microscope

The miniaturized fluorescent microscope (Inscopix) was not removed following successful baseplate implantation and remained attached to the birds' head until either the cranial window closed or 7-10 days had passed. The counterbalance was adjusted based on the observed behavior of the bird and its ability to move freely. The female was not housed in the cage with the male bird, but instead was introduced to the males during a minimum of 3 morning and afternoon sessions to evoke directed song. Video recording was first started followed by 5 to 10 seconds of spontaneous recording with the miniaturized fluorescent microscope. The female bird was placed in the cage as quickly and as with little disruption as possible for each session. If the male bird did not sing within a minute of the females' presence, the session was stopped, and the female was removed. All trials were recorded on video, and audio was recorded using Sound Analysis Pro (SAP) software and the HD video camera microphone. Calcium imaging was performed at 30 frames per second (fps), at 1080x1920 resolution, Gain was set to 4, and Power was set to 90% for all birds, behavioral videos were collected at 24 fps. Calcium imaging data and behavioral data was synchronized using start of calcium imaging on a frame-by-frame basis.

Calcium image processing and analysis

Calcium images were collected using the miniaturized fluorescent microscope developed by Inscopix (Ghosh et al 2011). Video recordings of birds behavior and singing were manually synchronized on a frame by frame basis to the onset of calcium imaging, visualized by turning of the blue LED on the miniscopes. For processing of calcium imaging data the FOV (Field of View) was spatially cropped to exclude pixels that did not include neurons or observable changes in fluorescence. Next, the preprocessing utility within the Mosaic data analysis software was used to spatially bin the images by a factor of 2 to reduce demands on computer memory and enable faster data processing. The TurboReg implementation within Mosaic was used to perform motion correction. A reference image was created using a maximum intensity projection of the dataset and the images were aligned in the x and y dimension to the reference image. Imaging datasets with translational motion greater than 20 pixels in either the x or y dimensions were excluded from further data analysis. Post-registration black borders were spatially cropped out. The resulting spatially-cropped, preprocessed, and motion corrected calcium imaging datasets were exported for further analysis in custom Matlab scripts.

We performed ROI-based analysis on the motion-corrected calcium imaging datasets using previously described methods(Peters et al 2014)(see Source Code Files 1-4). ROIs were manually drawn around identifiable soma and a secondary ROI that extended 6 pixels around the boundaries of the neuronal ROI was used to estimate background fluorescence (i.e. neuropil or other neurons). The pixel values were averaged within the neuronal and background ROIs, and background fluorescence signal was subtracted from neuronal

signal. An iterative procedure using custom Matlab scripts were used to estimate baseline fluorescence, noise, and active portions of the traces (Peters et al 2014). A subset of calcium images were re-analyzed using previously described constrained non-negative matrix factorization (CNMF) methods, but calcium fluorescence traces were identical to the traces pulled out by the ROI-based analysis (Pnevmatikakis et al 2016). Calcium traces generated by ROI-based analysis were further deconvolved to produce inferred calcium traces using the pool adjacent violators algorithm (PAVA)(Friedrich et al 2017). The deconvolved calcium traces were normalized to values between 1 and 0 to enable visualization of activity across different neurons during the same trial. Calcium transients that were 3 SD. above baseline activity were recorded as events. The corresponding onset times and the rise times to peak fluorescence of individual calcium transients were correlated with synchronized behavior.

All calcium events were first categorized as falling into peri-song or song behavioral epochs on a frame-by-frame basis. Peri-song was limited to the 5 second period before the onset of vocalizations, including introductory notes, and the 5 second period after the offset of the last syllable. These event counts were used to assign a Phrase index to all imaged neurons. Neurons that had fewer than 2 calcium events recorded over a day of singing were excluded from further analysis because sparsity of calcium events could spuriously identify neurons as peri-song or song exclusive. We combined the number of calcium events from neurons imaged across multiple trials during the same day. Neurons imaged across multiple days were treated as unique neurons. The phrase index was calculated as a ratio of the total number of song events imaged from a neuron during a day subtracted by the

number of peri-song events to the total number of calcium events. This bounded the phrase index to values of -1 (peri-song exclusive) and +1 (Song exclusive). We used the phrase index to examine the timing properties of neurons active only during peri-song, song, or both behavioral epochs.

To examine the distribution of calcium events, we generated histograms with bin sizes of 200 ms. Peri-song event rates were first calculated in 100ms bins and then a plotted using a 1 second moving average window that reaches a minimum of 500 ms at boundaries (-5, +5 seconds, and at song onset and offset). The average event rate and standard deviation was calculated using all pre and post phrase event rates from all birds.

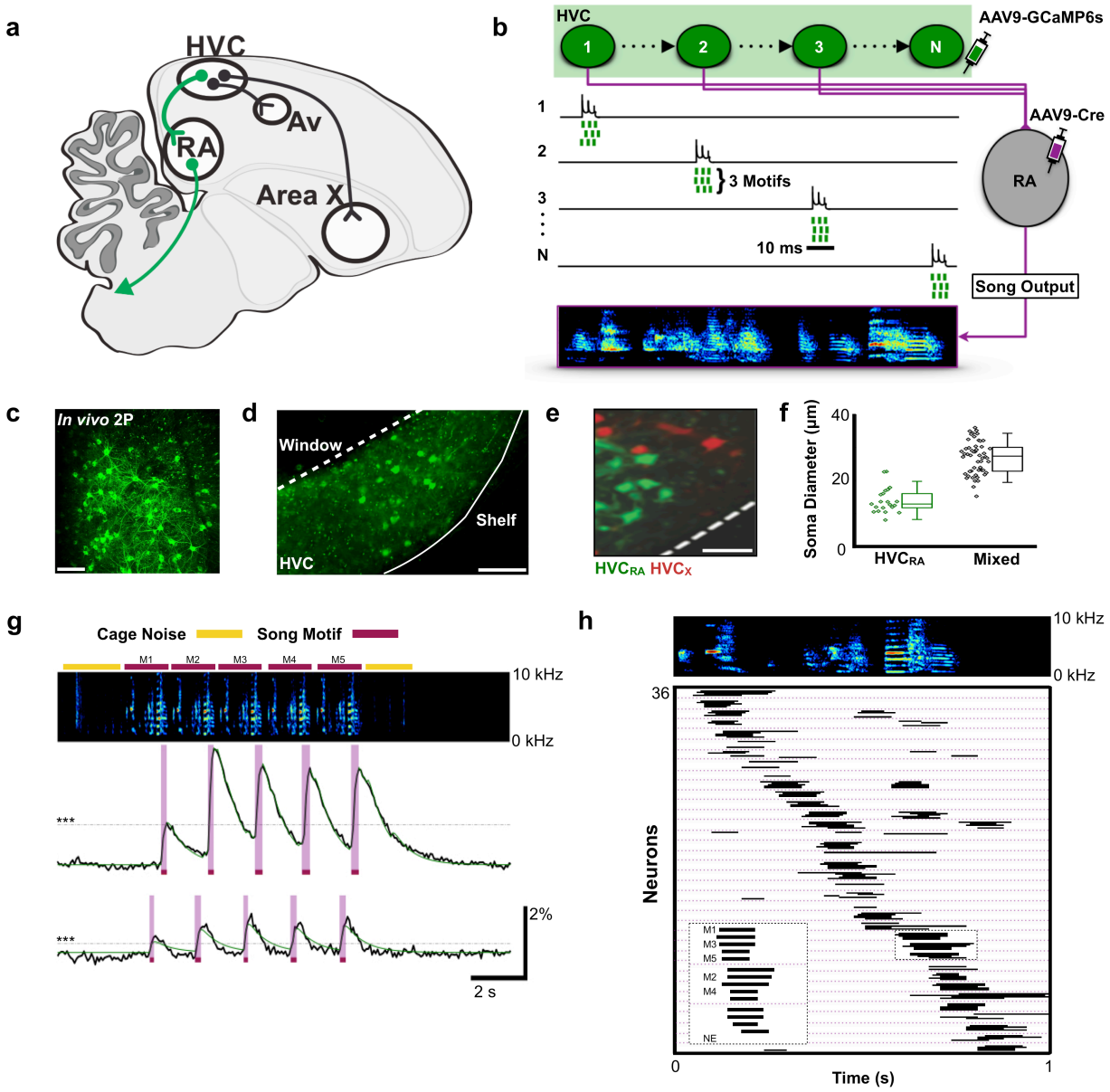
a
HVC
Av
RA
Area X
b
HVC
1
2
3
N
AAV9-GCaMP6s
AAV9-Cre
RA
3 Motifs
10 ms
Song Output
c
In vivo 2P
d
Window
Shelf
HVC
e
HVCRA HVCX
f
Soma Diameter (µm)
40
20
0
HVCRA
Mixed
g
Cage Noise
Song Motif
M1
M2
M3
M4
M5
10 kHz
0 kHz
***
***
2%
2 s
h
10 kHz
0 kHz
36
Neurons
M1
M3
M5
M2
M4
NE
0
1
Time (s)

Figure 1. Population imaging of song-related HVC_{RA} sequences. a) Diagram showing 3 distinct projection neuron targets of the vocal premotor nucleus HVC. The projection neurons connecting HVC to the downstream motor nucleus RA (HVC_{RA} neurons) are shown in green. Auditory region Avalanche (Av), robust nucleus of the arcopallium (RA), nucleus HVC of the nidopallium (HVC). **b)** Schematic showing HVC_{RA} neuron somata (green) and their outputs (magenta) to the downstream motor nucleus RA. AAV9-Flex-CAG-GCaMP6s was injected into HVC (green syringe) and AAV9-CAG-Cre was injected into RA (magenta syringe) to selectively label HVC_{RA} neurons. **c)** In vivo two-photon maximum density projection of retrogradely labeled HVC_{RA} neurons expressing GCaMP6s. Scale bar = 100 μm. **d)** A cross-section of HVC showing GCaMP6s-labeled HVC_{RA} neurons (green). The dashed line indicates where the cranial window was made over HVC. Note the lack of labeling in the region directly ventral of HVC, known as the HVC shelf. Scale bar = 100 μm. **e)** A sagittal section of HVC showing HVC_{RA} neurons (green) and retrogradely labeled HVC_X neurons (red). The dashed line indicates the border between HVC and HVC shelf. Scale bar = 50 μm. **f)** Whisker and scatter plots of soma diameters of GCaMP6s expressing cells show that retrogradely labeled HVC_{RA} neurons (green) have smaller diameters than neurons labeled using only direct viral injections (AAV9-CAG-GCaMP6s) into HVC (mixed population neurons, black). Boxes depict 25th and 75th percentiles, whiskers depict SD. HVC_{RA}: N=21 neurons; mean diameter = 14.0 ± 3.8 μm (SD); Mixed: N=52 neurons; mean=26.9 ± 4.9 μm; t = -10.7, p = 2.0 x 10^{-16}, two-sample t test. **g)** Example calcium traces from 2 HVC_{RA} neurons in a bird that sang 5 consecutive motifs. Shown are the background-subtracted traces (black) and the inferred calcium traces (green). The magenta overlays indicate the rise time (intervals between onset and peak times) of the recorded calcium transients. The horizontal dashed line (gray) denotes 3 SD above baseline activity. The bars above the spectrogram denote cage noise associated with birds hopping or flapping their wings (yellow) or production of song motifs (red). **h)** Motif-related activity of 36 HVC_{RA} neurons across 5 motifs. Each row shows activity of a neuron from 1 trial. The dashed magenta lines separate different neurons. Empty spaces indicate trials wherein neurons were not active (no event, NE). The inset shows a zoom-in of activity from 3 separate HVC_{RA} neurons.

CHAPTER 3

Transitioning between preparatory and precisely sequenced neuronal activity in production of skilled behavior

The sequential activation of neurons is implicated in a wide variety of behaviors, ranging from episodic memory encoding and sensory processing to the voluntary production of skilled motor behaviors (Fee et al 2004, Fiete et al 2010, Hahnloser et al 2002, Li et al 2015, Lynch et al 2016, Markowitz et al 2015, Okubo et al 2015, Peters et al 2014, Rajan et al 2016, Svoboda & Li 2017). Neural sequences develop through experience and have been described in several brain areas, including the motor cortex, hippocampus, cerebellum, and the basal ganglia(Barnes et al 2005, Dragoi & Buzsaki 2006, Foster & Wilson 2006, Harvey et al 2012, Jin et al 2009, Li et al 2015, Luczak et al 2007, Mauk & Buonomano 2004, Peters et al 2014, Pfeiffer & Foster 2013, Pfeiffer & Foster 2015, Schwartz & Moran 1999). Although computational models provide important insights into circuit architectures capable of sustaining sequenced activity(Churchland et al 2010, Fiete et al 2004, Fiete et al 2010, Haga & Fukai 2018, Harvey et al 2012, Kumar et al 2010, Rajan et al 2016), our understanding of sequence initiation and termination is still limited.

The precise neural sequences associated with birdsong may provide a useful biological model for examining this issue. Premotor projection neurons in the cortical vocal region HVC (HVC_{RA} neurons, see Figure 1 legend for anatomical abbreviations) exhibit precise sequential activity during song and current evidence suggests that this activity is acutely necessary for song production (Hahnloser et al 2002, Kozhevnikov & Fee 2007, Long & Fee 2008, Long et al 2010, Scharff et al 2000). HVC_{RA} neurons are thought to be exclusively active during vocal production in waking adult birds, yet ~50% of recorded

HVC_{RA} neurons do not exhibit any activity during singing(Hahnloser et al 2002, Hamaguchi et al 2016, Kozhevnikov & Fee 2007, Long et al 2010, Lynch et al 2016), leaving the function of much of the HVC_{RA} circuitry unresolved.

Neuronal activity related to motor planning and preparation has been associated with accurate production of volitional motor movements (Churchland et al 2010, Svoboda & Li 2017) but is still poorly described in the context of initiating precise neural sequences for motor behaviors, like those exhibited in HVC_{RA} neurons. Although it is not known if HVC_{RA} neurons exhibit activity related to motor planning and preparation, previous studies have identified anticipatory or preparatory activity in other classes of HVC neurons and in other regions of the songbird brain(Goldberg et al 2010, Goldberg & Fee 2012, Kao et al 2008, Keller & Hahnloser 2009, Rajan 2018, Roberts et al 2017). HVC contains interneurons and at least three classes of projection neurons, including neurons projecting to the striatopallidal region Area X (HVC_X), neurons projecting to a portion of the auditory cortex termed Avalanche (HVC_{Av}), and the aforementioned HVC_{RA} neurons that encode precise premotor sequences necessary for song production(Akutagawa & Konishi 2010, Mooney & Prather 2005, Roberts et al 2017). Multi-unit recordings from HVC, which are typically dominated by the activity of interneurons, show increases in activity tens to hundreds of milliseconds prior to singing(Crandall et al 2007, Day et al 2009, Rajan 2018). Calcium imaging from HVC_{Av} neurons and electrophysiological recordings from HVC_X neurons indicate that they also become active immediately prior to song onset (Rajan 2018, Roberts et al 2017). These data are consistent with recordings from the downstream targets of HVC_{Av} and HVC_X neurons. Portions of the auditory cortex (Keller & Hahnloser 2009) and

the basal ganglia pathway involved in song learning show changes in activity immediately prior to singing (Goldberg et al 2010, Goldberg & Fee 2012, Kao et al 2008). Given this background, and that ~50% of HVC_{RA} neurons may not exhibit any activity during singing (Hamaguchi et al 2016, Long et al 2010), we sought to examine if the precise neural sequences associated with song arise as part of larger changes in activity among populations of HVC_{RA} neurons.

To examine the neural circuit activity associated with the initiation and termination of singing we imaged from populations of HVC_{RA} neurons in freely singing birds. We show that ~50% of HVC_{RA} neurons are active during periods associated with preparation to sing and recovery from singing and that their activity presages the volitional production of song by 2-3 seconds. One population of HVC_{RA} neurons is only active immediately preceding and following song production, but not during either singing or non-vocal behaviors. A second population of neurons exhibits ramping activity before and after singing and can also participate in precise neural sequences during song performance. Recordings from downstream neurons in the motor cortical nucleus RA reveal neural activity prior to song initiation and following song termination. The control of respiratory timing is essential for song (Schmidt & Goller 2016), and our measurements of respiratory activity suggest that one function of pre-singing activity in HVC_{RA} neurons is to coordinate changes in respiration necessary for song initiation. From these findings, we reason that subpopulations of HVC_{RA} neurons are involved in motor planning and motor preparation, encoding the neural antecedents of song that drive recurrent pathways through the brainstem to prepare the motor periphery for song production.

Results

Activity Sequences in Populations of HVCRA Neurons

We used miniscope calcium imaging to examine the activity of populations of HVC_{RA} neurons in singing zebra finches(Chen et al 2013, Ghosh et al 2011). A total of 223 HVC_{RA} neurons were imaged during production of 1,298 song syllables from 6 birds (30 song phrases across 18 imaging trials, **Table 1**). To selectively target HVC_{RA} neurons, we combined retrograde viral expression of cre recombinase from bilateral injections into RA with viral expression of cre-dependent GCaMP6s from injections into HVC (**Figure 1a-b and legend, see Methods**)(Chen et al 2013). We confirmed the identity of imaged neurons using conventional retrograde tracing, anatomical measures of neuronal features, and post-hoc histological verification. Although this did not label all RA projecting neurons in HVC, we found that this approach exclusively and uniformly labeled populations of HVC_{RA} neurons (**Figure 1c-f**).

To elicit courtship singing, we presented male birds with a female and imaged HVC_{RA} neurons during song performance (**Video 1, see Methods for definitions song**). On average birds engaged in singing in 24 seconds (±49s) of a female bird being presented. Given the slow decay times of calcium signals relative to singing behavior, we defined neuronal activity by the rise times of calcium events that were >3 standard deviations (SD) above baseline (**Figure 1g,** average rise time: 0.112 ± 0.047 s SD, **see Methods**). The activity of individual HVC_{RA} neurons was time-locked to a moment in the birds' song, with different neurons active at different moments in the song motif (**Figure 1g-h**; onset jitter =

55.0 ± 60.9 ms, populations imaged at 30 frames per second). We found that the sequential activity of HVC_{RA} neurons roughly coded for all moments in the song motif (**Figure 1h**). These results provide the first glimpse of activity across populations of identified HVC_{RA} neurons during singing and support the idea that sparse and precise neuronal sequences underlie the sequential structure of birdsong(Amador et al 2013, Hahnloser et al 2002, Long et al 2010, Lynch et al 2016, Picardo et al 2016).

Peri-Song Activity in Populations of HVC_{RA} Neurons

The sequence of syllables in zebra finch song is stereotyped and unfolds in less than a second. Like other rapid and precise motor movements, song may benefit from motor planning and preparatory activity unfolding on much longer timescales than the synaptic delays associated with descending motor commands, which in zebra finches are estimated to be ~25-50ms (Amador et al 2013, Fee et al 2004); however, HVC_{RA} neurons have been hypothesized to exclusively represent temporal sequences for songs and calls, and to remain quiescent at other times (Hahnloser et al 2002, Hamaguchi et al 2016, Kozhevnikov & Fee 2007, Long et al 2010). We examined the activity of HVC_{RA} neurons prior to song onset, in between song bouts, and immediately after singing (**Figure 2a-c, Figure 2-figure supplement 1**). Song onset was defined by the onset of introductory notes that preceeded the bird's song phrase. A song phrase was defined as one or more repetitions of a bird's motif with less than 2 s between onset of the next song bout (see Methods for detailed definitions of phrases, song, and peri-song behavior). For any given song phrase, we observed significant activity surrounding singing behavior, indicating that HVC_{RA} neuronal activity is not restricted only to the production of precise neural sequences for song in

waking birds. 30 out of 30 song phrases from 6 birds exhibited 'peri-song' activity, defined as the 5 second intervals before and after singing, plus silent gaps within song phrases. Slightly fewer HVC_{RA} neurons were active during peri-song intervals (54.3% of neurons) than during singing (59.9%), (t = -1.1, p = 0.29 two-sample t test; **Figure 2b)**. Of the neurons that were active during peri-song intervals, 40.6% were active prior to song onset, 17.8% were active following song offset, and 41.6% were active before and after song (N=197 neurons, 6 birds, **Figure 2-figure supplement 2**). When we examined the timing of peri-song events, we found no correlation in the timing of pre-song and post-song event onsets in neurons that were sparsely active both before and after song (**Figure 2-figure supplement 3**). Although neuronal populations displayed considerably more calcium events during song (t = 5.635, p = 5.65 x10^{-7} two-sample t, normalized song event rate = 24.09 events/s ± 15.95 SD, normalized peri-song event rate = 6.97 events/s ± 3.72 SD), a substantial fraction of all recorded calcium events occurred within the 5 second intervals before or after song (997/2366 or 32.5% of all calcium events).

To better characterize these newly discovered activity profiles, we indexed the song and peri-song activity of all HVC_{RA} neurons throughout a day of singing (phrase index: range -1 to +1, with neurons exclusively active outside of singing scoring -1 and neurons active only during singing +1, **Figure 2c-d, see Methods**). We found that HVC_{RA} phrase indices were not uniformly distributed (χ^2 (7, N = 223) = 46.3, p = 7.6 x 10^{-8}, Chi-square goodness of fit test), with a significant fraction (36%) falling at the extremes of this scale (**Figure 2d**), and that neurons with different phrase indices were anatomically intermingled throughout HVC (**Figure 2-figure supplement 4**)**.** Most neurons (64.1%) displayed sparse heterogenous

activity during peri-song periods and transitioned to temporally precise activity during singing (referred to here as '**pan-song neurons**'; **Figure 2-figure supplement 5**). At the extremes of the phrase index scale (phrase indices -1 or +1), we found that 18.4% of neurons were exclusively active during peri-song intervals (phrase index = -1, referred to here as '**peri-song neurons**'), while 17.5% participated exclusively in neural sequences during singing (phrase index = +1, referred to here as '**song neurons**').

These results reveal that a substantial portion of HVC_{RA} neurons are active outside of the precise neuronal sequences associated with song, expanding our view of the potential functional role of this neuronal population. One interpretation is that HVC_{RA} neurons may play a role in motor planning and in preparation to sing. That more than half of all HVC_{RA} neurons can be active during peri-song intervals also raises the prospect that precise neural sequences emerge as part of changing network dynamics across subpopulations of HVC_{RA} neurons. These results also lend insight into why approximately half of HVC_{RA} neurons recorded using electrophysiological methods appear to be inactive during song (Fee et al 2004, Hamaguchi et al 2016, Kozhevnikov & Fee 2007, Long et al 2010). Nonetheless, this result also raises questions as to why previous studies have not identified peri-song activity. First, previous calcium imaging experiments have not restricted GCaMP expression to HVC_{RA} neurons, but rather relied on either non-selective labeling of neuronal populations in HVC(Katlowitz et al 2018, Liberti et al 2016, Markowitz et al 2015, Picardo et al 2016) or have been restricted to imaging small populations of other classes of HVC neurons(Roberts et al 2017). Second, electrophysiological studies of identified HVC_{RA} neurons have been mostly confined to recording one neuron at a time and these

experiments have focused on understanding coding during song production, often using short (~500 ms) buffering windows triggered by singing behavior. Therefore, sparse heterogenous activity occurring seconds before or after song could be simply overlooked or could appear irrelevant unless viewed through the lens of population dynamics. Consistent with this idea, previous multi-unit recordings in zebra finches and mockingbirds, which are dominated by activity of interneurons or neurons projecting to the basal ganglia, have identified 'anticipatory' activity in HVC hundreds of milliseconds prior to song onset, but the role of this activity and whether HVC_{RA} neurons are active prior to song onset have not been examined(McCasland 1987, Rajan 2018, Rajan & Doupe 2013).

Another possibility is that peri-song activity is unrelated to singing and merely reflects low levels of spontaneous activity intrinsic to HVC_{RA} neurons. This was not the case, however, as HVC_{RA} neurons were largely inactive outside of peri-song intervals and were significantly more active during the peri-song periods than baseline (baseline calculated from periods ≥10 s removed from periods of singing or calling, $p = 8.4 \times 10^{-5}$, Chi-square = 18.78 Friedman test, baseline = 12.9% ±5.7 SD of fluorescence values normalized to song, pre-song = 26.9% ±14.7, and post-song = 30.2% ±10.7). In addition, we examined the amplitudes of peri-song calcium events and found that they were larger than events occurring during song ($t = 3.2769$, $p = 0.0012$, two-tailed t test, 279 fluorescence peaks measured from neurons active during both peri-song and song, pan-song neurons with phrase indices between -0.18 to 0.18). We also asked whether peri-song activity might relate to factors other than singing. We examined trials in which birds did not sing to female birds but did not find HVC_{RA} neurons that responded solely to presentation of the

female or during non-song related movements of the head, beak, or throat, such as during eating, grooming, and seed-shelling (**Figure 2e, Figure 2-figure supplement 6)**. Indeed, populations of HVC_{RA} neurons only became substantially active prior to singing or calling. Moreover, in a single bird in which we were able to image neuronal activity during undirected singing, that is song produced when the bird was alone in its cage, we also found peri-song activity in the moments before and after (**Figure 2-figure supplements 6 - 7**), suggesting that peri-song activity is unlikely to be solely associated with extraneous nonvocal singing behaviors such as courtship dance.

We next examined the possibility that HVC_{RA} neurons play a role in motor planning or preparation as birds prepare to sing. We found pre-song activity in 28/30 song phrases analyzed. In the two instances when we did not detect any pre-song activity less than 6 HVC_{RA} neurons were active within our imaging window during singing, indicating that the lack of activity was likely the result of under sampling from the population. Electrophysiological recordings in young zebra finches have identified HVC neurons that mark the onset of song bouts(Okubo et al 2015), 'bout neurons' that burst immediately prior to vocalizations. The vast majority of pre-song activity we describe occurs hundreds of milliseconds to seconds prior to vocalizations, suggesting a role in planning or preparation to vocalize (96.2% of calcium events occurred more than 100 ms prior to vocal onset and 65.6% occurred more than 1 second prior to vocal onset). Zebra finches often sing a variable number of introductory notes prior to the first motif of a song bout. Pre-song activity (prior to introductory notes) could be related to the number of introductory notes to be sung, but we found no correlation between pre-song event rates and the

number of introductory notes (**Figure 2-figure supplement 8**). In 27/28 song phrases we found increases in population activity greater than 3 SDs above baseline predicted song onset within the following 4-5 seconds (2.44 s ±1.0 s SD, 28 song phrases from 5 birds). Calcium activity reached two-thirds of the maximum pre-song activity only prior to song onset or prior to short vocalizations (**Figure 2-figure supplement 9**). Together, these results indicate that HVC_{RA} neuron activity is predictive of the voluntary production of courtship song and suggests a role for this network in motor planning and in preparation to sing.

Peri-Song and Pan-Song Neurons

A substantial fraction of all imaged neurons (41/223 neurons) were active exclusively before or after singing (**Figure 2d**, neurons with a phrase index of -1). These peri-song neurons exhibited sparse heterogeneous activity before song phrases and were occasionally active in the silent intervals between song motifs (**Figure 3a-c, and Figure 3-figure supplement 1**). Both the number of active peri-song neurons and the density of calcium events increased 1-3 s prior to song onset, with the event rate peaking 1.5 s prior to singing (**Figure 3b-c, i**) and then declining sharply in the last second before song onset (**Figure 3i**). Most of the neurons we imaged, pan-song neurons (143/223 neurons), exhibited sparse, heterogeneous activity before and/or after song and exhibited time-locked sequences during singing (**Figure 3d-f**). Pan-song neurons exhibited substantial increases in their activity in the last ~2 s prior to song onset. Their activity continued to increase as the activity of peri-song neurons began to ramp-off prior to song onset (**Figure 3g,I, and Figure 3-figure supplement 2**). Differences in pre-song activity profiles

between peri-song and pan-song neurons (Kolmogorov-Smirnov, K-S test, $k = 0.26$, $p = 0.056$) may support temporally coordinated network transitions as birds prepare to sing, suggesting that neural sequences for song could emerge as part of changing network dynamics in HVC.

During production of song motifs, pan-song neurons exhibited sequential bursts of activity that roughly coded for all moments in the bird's song, similar to sequencing previously described in song neurons. We found that pan-song and song neurons had a similar probability of being active with each motif (song neurons probability of at least one calcium event per motif P(motif) = 0.72 ± 0.32, pan-song neurons P(motif) = 0.66 ± 0.29, K-S test, $p = 0.11$; **Figure 3-figure supplement 3**); however, we also noted that the probability of being active was lower than in electrophysiological recordings(Hahnloser et al 2002, Kozhevnikov & Fee 2007). This likely reflects limitations in event detection using single-photon calcium imaging. To better understand this, we calculated signal to noise ratios (SNRs, signal defined as peak fluorescence of calcium events during song) between pan-song neurons and song neurons during singing (SNR song neurons = 913.8 ±405.4 (7 neurons), pan-song neurons = 638.3±248.2 SEM, n=36 neurons). We found no difference in SNR between these neurons (two-sample t test, $p = 0.6$; SNR calculated from 156 calcium events (28 from song neurons and 128 from pan-song neurons), suggesting that although we are underestimating activity during singing, these limitations are unlikely to obscure differences between pan-song and song neurons.

In addition to preceding song onset, neurons also marked the end of song phrases. Within 5 seconds after song offset, peri-song neurons exhibited a sharp increase in activity followed by a gradual ramp-off (**Figure 3a-c, h, j, and Figure 3-figure supplement 2**) whereas pan-song neurons only exhibited a ramp-off (**Figure 3d-f, h, j**). Although the distribution of post-song activity differed between peri-song and pan-song neurons (K-S test, $k = 0.2692$, $p = 0.0373$), both populations returned to baseline activity over similar timescales. The function of post-song activity is unclear but may provide a circuit mechanism for birds to rapidly re-engage in song performances given appropriate social feedback or context. Courtship singing is tightly coupled to social interaction with female birds and it is common for male birds to string two or more song phrases together during courtship song(Williams 2004) (see **Figure 2-figure supplements 1 & 6**). Post-song activity could also reflect moments when birds are unable to continue singing due to hyperventilation induced by the rapid respiratory patterns associated with song(Franz & Goller 2003). To explore this idea, we examined whether the duration of song phrases was correlated with the number of active neurons in the post-song period, but did not find a significant correlation ($r^2 = 0.03$). Although the function of post-song activity is unclear, our results indicate that pre-song activity forecasts impending song and suggest a previously unappreciated role for the HVC_{RA} network in planning or preparing to sing.

Common Preparatory Activity in Premotor Circuits Across Multiple Species

To examine whether preparatory activity is a common circuit mechanism for the production of birdsong, we recorded HVC and RA neural activity in another songbird species, Bengalese finches (*Lonchura striata domestica*). Motor planning and preparation

facilitate the accurate execution of fast and precise movements, which are common to the songs of zebra finches and Bengalese finches, however, syllable sequences in Bengalese finches are less stereotyped than those in zebra finches(Okanoya 2004). Using multi-channel neural recordings in HVC, we identified robust preparatory activity several hundreds of milliseconds prior to song onset (**Figure 4a-g**). The pre-song and song–related multiunit spike rates were significantly above baseline (Wilcoxon signed-rank test after Bonferroni correction, n = 29 MU sites. pre-song: $z = 4.62$, $p = 0.030$; song: $z = 4.70$, $p < 0.001$), whereas the post-song spike rates was not ($z = 2.17$, $p = 0.089$). Pre-song activity increased above baseline -1.47 ± 1.05 s prior to song onset, a timescale that closely matched the timing of peak calcium-event rates in peri-song neurons in zebra finches. The offset timing of post-song activity was 0.42 ± 0.23 s. This indicates that preparatory activity in HVC is a common network motif important for song generation and the onset of precise neural sequences.

HVC contains multiple cell types, including interneurons and at least three different classes of projection neurons(Mooney & Prather 2005, Roberts et al 2017). Multichannel recordings in HVC provide an important read-out of the network activity prior to song onset but alone are insufficient to assess whether this preparatory activity influences descending cortical pathways involved in song motor control. Therefore, we recorded single unit electrophysiological activity from the downstream targets of HVC_{RA} neurons within the cortical premotor nucleus RA. Projection neurons in RA are tonically active at baseline (**Figure 5a**, "Spontaneous") and exhibit precise bursts of activity during singing (**Figure 5a**, "Song"), a transition well captured by changes in the coefficient of variation of

the inter-spike intervals (CV_{ISI}, **Figure 5c**). We measured changes in RA neuron activity in the period just prior to song initiation and just after the conclusion of each song bout (between 0.5 and 2.5 s before/after the first/last song syllable). As expected, we did not find substantial differences in spike rates between non-singing and singing states (not shown) but found that the CV_{ISI} for RA neurons changed significantly during song, reaching higher values during pre-song, song, and post-song epochs as compared to spontaneous activity (**Figure 5d and Figure 5-figure supplement 1,** $p<0.005$, two-sided K-S tests). This suggests that HVC_{RA} sequences associated with preparation to sing propagate to downstream premotor circuits prior to song onset and that HVC continues to influence descending motor pathways following song cessation.

Peripheral Preparation to Sing

Pre-song activity could reflect motor planning (changes in network activity independent of changes in the motor periphery) and/or motor preparation that functions to coordinate changes in the motor periphery as birds prepare to sing. Song is a respiratory behavior that is primarily produced during expiration and silent intervals in the song correspond to mini-breaths, which are rapid, deep inspirations (Hartley & Suthers 1989, Schmidt & Goller 2016). How birds plan to sing or prepare the respiratory system to sing is poorly understood, but there is evidence that prior to song onset, oxygen consumption decreases and respiratory rate increases(Franz & Goller 2003). To explore the time course of changes in respiratory patterns in more detail, we used air sac pressure recordings in singing zebra finches (**Figure 6a-c**). During singing, birds significantly accelerated the respiratory rhythm and marginally shifted towards longer periods of expiration during each cycle

(**Figure 6b,** respiratory duration pre-song = 0.38 ±0.04 s (SD), song = 0.18 ±0.03 s, post-song = 0.39 ±0.06 s: $F(2,10) = 46.63$, $p < 0.001$; duty cycle (% of time in expiration) pre-song = 58% ±3 (SEM), song = 57% ±2.5, post-song = 61% ±2.4: $F(2,10) = 3.56$, $p = 0.07$). We found that significant changes in respiration also preceded song onset. Respiratory cycle duration significantly accelerated in the last second prior to song onset with relative decreases of expiratory phases (respiratory duration: $F(3,15) = 7.67$, $p = 0.02$, duty cycle: $F(3,15) = 4.077$, $p = 0.07$; **Figure 6d**). Following song termination, birds immediately returned to longer respiratory cycles but during the first second post-song, they spent more time exhaling compared to inhaling, a behavior likely involved in helping to recover from singing-related hyperventilation (respiratory duration: $F(2,10) = 0.509$, $p <$ n.s., duty cycle: $F(2,10) = 6.553$, $p <0$ .01; **Figure 6e**). These changes in respiration during the last second before and first second following song support the idea that HVC_{RA} neurons provide descending motor commands that coordinate transitions between non-vocal and vocal states by coordinating respiratory patterns. The lack of changes at earlier time-points prior to singing also indicate that pre-song activity 1-3 s prior to song onset may reflect motor planning or the decision to sing, rather than respiratory preparation. Together these, findings support the idea that HVC_{RA} neurons could function in aspects of motor planning as well as preparation.

Table 3

Bird	Trial	Type	Syllables	Motifs	Bouts	Phrases	Singing Duration (s)
O262	132226	Directed	30	6	3	1	4.92

	135632	Directed	25	5	1	1	4.16
	142315	Directed	15	3	1	1	2.43
	173107	Directed	25	5	1	1	3.29
	174745	Directed	25	5	2	1	4.08
	165515	Directed	25	5	1	1	4.54
	170812	Non-Singing*	N/A	N/A	N/A	N/A	N/A
O248	162048	Directed	244	49	24	10	31.73
	162201	Directed	85	17	7	5	10.58
	160046	Directed	170	34	21	4	22.92
	152940	Directed	25	5	1	1	3.625
	140745	Undirected	60	12	3	2	8.68
	141006	Undirected	100	20	4	2	15.952
	141059	Undirected	130	26	4	2	19.918
	131612	Undirected	110	22	4	3	16.83
	132211	Non-Singing	N/A	N/A	N/A	N/A	N/A
	131904	Non-Singing	N/A	N/A	N/A	N/A	N/A
	123106	Non-Singing**	N/A	N/A	N/A	N/A	N/A
O213	164915	Directed	30	7	4	1	5.1
	170209	Directed	27	6	3	1	4.499
	163439	Directed	27	6	3	1	4.55
	165959	Directed	12	3	2	1	2.07
Y204	151708	Directed	30	9	2	1	5.61
	155748	Directed	14	4	1	1	2.57

B89	162205	Directed	26	8	1	1	4.68
B263	163144	Directed	21	3	2	1	7.34
	162125	Directed	14	2	1	1	2.72
	140432	Directed	28	4	2	1	4.4
	135424	Non-Singing***	N/A	N/A	N/A	N/A	N/A
TOTALS	29		1298	266	98	45	197.194

Figure 1 Supplemental Table 1. Summary of behavioral data set for *in vivo* calcium imaging experiments. *Male did not sing despite having a female present. **Male was actively calling during this trial. ***Male did not sing despite being in the presence of a female, however, the bird does perform introductory notes.

Figures

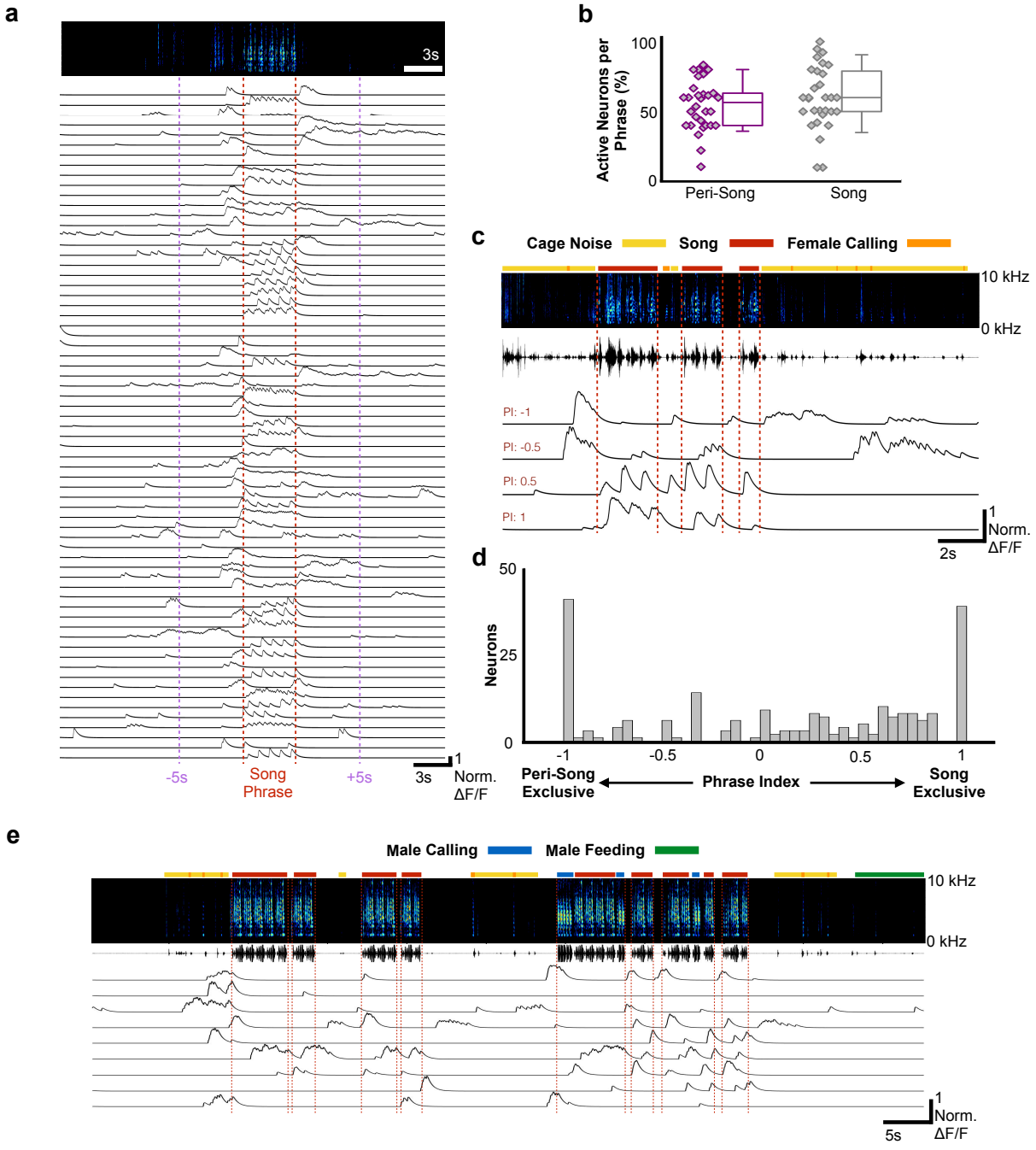

Figure 2. Most HVCRA neurons exhibit peri-song activity. a) Normalized calcium transients from 67 simultaneously recorded HVC_{RA} neurons during production of a song phrase. The red dashed lines delimit 5 consecutive motifs. **b)** Percentages of active neurons

during peri-song (54.3 ± 17.8 %, SD, purple) and song (59.9 ± 22.5 %, gray) are similar (30 phrases, t = -1.1, p = 0.29 paired two-sample t test). Box plots show the median, 25th and 75th percentiles with whiskers showing ±1.5 IQR. **c)** Sample neurons with diverse phrase indices ranging from -1 to 1 and their corresponding calcium traces during 6 motifs over 3 bouts. Dashed lines indicate bout onsets and offsets. Bars above spectrogram indicate the presence of cage noise related to hopping and wing flapping (yellow) or female calling (FC, orange). **d)** Histogram of phrase indices for all 223 neurons from 6 birds. **e)** Undirected song from a different male showing periods of cage noise or hopping behavior (yellow) and feeding behavior (green). Blue boxes indicate the male calling. Red dashed lines indicate onsets and offsets of song bouts.

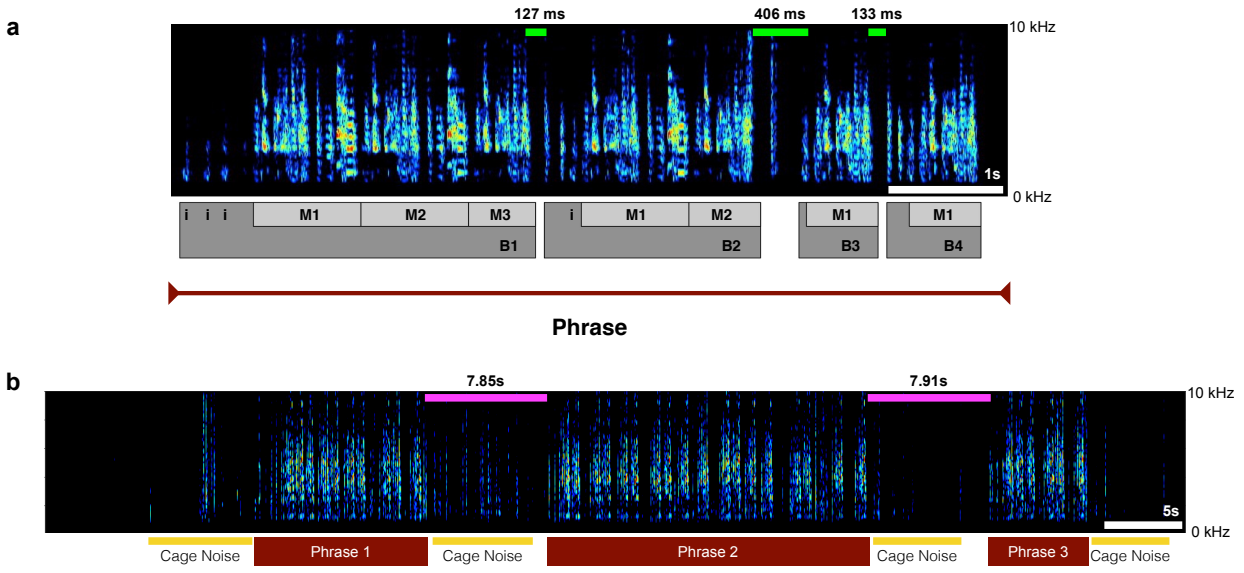

Figure 2 Supplement 1. a) A spectrogram of a single song phrase composed of 4 bouts and 7 motifs (Bout 1: 3 motifs, Bout 2: 2 motifs, Bout 3: 1 motif, Bout 4: 1 motif). Green bars on

top of spectrogram indicate representative silent periods between bouts and numbers above indicate duration in milliseconds. b) A spectrogram highlighting a trial where the bird sang 3 different phrases. The magenta bars above the spectrogram indicate silent periods between phrases and the numbers above indicate duration in seconds. Yellow bars below spectrogram indicate cage noise.

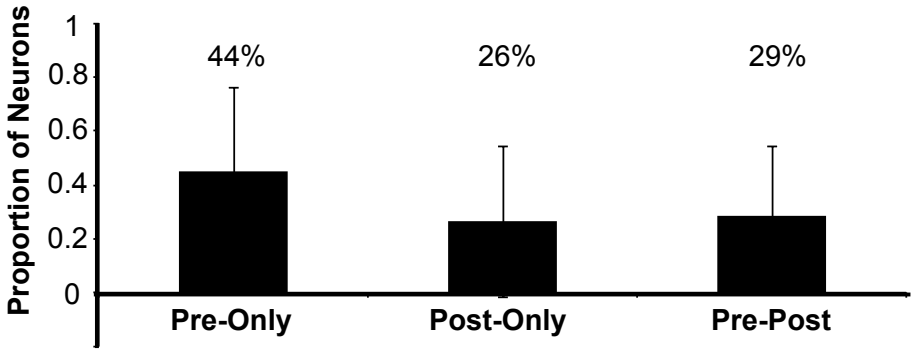

Figure 2 Supplement 2. Proportion of imaged neurons by bird (N = 6 birds, 197 neurons) that exhibited calcium events only before song onset calcium events (Pre-only, 0.44 ± 0.31, SD), only after song offset calcium events (Post-only, 0.26 ± 0.28), or were active before and after song (Pre-Post, 0.29 ± 0.25).

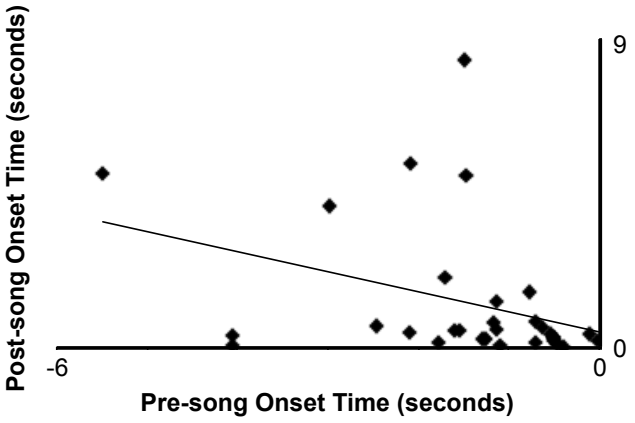

Figure 2 Supplement 3. 62 events (31 paired pre-song and post-song events) from 31 neurons from 6 birds. Showing a small positive correlation ($r^2 = 0.127$) between pre-song onset time to post-song onset time in cases where a neuron was active only once before and after singing.

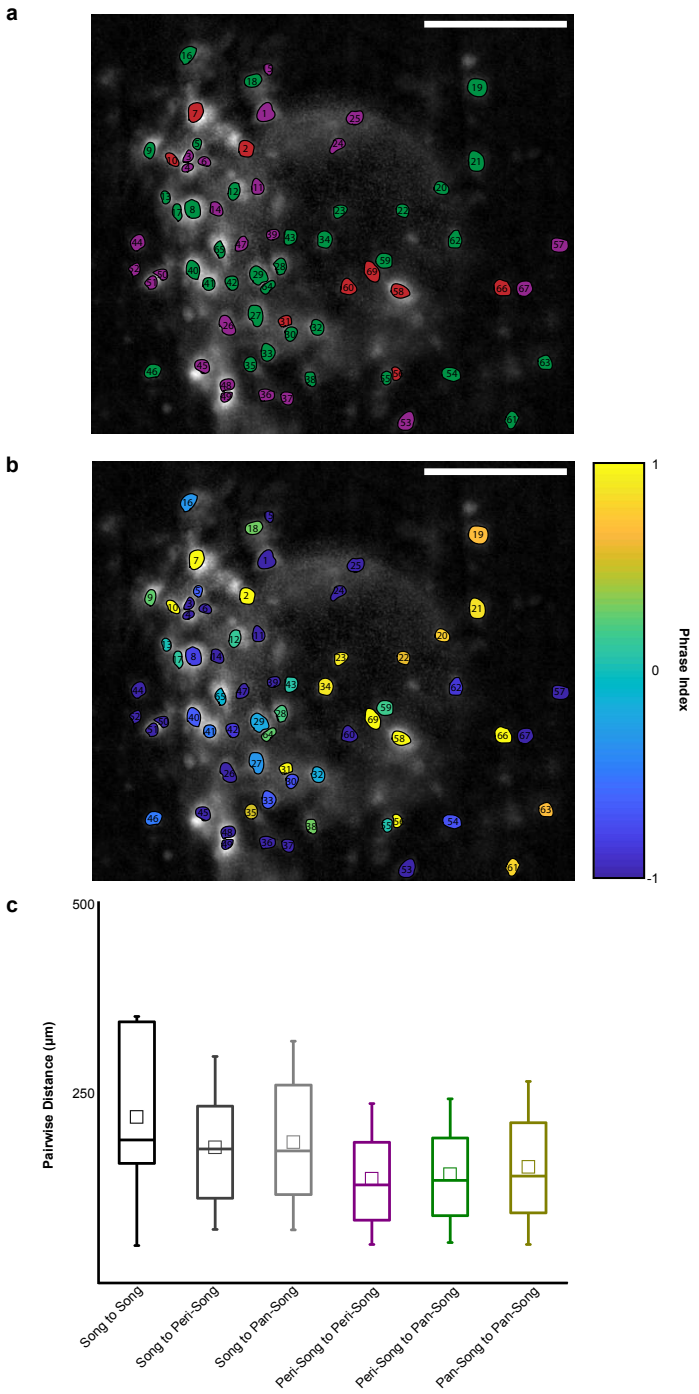

Figure 2 Supplement 4. a) FOV of ROIs identified in one exemplary bird (O262). Peri-song neurons are shown in purple, pan-song neurons are shown in green, and song neurons are shown in red. Scale bar is 100 micrometers. b) Same FOV as in a, but neurons are color coded by their phrase index. c) Euclidean distances between neurons shown in figure a. Distances (in micrometers) were calculated between the three functional neuron pools mentioned in this paper: peri-song neurons, pan-song neurons, and song neurons. Song-

song to peri-peri, p=0.02, song-song to peri-pan, p = 0.04, Mann-Whitney U Test. 2278 pairwise distances.

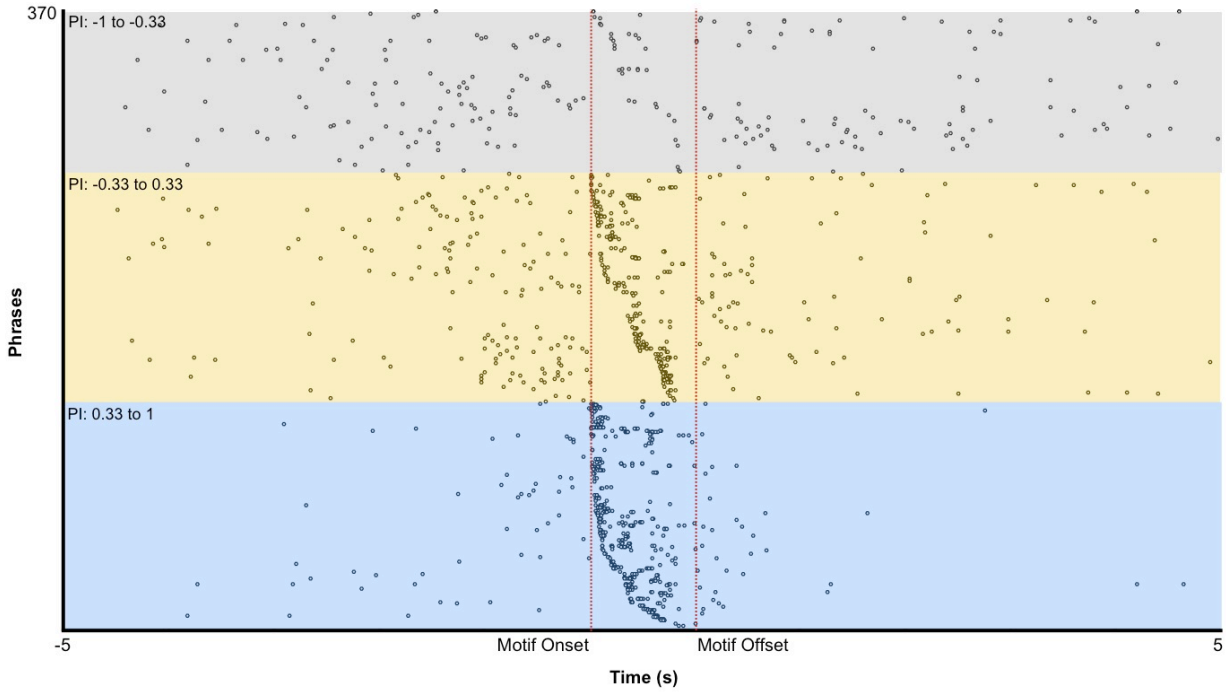

Figure 2 Supplement 5. Pan-song neuron events organized in tripartite groups according to phrase index. Within each subdivision neurons are organized by Motif onset times. 23 neurons are shown between -1 to -0.33. 56 neurons are shown between -0.33 to 0.33. 53 neurons are shown between 0.33 to 1.

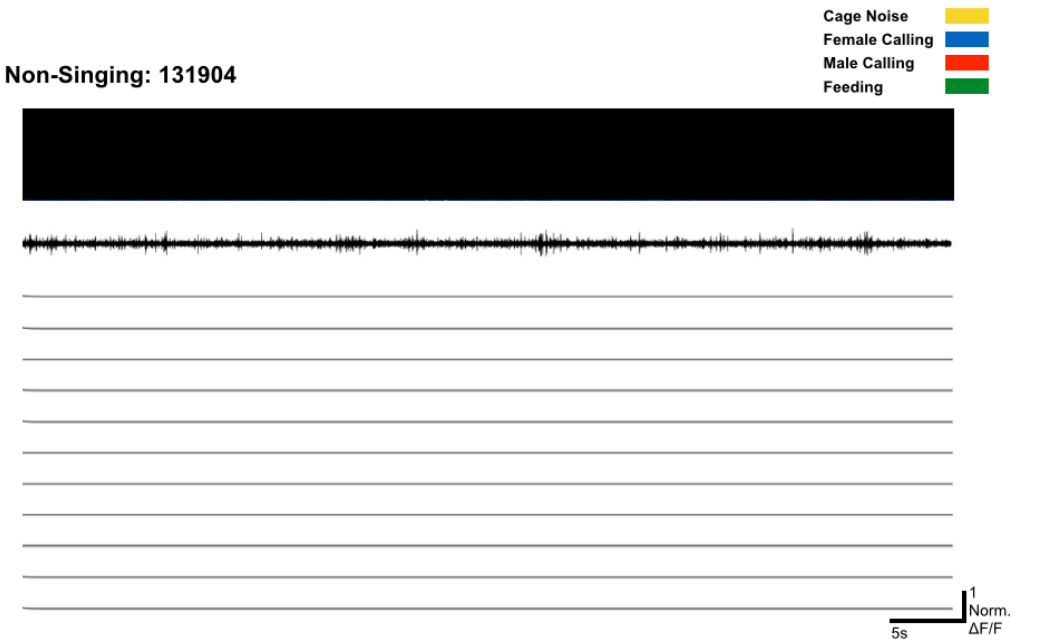
Cage Noise
Female Calling
Male Calling
Feeding
Non-Singing: 131904
1
Norm.
ΔF/F
5s
Directed Singing: 162201
1
Norm.
ΔF/F
5s
Directed Singing: 162048
1
Norm.
ΔF/F
5s

Figure 2 Supplement 6. Synchronized calcium traces for all available trials for one bird (O248) across directed, and non-singing behaviors. Bars above spectrograms indicate cage noise (yellow), female calling (blue), and male calling (red). Each trace under the spectrograms corresponds to different neurons but they are not necessarily the same neuron across the trials.

Directed Singing: 160046

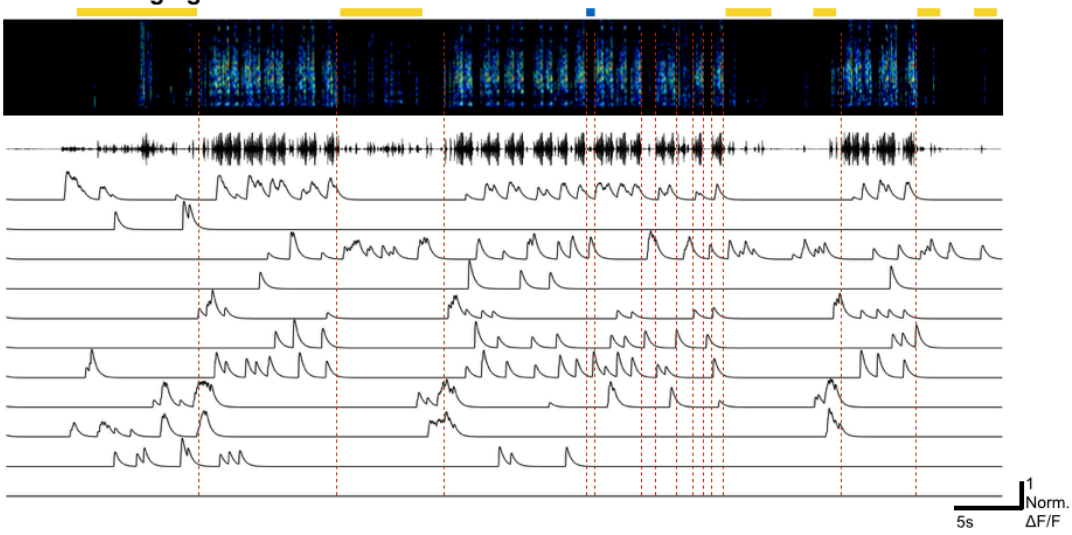

Directed Singing: 152940

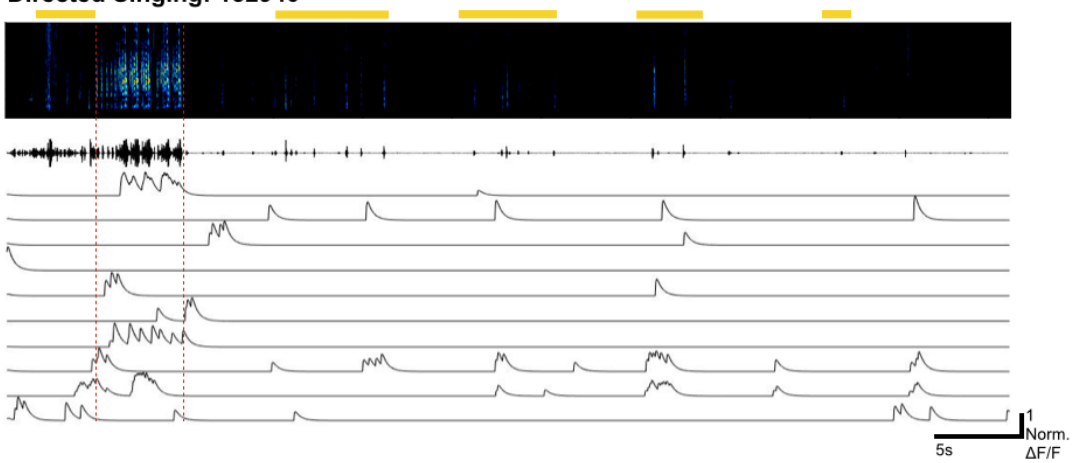

Undirected Singing:141059

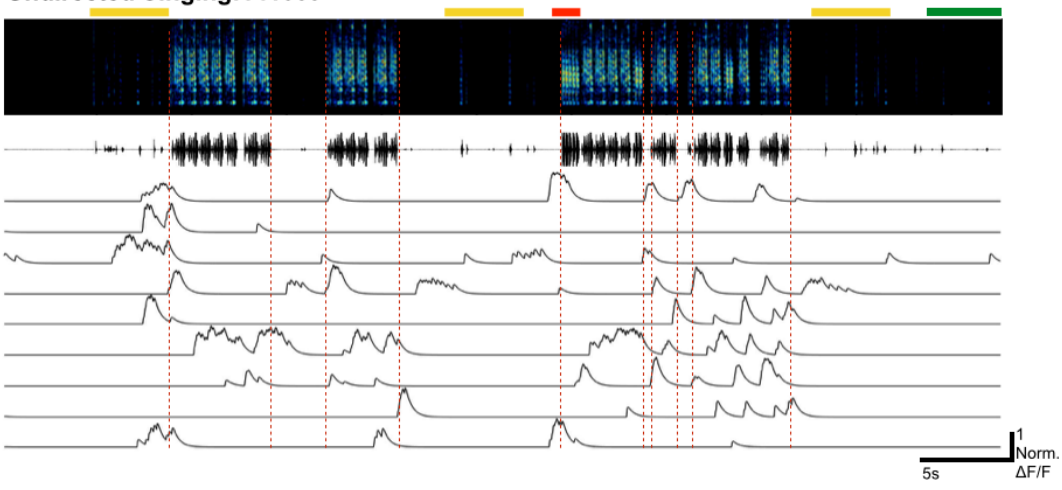

Figure 2 Supplement 6-2. Synchronized calcium traces for all available trials for one bird (O248) across directed and undirected. Bars above spectrograms indicate cage noise (yellow), female calling (blue), and male calling (red). Each trace under the spectrograms corresponds to different neurons but they are not necessarily the same neuron across the trials.

Undirected Singing: 141006

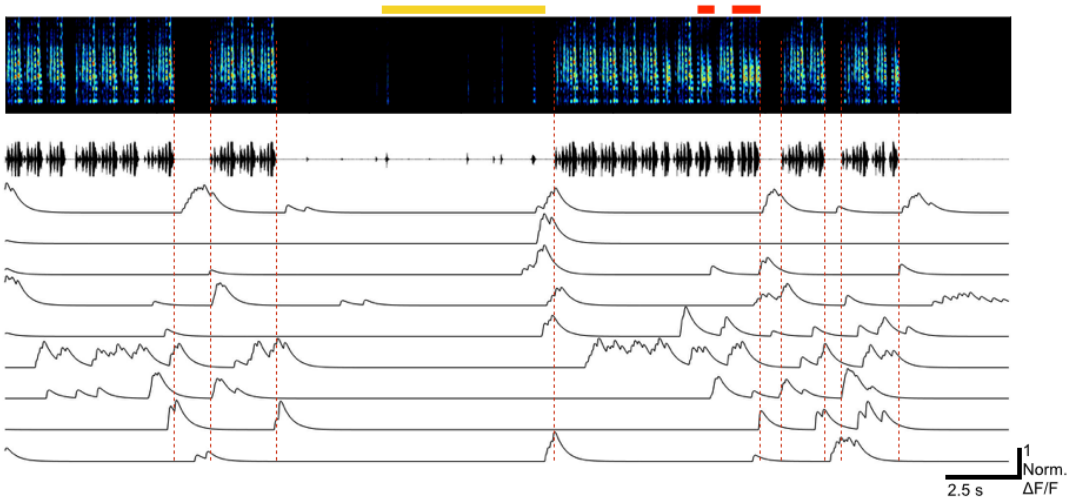

Undirected Singing: 140745

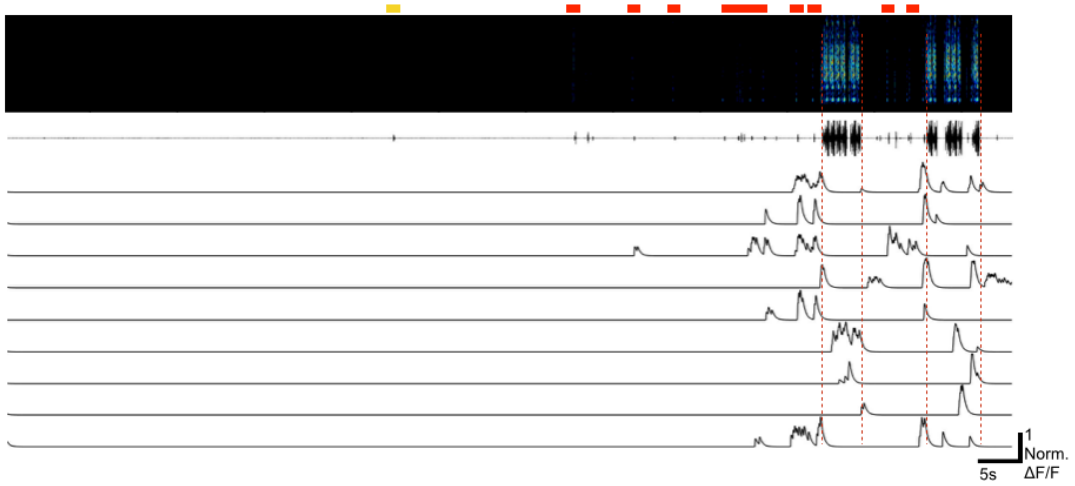

Undirected Song: 131612

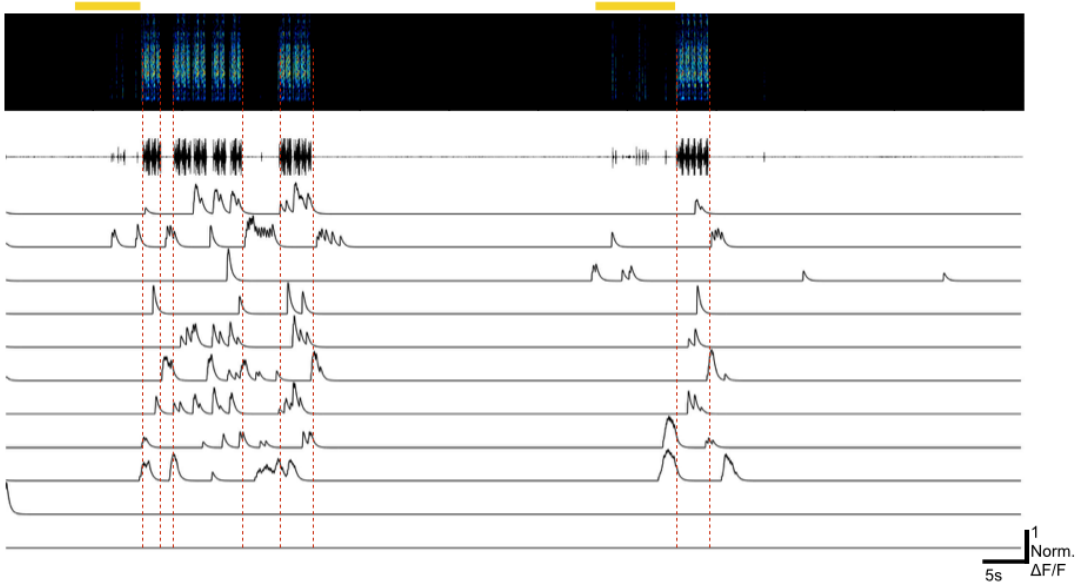

Figure 2 Supplement 6-3. Synchronized calcium traces for all available trials for one bird (O248) across undirected song. Bars above spectrograms indicate cage noise (yellow), female calling (blue), and male calling (red). Each trace under the spectrograms corresponds to different neurons but they are not necessarily the same neuron across the trials.

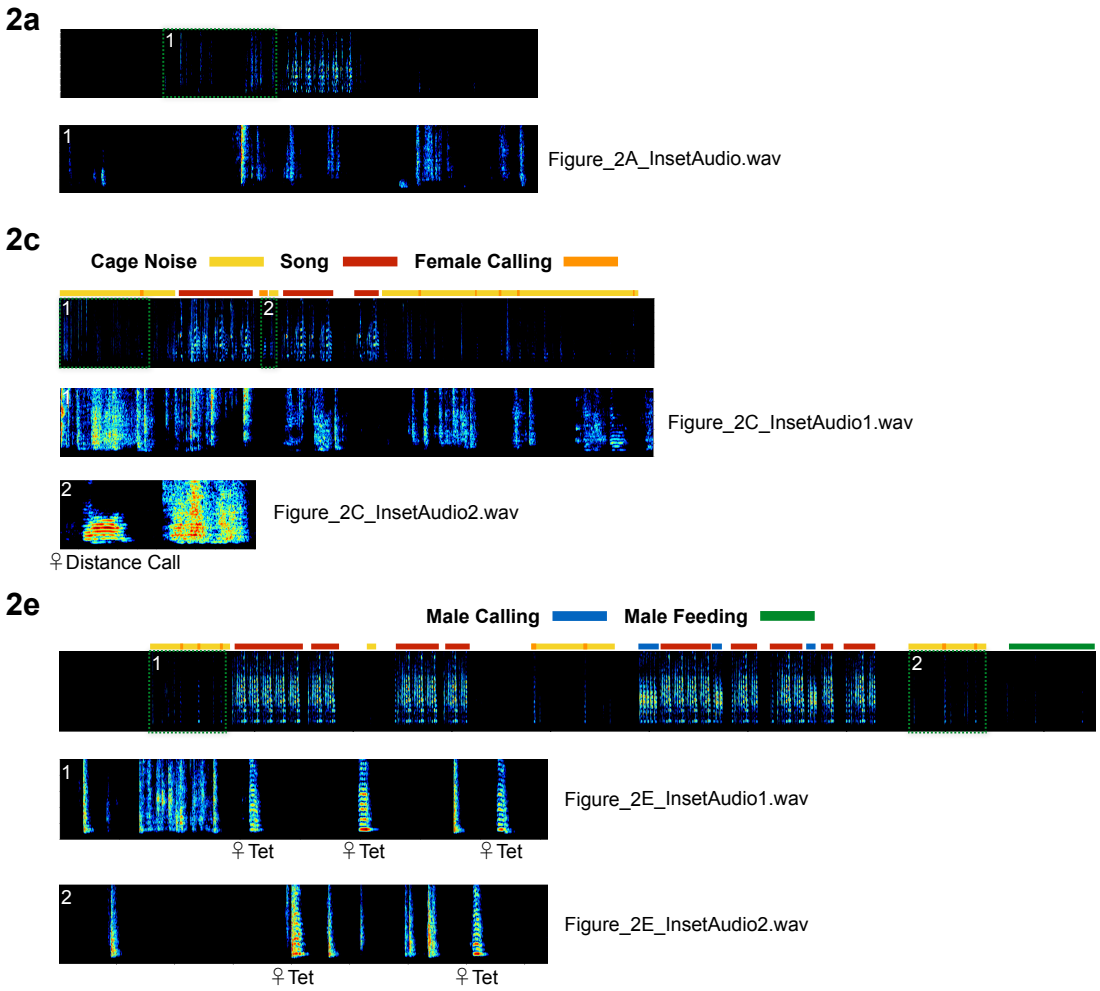

Figure 2 Supplement 7. Expanded insets showing where female calls occurred within the trials displayed in Figure 2.

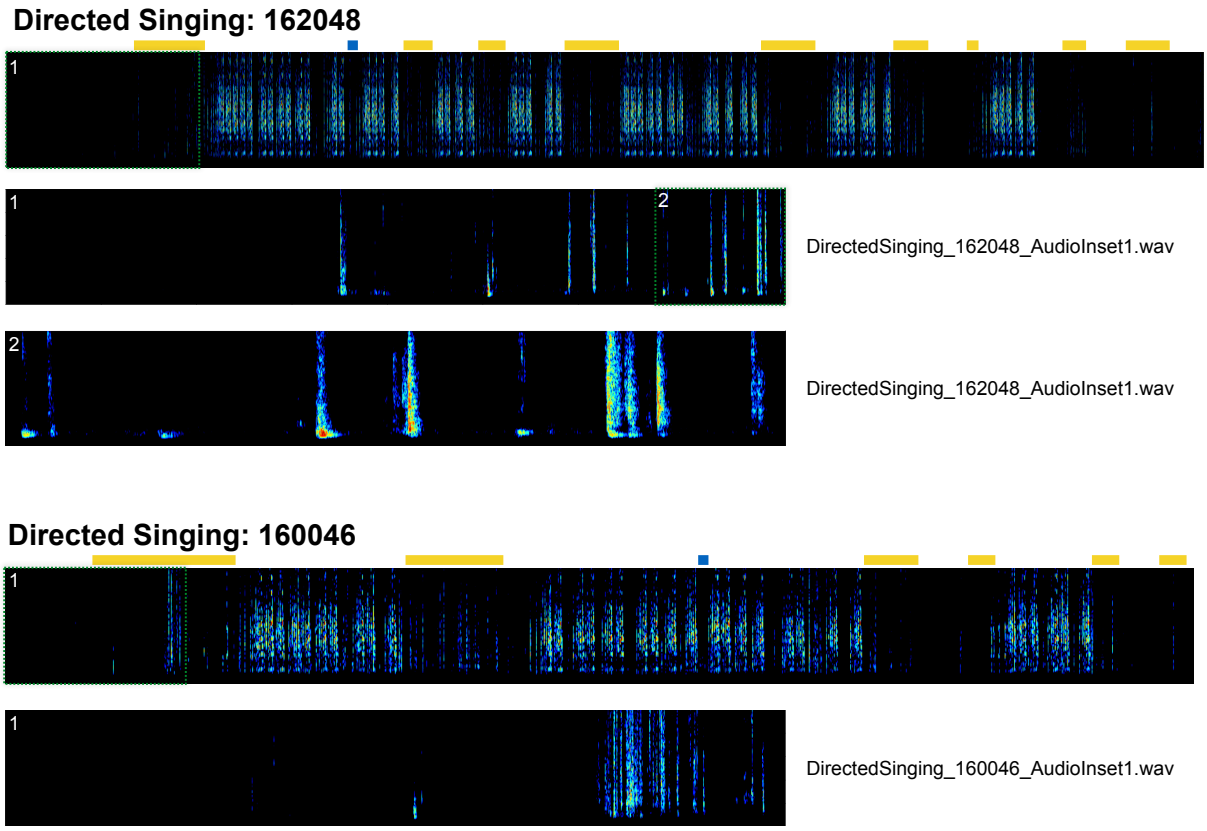

Figure 2 Supplement 8. Expanded insets showing where cage noise with no spectral structure in two directed song trials.

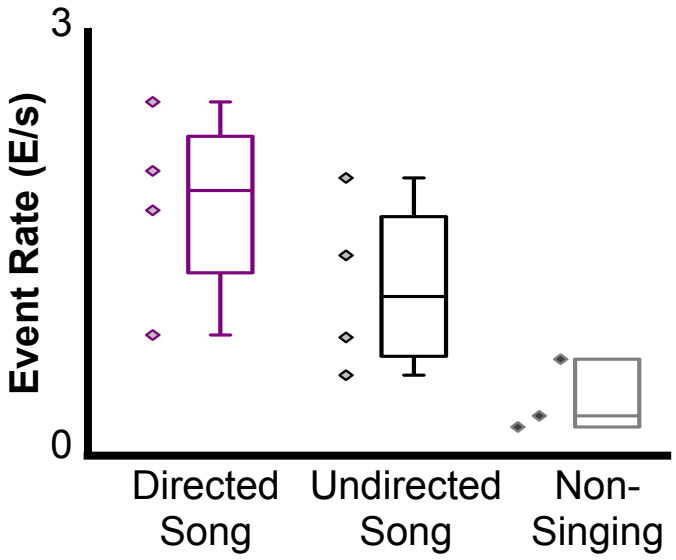

Figure 2 Supplement 9. a) Event rates for a bird during Directed (561 CEs, 1.67 ± 0.74 std), Undirected (252 CEs, 1.06 ± 0.66), and Non-Singing (53 CEs, 0.19 ± 0.27) periods of behavior (Directed song is significantly different from non-singing, $F(2,10) = 4.83$, $p < 0.05$). Each marker on the plot corresponds to a different trial. Event rate was calculated as the ratio of the number of events to the duration of the trial.

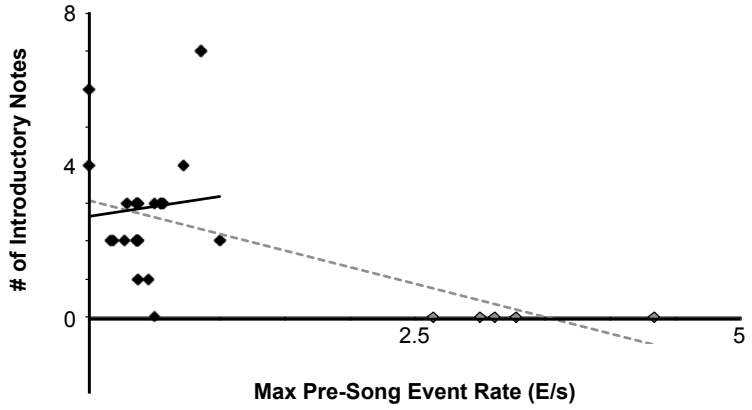

Figure 2 Supplement 10. Comparison between maximum pre-song event rate to the number of introductory notes prior to motif onset across 5 birds (Mean Event Rate = 0.91 E/s, Mean Introductory notes = ~2). 1 bird did not have any introductory notes during the imaged trials.

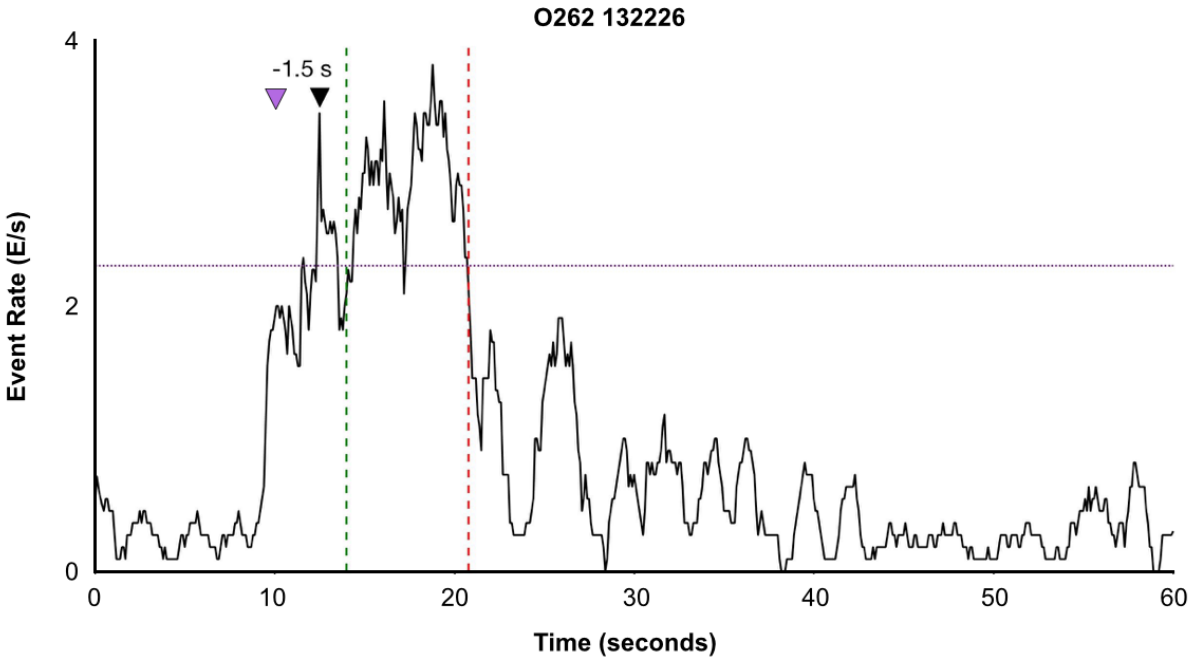
O262 132226
-1.5 s
Event Rate (E/s)
Time (seconds)
0
2
4
0
10
20
30
40
50
60

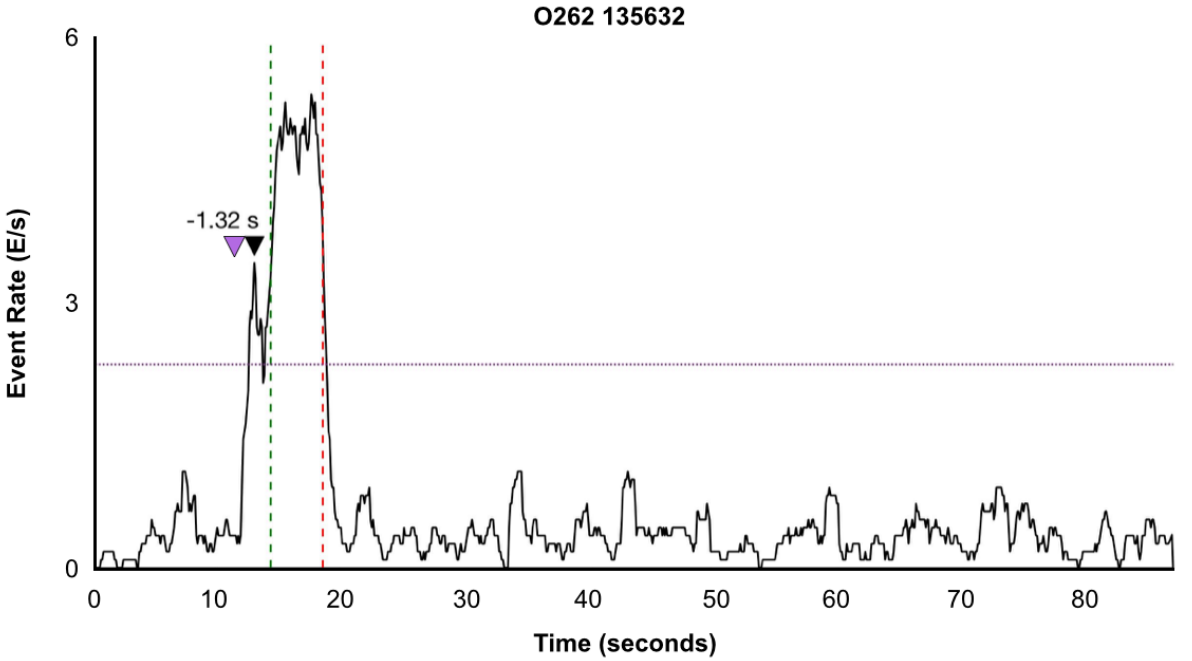
O262 135632
-1.32 s
Event Rate (E/s)
Time (seconds)
0
3
6
0
10
20
30
40
50
60
70
80

Figure 2 Supplement 11. Event rate calculated across the full length of 5 trials for 1 bird (O262). Event rate was calculated by first binning calcium onsets in 100ms bins and smoothing with a 1 second moving window. Green dashed line indicates onset of song phrase and red dashed line indicates offset of song phrase. Purple (horizontal) line indicates 2/3s of the maximum value during the pre-song period. Black arrow with time marks maximum peak song event rate. Magenta arrow indicates when female was introduced. Asterisk indicates onset of short call.

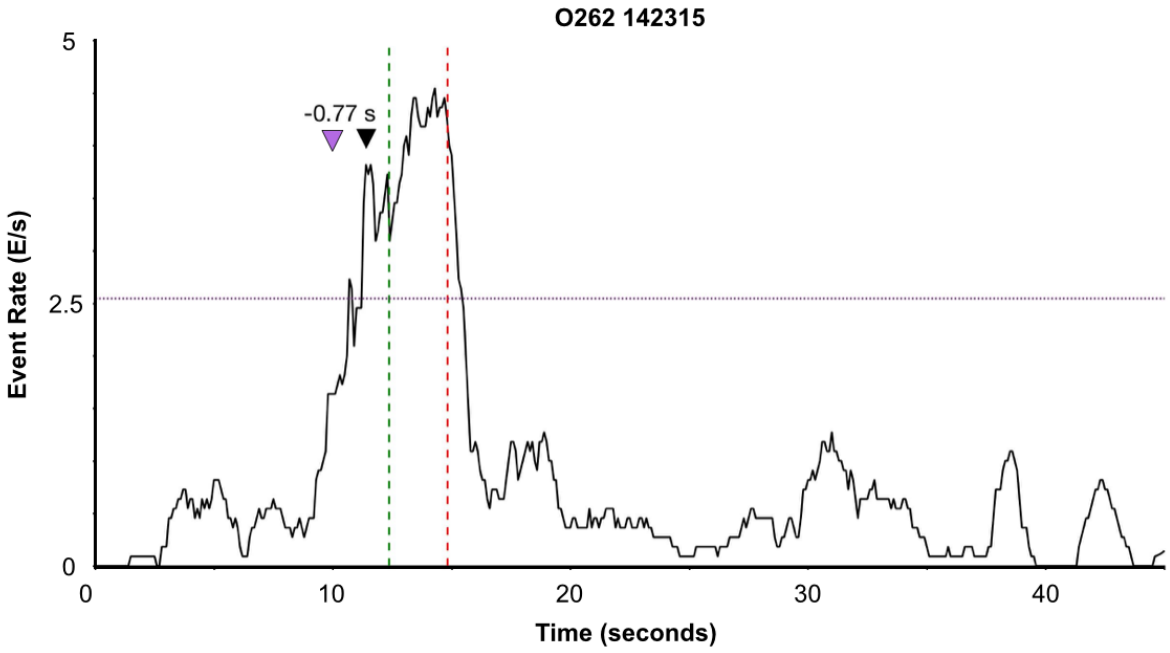
O262 142315
-0.77 s
Event Rate (E/s)
Time (seconds)
0
2.5
5
0
10
20
30
40

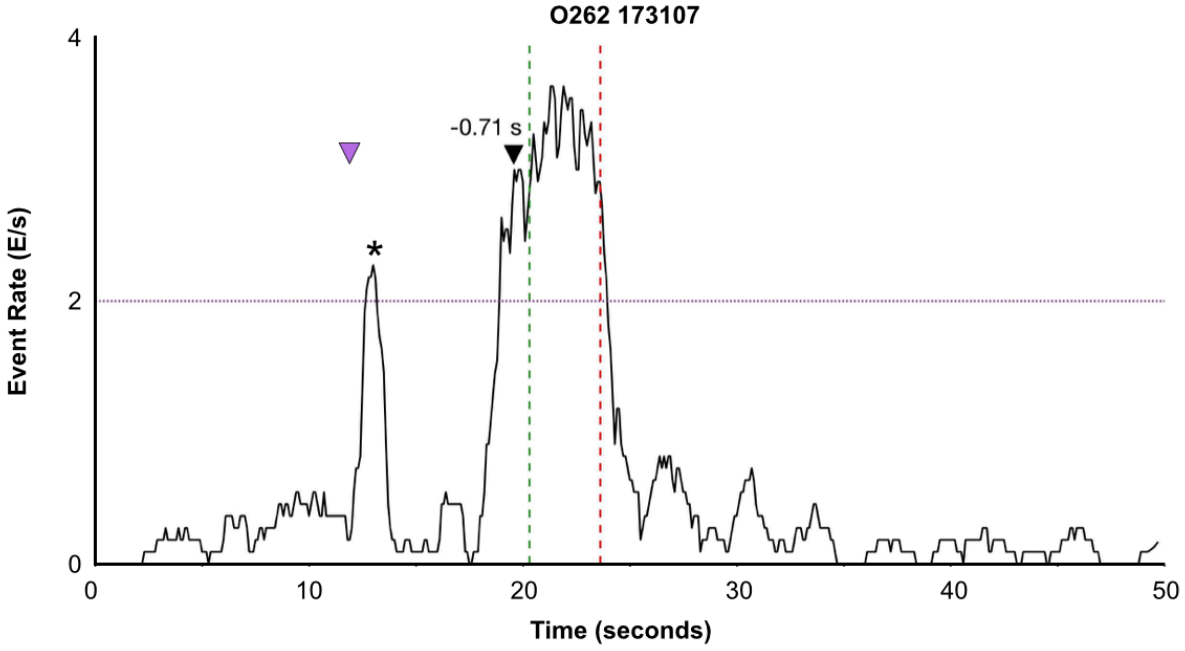
O262 173107
-0.71 s
*
Event Rate (E/s)
Time (seconds)
0
2
4
0
10
20
30
40
50

Figure 2 Supplement 11-2. Event rate calculated across the full length of 5 trials for 1 bird (O262). Event rate was calculated by first binning calcium onsets in 100ms bins and smoothing with a 1 second moving window. Green dashed line indicates onset of song phrase and red dashed line indicates offset of song phrase. Purple (horizontal) line indicates 2/3s of the maximum value during the pre-song period. Black arrow with time marks maximum peak song event rate. Magenta arrow indicates when female was introduced. Asterisk indicates onset of short call.

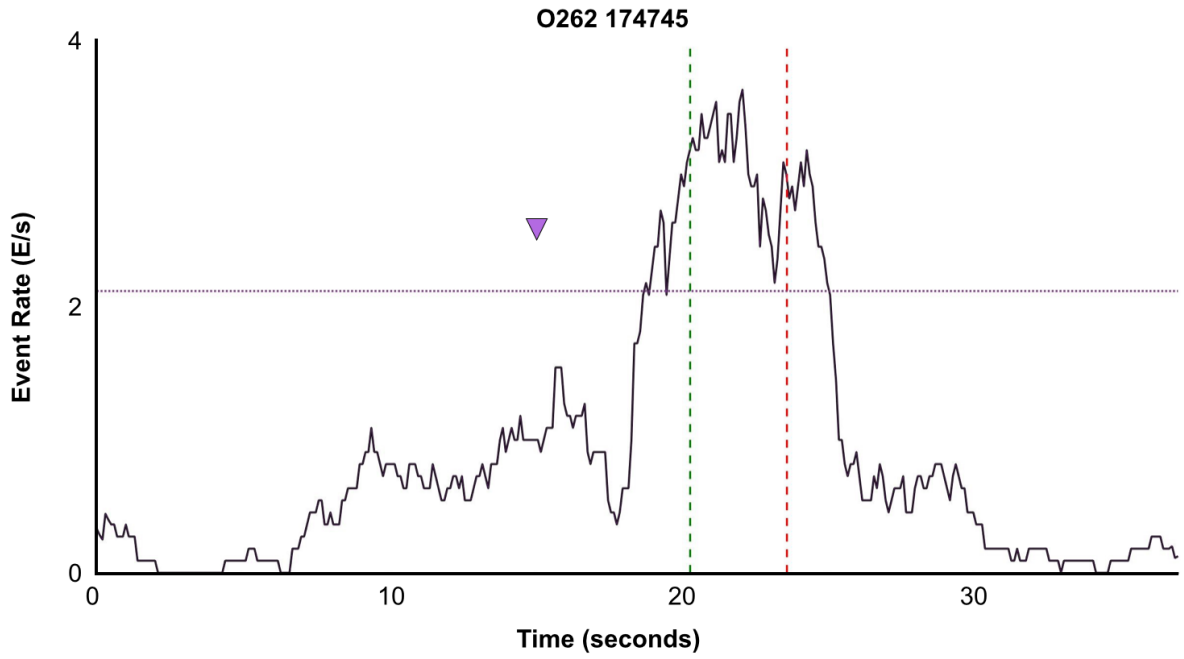

Figure 2 Supplement 11-3. Event rate calculated across the full length of 5 trials for 1 bird (O262). Event rate was calculated by first binning calcium onsets in 100ms bins and smoothing with a 1 second moving window. Green dashed line indicates onset of song phrase and red dashed line indicates offset of song phrase. Purple (horizontal) line indicates 2/3s of the maximum value during the pre-song period. Black arrow with time marks maximum peak song event rate. Magenta arrow indicates when female was introduced. Asterisk indicates onset of short call.

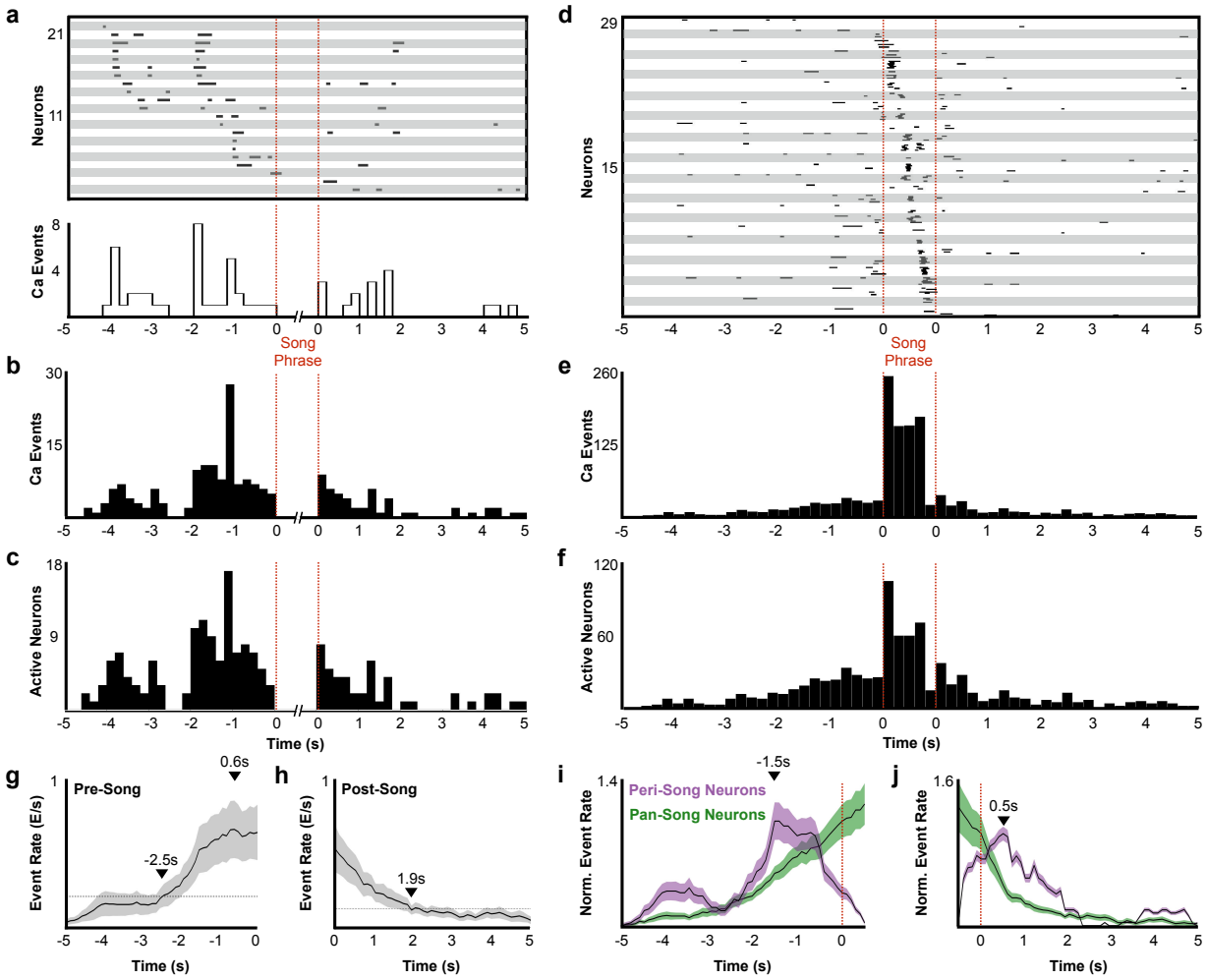
a
Neurons
21
11
Ca Events
8
4
-5 -4 -3 -2 -1 0 0 1 2 3 4 5
Song
Phrase
b
Ca Events
30
15
c
Active Neurons
18
9
Time (s)
d
Neurons
29
15
e
Ca Events
260
125
f
Active Neurons
120
60
Time (s)
g
Pre-Song
Event Rate (E/s)
1
0.6s
-2.5s
Time (s)
h
Post-Song
Event Rate (E/s)
1
1.9s
Time (s)
i
Norm. Event Rate
1.4
-1.5s
Peri-Song Neurons
Pan-Song Neurons
Time (s)
j
Norm. Event Rate
1.6
0.5s
Time (s)

Figure 3. Description of peri-song and pan-song neuron activity. a) 21 peri-song neurons from one bird singing 3 bouts containing 6 motifs (1st bout: 3 motifs; 2nd bout: 2 motifs; 3rd bout: 1 motif, the dashed red lines indicate the onset and offset of the three bouts). Each row shows song-aligned calcium events (CEs N=54 CEs; average rise time = 0.18 ± 0.09 s SD). The shaded horizontal bars separate different neurons. One CE is seen to overlap with the beginning of the song phrase. The onset time for this event is 170 ms before song, but the rise time is slow and extends to 100 ms after song onset. Below the CE raster plot is a peri-event histogram with the event rate in 200 ms bins shown for the trial above. **b)** Song-aligned CEs in peri-song neurons 5 s before and after phrase onset (41 neurons, 190 CEs). The activity rate peaks ~1.2 s before phrase onset. **c)** The number of active peri-song neurons in 200 ms bins before and after phrase onset (41 neurons, 169 CEs). **d)** Song-aligned activity of pan-song neurons (same trial as shown in panel **a**, N=29 neurons, 253 CEs). **e)** Peri-event histogram of pan-song neurons (143 neurons, 1,333 CEs). **f)** The number of active pan-song neurons in 200 ms bins (143 neurons, 853 CEs). **g)** Pre-phrase event rate for all pan-song neurons. The event rate was calculated by counting event onsets in 100 ms bins and then smoothed with a 1 second moving window. 28 trials are shown from 5 birds, the black line indicates the average event rate. The black triangles mark the peak event rate occurring 0.6 s before song onset and 2.5 s when the event rate reaches 3 SD above the baseline event rate, respectively. Baseline event rate was determined by measuring the average event rate from -5 to -4 seconds before song onset. Shaded region indicates standard deviation. **h)** Post-phrase event rate for all neurons. 27 trials are shown from 5 birds. The black triangles mark when the event rate reaches 3 SD above the baseline event rate. Baseline event rate was determined by measuring the average event rate during -5 to -4 seconds before song onset. **i)** Pre-phrase event rate for peri-song and pan-song neurons calculated as calcium events in moving 1 s windows. The black line indicates average event rate. The black triangle indicates peak event rate occurring 1.5 s before phrase onset. **j)** Same as **i**, but post-phrase event rates for peri-song and pan-song neurons. The black triangle indicates peak event rate occurring 0.5 s after phrase offset.

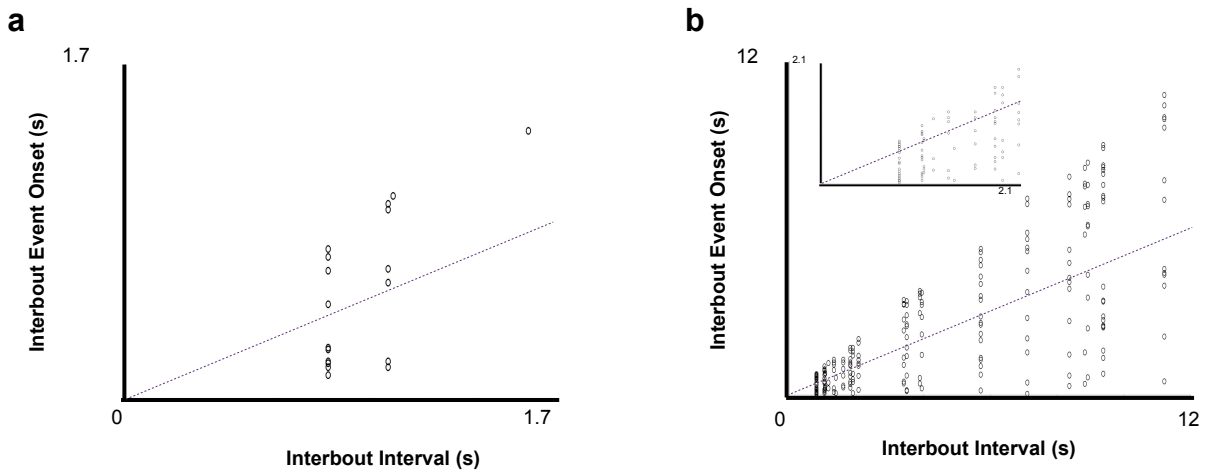

Figure 3 Supplement 1. a) Inter-bout events for peri-song neurons (N = 27 events, each event was aligned to the end of the previous bout). Dashed line indicates midway point between start of next bout and end of previous bout. These events were excluded from the analysis shown in Figure 3. b) Same as A but for pan-song neurons (N= 231 events). The inset shows a zoomed in portion of events occurring during Interbout Intervals less than 2 seconds. These events were excluded from the analysis shown in Figure 3.

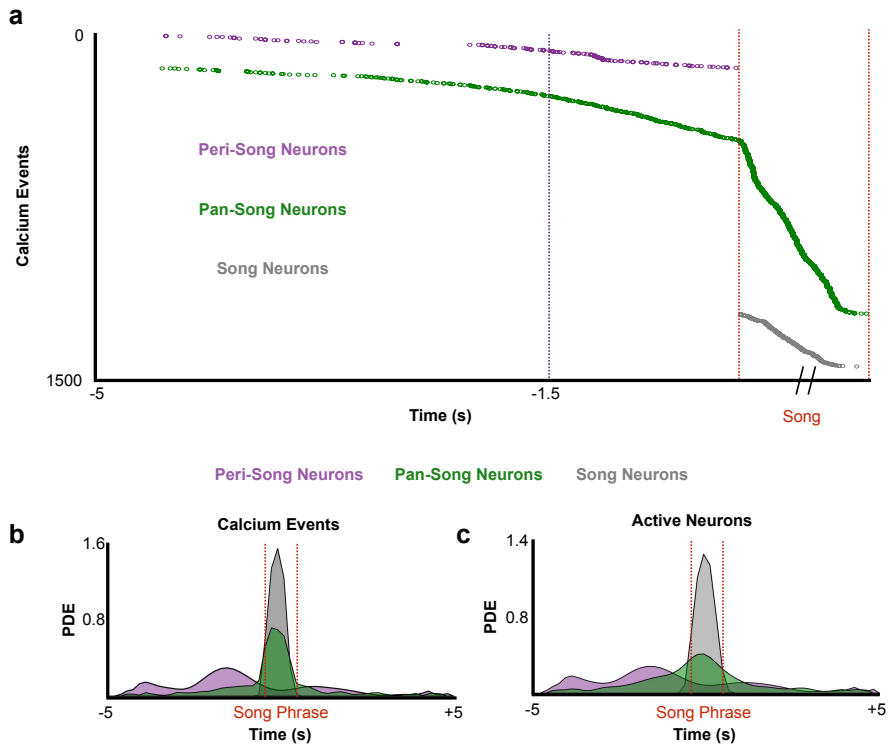

Figure 3 Supplement 2. **a)** Cumulative calcium event onset times across all birds and all trials. Time corresponding to peak event rate for peri-song neurons is shown (magenta line, 1.5 s). **b)** Probability density estimates of calcium events organized by neuron type. (pan-song neurons: 1,333 CEs, 143 neurons from 6 birds; peri-song neurons: 190 CEs, 41 neurons from 3 birds). **c)** Same as **b** but for active neurons (pan-song neurons: 853 CEs, 143 neurons, 5 birds; peri-song neurons: 169 CEs, 41 neurons, 3 birds).

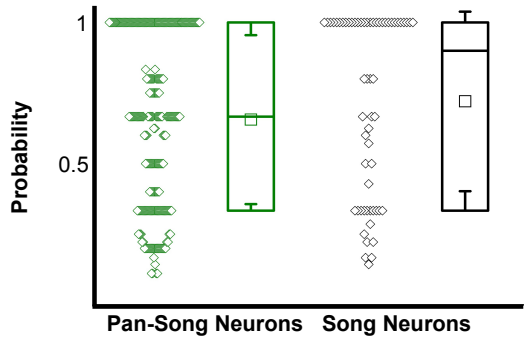

Figure 3 Supplement 3. Comparison of the probability of pan-song neuron and song neuron events occurring during a motif (Kolmogorov-Smirnov test, n.s., $p > 0.05$; song neurons P(motif) = 0.72 ± 0.32, pan-song neurons P(motif) = 0.66 ± 0.29). Bouts consisting of a minimum of 2 motifs where the neuron was active during at least one of those motifs were used to calculate the probability (29 bouts had greater than 1 motif out of a possible 32 bouts; 28 song neurons; 132 pan-song neurons). Probability was calculated at the bout level for each neuron, probabilities across different bouts were treated as independent variables.

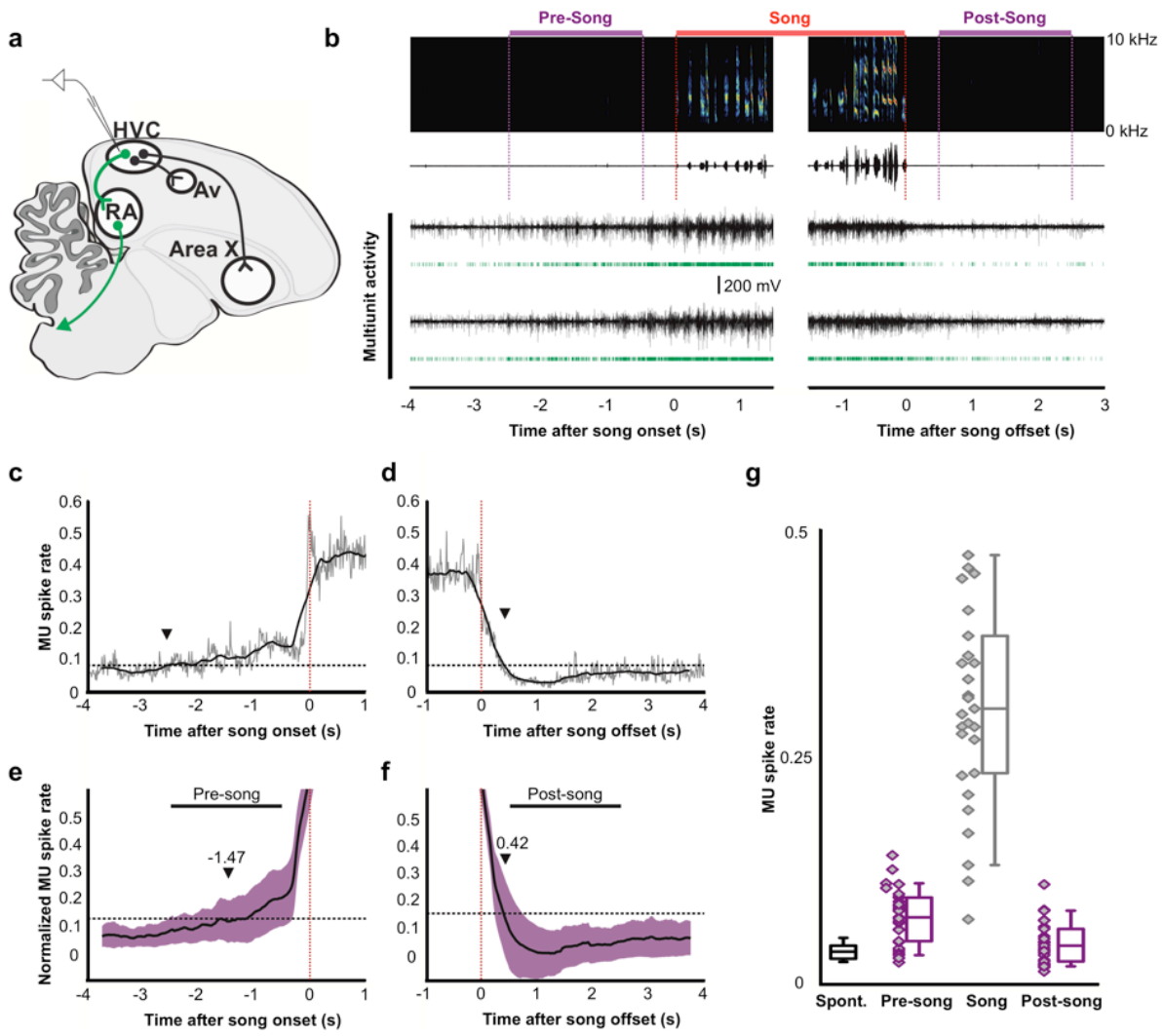
a
HVC
Av
RA
Area X
b
Pre-Song
Song
Post-Song
10 kHz
0 kHz
Multiunit activity
200 mV
Time after song onset (s)
Time after song offset (s)
c
MU spike rate
Time after song onset (s)
d
Time after song offset (s)
e
Pre-song
-1.47
Normalized MU spike rate
Time after song onset (s)
f
Post-song
0.42
Time after song offset (s)
g
MU spike rate
Spont.
Pre-song
Song
Post-song

Figure 4. Pre-song and post-song firing in HVC of Bengalese finches. a) Schematic of recording site. **b)** An example of song initiation and termination (dashed lines indicate phrase onset and offset, pre and post-song period marked in purple and song marked in red) and simultaneously recorded HVC multiunit activity on two electrodes (channels #4 and #15, bird p15o56). Green raster plots represent detected spikes on the two electrodes. **c,d)** Phrase onset (c) and offset (d) related average multiunit activity obtained from an example electrode channel (vertical dashed lines indicate phrase onset and offset, respectively). The spike rate was averaged across multiple song onsets or offsets and was first calculated in 10 ms bins (gray thin line) and then smoothed with a 500 ms window (bold line). Upper and lower horizontal dotted lines show mean spike rates during singing and baseline, respectively. Arrowheads indicate onset (c) and offset (d) timings of spike rate, as assessed by crossing of a pre-defined threshold (red line). **e,f)** Normalized multiunit activity related to phrase onset (e) and offset (f). Before averaging, the spike rate trace of each electrode channel was normalized such that 0 corresponds to the mean rate during baseline and 1.0 to the mean rate during singing (see Method). The bold line shows an average across all electrodes and birds (n = 29 channels). Purple area indicates ± one SD. Arrowheads show mean onset (e) and offset (f) timing of pre-song and post-song activity, respectively. **g)** Mean multiunit spike rates during spontaneous (black), pre-song (purple with diamonds), song (gray with diamonds), and post-song (purple with diamonds) periods. Pre-song and post-song periods are indicated by the horizontal bars in panels e and f. Box plots show the median, 25^{th} and 75^{th} percentiles with whiskers showing ±1.5 IQR.

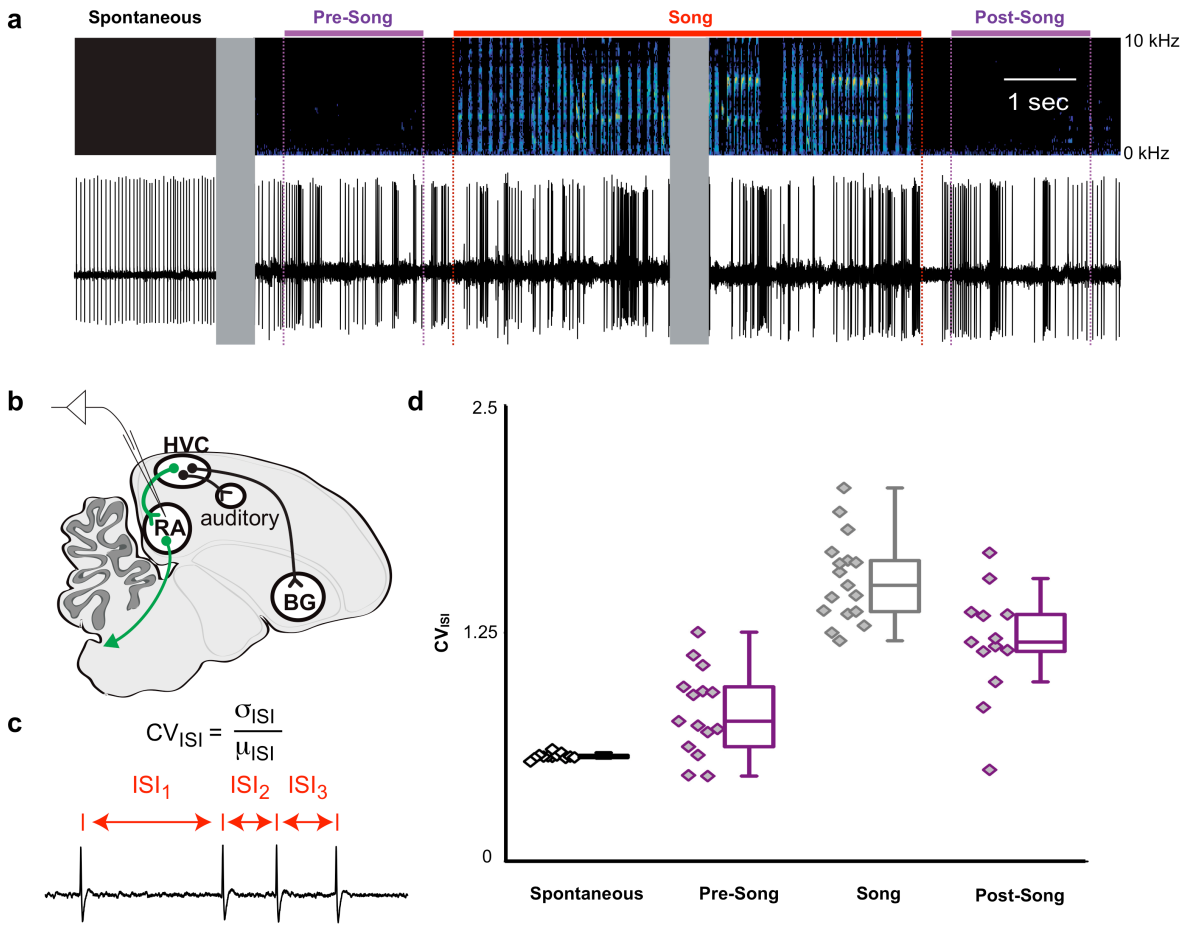

Figure 5. a) Example extracellular recording from a single RA neuron. Colored lines highlight four epochs (pre-song (purple), song (red), and post-song (purple)) relative to the beginning and ending of a song phrase (see main text). Grey areas indicate discontinuities in time (pauses between "spontaneous" epoch and song initiation and within the middle portion of the song bout). **b)** Schematic of recording site. **c)** We quantified inter-spike-intervals (ISIs) and computed the coefficient of variation (CV) in each epoch. **d)** We found significantly higher ISI variability in the pre-song epoch (purple with diamonds) compared to spontaneous (p<0.005, two-sided K-S test). Box plots show the median, 25th and 75th percentiles with whiskers showing ±1.5 IQR.

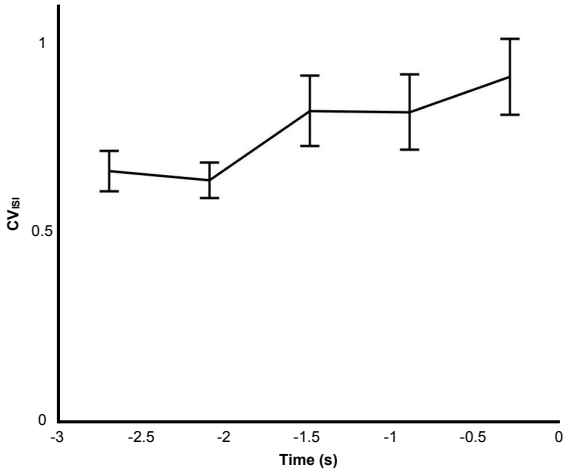

Figure 5 Supplement 1. Pre-song changes in CV_{ISI} in 600ms bins from single units in the RA of Bengalese finches singing undirected song. There is a significant difference in spiking variability when comparing the first bin (-3 to -2.5s) to the last bin before song onset (-0.5 to 0s, Kolmogorov-Smirnov test, $p = 0.023$).

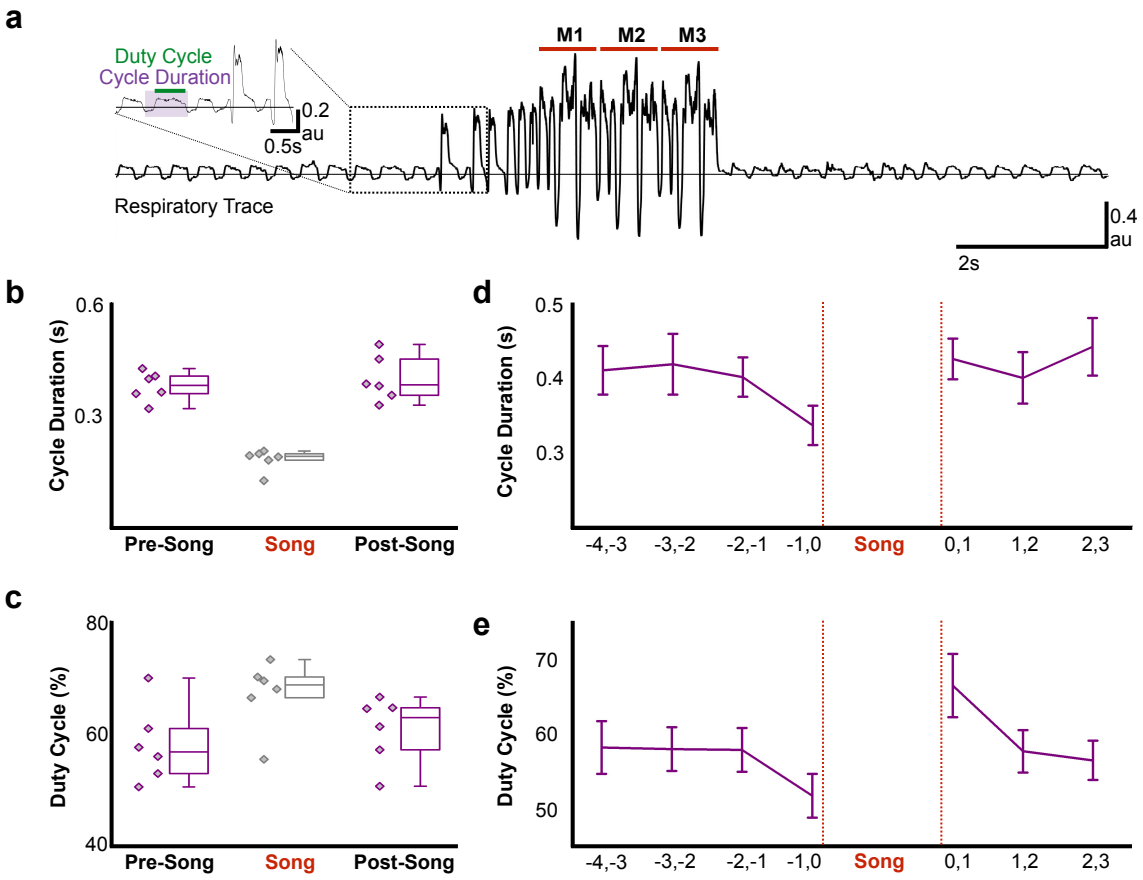

Figure 6. Air sac pressure recording in zebra finches. a) Waveform of pressure changes during non-singing and singing periods. Waveforms above the horizontal line (suprambient pressurization) indicate expiration and below the line (subatmospheric pressurization) indicate inhalation. Song start was identified by the presence of introductory notes preceeding the song phrase. M1-3 corresponds to three repetitions of the bird's motif. Inset illustrates measurements for respiratory cycle duration and duty cycle (% time in expiration) and the first two introductory notes. **b)** Respiratory cycle duration and **c)** duty cycle of expiratory phase before (Pre), during (Song), and after (Post) song production (N = 6 birds). **d)** Plots of average respiratory cycle durations and **e)** duty cycles during pre-song and post song periods (N = 6 birds). Longer duty cycles correspond to increased periods of expiration. Data in panels b-e is derived from the same 6 birds.

Methods

Key Resources Table 4

Reagent type (species) or resource	Designation	Source or reference	Identifiers	Additional information
strain, strain background (adeno-associated virus)	AAV9.CMV.HI.eGFP-Cre.WPRE.SV40	James M. Wilson	Addgene viral prep # 105545-AAV9; http://n2t.net/addgene:105545 ; RRID:Addgene_105545	
strain, strain background (adeno-associated virus)	AAV9.CAG.Flex.GCaMP6s.WPRE.SV40	Chen et al., 2013	Addgene viral prep # 100842-AAV9; http://n2t.net/addgene:100842 ; RRID:Addgene_100842	
strain, strain background (adeno-associated virus)	AAV9.CAG.GCaMP6s.WPRE.SV40	Chen et al., 2013	Addgene viral prep # 100844-AAV9; http://n2t.net/addgene:100844 ; RRID:Addgene_100844	
commercial assay or kit	Miniature Microscope	Inscopix	https://www.inscopix.com/nvista	
software, algorithm	Matlab	Mathworks	http://www.mathworks.com/products/matlab/; RRID:SCR_001622	
software, algorithm	Calcium Analysis	Peters et al., 2014		
software, algorithm	CNMF	Pnevmatikakis et al., 2016	https://github.com/epnev/ca_source_extraction	

Software and Data Availability

All custom analysis codes and calcium imaging data are publically available as a Github repository. https://github.com/TRobertsLab/HVCRA_PreparatoryActivityData

Animals

Experiments described in this study were conducted using adult male zebra finches and Bengalese finches (>90 days post hatch). During experiments, birds were housed individually in sound-attenuating chambers on a 12/12 h day/night schedule and were given ad libitum access to food and water. All procedures were performed in accordance with established protocols approved by Animal Care and Use Committee's at UT Southwestern Medical Centers, Texas Christian University, Emory University, and the Korea Brain Research Institute.

Defining Song and Peri-Song Behavior

Zebra finch song is composed of a song motif which contains a stereotyped set of song syllables. The song motif is often produced two or more times in immediate succession – this is referred to as a song bout. Song bouts are often preceded by one or more introductory syllables. When a bird strings together more than one song bout, this is referred as a song phrase. In this study we defined song bouts separated by less than 2 seconds of silence as being part of a single song phrase, while any singing following silent gaps greater than two seconds from the last song phrase were considered as the beginning of a new song phrase. For analysis of pre-song activity we only analyzed data in which birds were not singing for a minimum of 5 seconds prior to production of their first introductory note or song motif. For analysis of post-song activity we only analyzed data from birds that did not engage in further singing for a minimum of 5 seconds following production of the last syllable in their song phrase or bout.

Viral Vectors

The following adeno-associated viral vectors were used in these experiments: AAV2/9.CAG.Flex.GCaMP6s.WPRE.SV40 (University of Pennsylvania Vetor Core; Addgene Catalog #: 100842-AAV9), AAV2/9.CMV.EGFP.Cre.WPRE.SV40 (University of Pennsylvania Vector Core; Addgene Catalog #: 105545-AAV9) and AAV2/9.CAG.GCaMP6s.WPRE.SV40 (University of Pennsylvania Vector Core; Addgene Catalog #: 100844-AAV9). All viral vectors were aliquoted and stored at -80°C until use.

Imaging Equipment

Head-mounted miniaturized fluorescent microscopy in freely behaving singing birds was conducted with an nVista system (Inscopix). Two-photon microscopy was conducted with a commercial microscope (Ultima IV, Bruker) running Prairie View software using a 20x (1.0 NA) objective (Zeiss) with excitation at 920 nm (Mai Tai HP DS, Newport). Two-photon and initial single photon imaging was conducted in lightly anesthetized head-fixed animals. Two-photon and single-photon images of HVC were acquired through the cranial window using a sCMOS camera (QImaging, optiMOS) and these images were used to guide placement of the baseplate for the miniaturized single-photon microscope (Inscopix). CAD files for head holders and stereotaxic devices are available upon request.

Stereotaxic Surgery

All surgical procedures were performed under aseptic conditions. Birds were anesthetized using isoflurane inhalation (~1.5-2%) and placed in a stereotaxic apparatus. Viral

injections were performed using previously described procedures (Roberts et al., 2012, 2017) at the following approximate stereotaxic coordinates relative to interaural zero and the brain surface (rostral, lateral, depth, in mm): HVC (0, 2.4, 0.1-0.6); and RA (-1.0, 2.4, 1.7-2.4). The centers of HVC and RA were identified with electrophysiology. For calcium imaging experiments, 1.0 – 1.5 μL of Cre-dependent GCaMP6s was injected at 3 different sites into HVC and 350 nL of Cre was injected into RA. Viruses were allowed to express for a minimum of 6 weeks before a cranial window over HVC was made.

Cranial Windowing, Imaging and Baseplate Implantation

Briefly, a unilateral square craniotomy (~3.5 x 3.5 mm) was created over HVC and the dura was removed. A glass coverslip was cut to match the dimensions of the craniotomy and held in place with a stereotaxic arm as Kwik Sil was applied to the edges of the cranial window. Dental acrylic was applied over the Kwik Sil and allowed to slightly overlap with the glass coverslip to ensure the window would not move and would apply the appropriate amount of pressure to the brain. An aluminum head post was affixed to the front of the bird's head to enable head-fixed imaging under the 2-photon microscope and to enable head-fixation for baseplate implantation. Following verification of labeling, identification of HVC boundaries, and high-resolution images of neurons under the 2-photon microscope, the bird was lightly anesthetized with isoflurane and the miniaturized fluorescent microscope (Inscopix) was placed over the cranial window. The field of view that matched the 2-photon images was identified and the focal plane that enabled the largest number of neurons to be in focus was selected. Dental acrylic was used to fix the baseplate in the desired position and any exposed skull was covered with dental acrylic. Once the dental

acrylic dried, the microscope was removed from the baseplate and the bird was allowed to recover overnight. About 30 minutes before the birds' subjective daytime, the microscope was attached to the counterbalance (Instech) with enough cable to allow the bird to move freely throughout the cage. The microscope was then secured to the baseplate with a setscrew. The bird was allowed to wake up and accommodate to the weight of the microscope over the next 2-3 days. After the end of imaging experiments, the baseplate was removed and stereotactic injections of AlexFluor 594 were made into Area X. After 1 week, birds were given an overdose of Euthasol, perfused and tissue was sectioned.

GCaMP6s Imaging Using a Miniaturized Fluorescent Microscope

The miniaturized fluorescent microscope (Inscopix) was not removed following successful baseplate implantation and remained attached to the birds' head until either the cranial window closed or 7-10 days had passed. The counterbalance was adjusted based on the observed behavior of the bird and its ability to move freely. The female was not housed in the cage with the male bird, but instead was introduced to the males during a minimum of 3 morning and afternoon sessions to evoke directed song. Video recording was first started followed by 5 to 10 seconds of spontaneous recording with the miniaturized fluorescent microscope. The female bird was placed in the cage as quickly and as with little disruption as possible for each session. If the male bird did not sing within a minute of the females' presence, the session was stopped, and the female was removed. All trials were recorded on video, and audio was recorded using Sound Analysis Pro (SAP) software and the HD video camera microphone. Calcium imaging was performed at 30 frames per second (fps), at 1080x1920 resolution, Gain was set to 4, and Power was set to 90% for all birds,

behavioral videos were collected at 24 fps. Calcium imaging data and behavioral data was synchronized using start of calcium imaging on a frame by frame basis.

Calcium image processing and analysis

Calcium images were collected using the miniaturized fluorescent microscope developed by Inscopix(Ghosh et al 2011). Video recordings of birds behavior and singing were manually synchronized on a frame by frame basis to the onset of calcium imaging, visualized by turning of the blue LED on the miniscopes. For processing of calcium imaging data the FOV (Field of View) was spatially cropped to exclude pixels that did not include neurons or observable changes in fluorescence. Next, the preprocessing utility within the Mosaic data analysis software was used to spatially bin the images by a factor of 2 to reduce demands on computer memory and enable faster data processing. The TurboReg implementation within Mosaic was used to perform motion correction. A reference image was created using a maximum intensity projection of the dataset and the images were aligned in the x and y dimension to the reference image. Imaging datasets with translational motion greater than 20 pixels in either the x or y dimensions were excluded from further data analysis. Post-registration black borders were spatially cropped out. The resulting spatially-cropped, preprocessed, and motion corrected calcium imaging datasets were exported for further analysis in custom Matlab scripts.

We performed ROI-based analysis on the motion-corrected calcium imaging datasets using previously described methods(Peters et al 2014)(see Source Code Files 1-4). ROIs were

manually drawn around identifiable soma and a secondary ROI that extended 6 pixels around the boundaries of the neuronal ROI was used to estimate background fluorescence (i.e. neuropil or other neurons). The pixel values were averaged within the neuronal and background ROIs, and background fluorescence signal was subtracted from neuronal signal. An iterative procedure using custom Matlab scripts were used to estimate baseline fluorescence, noise, and active portions of the traces(Peters et al 2014). A subset of calcium images were re-analyzed using previously described constrained non-negative matrix factorization (CNMF) methods, but calcium fluorescence traces were identical to the traces pulled out by the ROI-based analysis(Pnevmatikakis et al 2016). Calcium traces generated by ROI-based analysis were further deconvolved to produce inferred calcium traces using the pool adjacent violators algorithm (PAVA)(Friedrich et al 2017). The deconvolved calcium traces were normalized to values between 1 and 0 to enable visualization of activity across different neurons during the same trial. Calcium transients that were 3 SD. above baseline activity were recorded as events. The corresponding onset times and the rise times to peak fluorescence of individual calcium transients were correlated with synchronized behavior.

All calcium events were first categorized as falling into peri-song or song behavioral epochs on a frame by frame basis. Peri-song was limited to the 5 second period before the onset of vocalizations, including introductory notes, and the 5 second period after the offset of the last syllable. These event counts were used to assign a Phrase index to all imaged neurons. Neurons that had fewer than 2 calcium events recorded over a day of singing were excluded from further analysis because sparsity of calcium events could spuriously identify

neurons as peri-song or song exclusive. We combined the number of calcium events from neurons imaged across multiple trials during the same day. Neurons imaged across multiple days were treated as unique neurons. The phrase index was calculated as a ratio of the total number of song events imaged from a neuron during a day subtracted by the number of peri-song events to the total number of calcium events. This bounded the phrase index to values of -1 (peri-song exclusive) and +1 (Song exclusive). We used the phrase index to examine the timing properties of neurons active only during peri-song, song, or both behavioral epochs.

To examine the distribution of calcium events, we generated histograms with bin sizes of 200 ms. Peri-song event rates were first calculated in 100ms bins and then a plotted using a 1 second moving average window that reaches a minimum of 500 ms at boundaries (-5, +5 seconds, and at song onset and offset). The average event rate and standard deviation was calculated using all pre and post phrase event rates from all birds.

Fluorescence Analysis Across Intervals

Average fluorescent changes were measured for each neuron across baseline, pre-song, post-song, and song behavioral periods. Baseline was defined as a behaviorally quiet period covering 5s of fluorescent activity that was ≥10 s removed from periods of singing or calling. Pre-song was 5s before phrase onset and post-song was 5s after phrase offset. The background subtracted fluorescent traces were used to measure average fluorescence across the above intervals for all phrases and all birds. Averaged fluorescent values were than normalized to the average fluorescence measured during song.

Comparison of Signal-to-Noise Ratio and Calcium Event Peak Magnitudes

We measured the SNR of events occurring during song for a subset of pan-song and song neurons. The SNR was calculated as a ratio of peak fluorescence for each song event per neuron to the average fluorescence from baseline period within the trial (as above, 5s of fluorescent activity that was ≥10s removed from periods of singing or calling). We determined the average SNR for each neuron and examined differences between pan-song and song neurons.

Peak magnitudes during peri-song and song periods of pan-song neurons were measured using normalized deconvolved fluorescent traces. The peak values for each pan-song neuron (with phrase indices between -0.18 to +0.18) during peri-song and song periods were used to evaluate potential differences between calcium events occurring outside of song versus during song.

Neural Recordings

Multiunit recordings of HVC neurons were collected from three adult (>90 days old) male Bengalese finches. All procedures were approved by the Korea Brain Research Institute. An array of 16 tungsten microwires (175 μm spacing, OMN1005-16, Tucker Davis Technologies) was implanted into left HVC. The location of HVC was identified by searching for spontaneous spike bursts and for antidromic response to stimulation in RA. The extracellular voltage traces of all channels from birds singing alone (without presentation of female) were amplified and recorded with an interface board (RHD2132, Intan

Technologies) at a sampling rate of 25kHz. The interface board was tethered to a passive commutator (Dragonfly Inc.) via a custom-made light-weight cable. In total we obtained HVC recordings from 35 electrode channels in three birds (15, 7, and 8 channels, respectively), all of which showed spontaneous bursts typical of HVC neurons. The impedance of successful electrodes was around 100-300 kΩ.

Recorded signals were bandpass filtered (0.3-5kHz) and negative signal peaks exceeding 4 SD from spontaneous activity (spontaneous activity was measured from time points greater than 10s from the nearest song bout) were interpreted as multi-unit spikes. In total 38, 62, and 212 song onsets, and 42, 23, and 280 offsets were identified in these birds, respectively. We produced firing rate-traces from each electrode channel with 10ms resolution and averaged them across song renditions. After smoothing with a 500ms moving average window, the averaged firing rates were normalized between 0 and 1 to enable comparisons of recordings from different channels and to obtain the general trend of onset- and offset-related firing across channels and birds.

The significance of activity elevation during pre-song, song, and post-song periods from the baseline was tested by Wilcoxon signed-rank test with significant level at 0.05 after Bonferroni correction for multiple comparison. Onset of pre-song and offset of post-song activity were estimated for each channel as the smoothed spike rate trajectory was exceeded a threshold which was defined as mean + 2 SD of the spontaneous spike rate.

Single-unit and multiunit recordings of RA neurons were collected from six adult (>140 days old) male Bengalese finches as described previously(Tang et al 2014). All procedures were approved by the Emory University Institutional Animal Care and Use Committee. Briefly, an array of four or five high-impedance microelectrodes was implanted above RA. We remotely advanced the electrodes through RA using a miniaturize motorized microdrive and recorded extracellular voltage traces as birds produced undirected song (i.e., no female bird was present). We used a previously described spike sorting algorithm to classify individual recordings as single-unit or multiunit(Sober et al 2008). In total, we recorded 19 single units (multiunit recordings were not analyzed further in this study). Based on the spike waveforms and response properties of the recordings, all RA recordings were classified as putative projection neurons(Leonardo & Fee 2005, Sober et al 2008, Spiro et al 1999).

Analysis of Chronic Recording Data

To analyze the variation in inter-spike-interval (ISI) in different time periods (Figure 5), we restricted our analysis to cases in which we collected at least one recording that included the relevant song epoch. “Spontaneous” epochs were sampled from neural activity recorded more than 10 sec after the nearest song bout. “Pre-song” activity was sampled from between 2.5 and 0.5 s prior to the first song syllable or introductory note. “Song” activity was sampled from the onset of the first song syllable until the offset of the last syllable in a bout. “Post-song” activity was sampled from between 0.5 and 2.5 s after the offset of the last syllable in a bout. In some cases, we did not have sufficient data available

from all epochs for all neurons (note the variation in the number of neurons included in the analyses shown in Fig. 5d).

Air Sac Recording Procedures

Subsyringeal air pressure was recorded from 6 adult male zebra finches in directed singing conditions. Directed song was defined as a female presented in an adjacent cage during a two-hour recording period. Data from four of the birds were re-analyzed from a previously published study (Cooper & Goller, 2006) and data from two additional birds were collected to replicate the effects observed in the previously collected data(Cooper & Goller 2006). As described in (Secora et al. 2004), each bird was accustomed to carrying a pressure transducer that was held in place on the bird's back with an elastic band(Secora et al 2012). To facilitate relatively free lateral and vertical movement in the cage, the weight of the transducer was offset by a counter-balance arm. Subsyringeal air pressure surgery was performed after birds sang while carrying the pressure transducer. Prior to insertion of the air pressure cannula, animals were deeply anesthetized as verified by an absence of a toe-pinch response. A small opening in the body wall below the last rib was made with a fine pair of micro-dissecting forceps, and a flexible cannula (silastic tubing, OD 1.65 mm, 6.5 cm length) was inserted into the body wall and suture was tied around the cannula and routed between the 2nd and 3rd ribs to hold it in place. The skin was sealed to the cannula with tissue adhesive (Nexaband). The free end of the cannula was attached to the pressure transducer. This allowed for measurement of relative subsyringeal air pressure changes inside the thoracic air sac before, during, and after spontaneously generated song events. Birds were monitored following surgery until they perched in the recording chamber.

The voltage output of the pressure transducer was amplified (50-100 x) and low-pass filtered (3 kHz cutoff; Brownlee, Model 440, Neurophase, Santa Clara, CA). Respiration was recorded for five seconds prior to and following singing epochs using a National Instruments analog-to-digital conversion board (NI USB 6251, Austin, TX) controlled by Avisoft Recorder software (Avisoft Bioacoustics, Berlin, Germany). Data were collected in wav file format, 16 bit resolution, with sampling rates varying from 22.05 to 40 kHz. Songs were selected for analysis that contained at least 3 s of uninterrupted quiet respiration prior to and following song. Songs that were preceded by calls, drinking, defecation, or movement-related activity were excluded from the analysis.

Air sac data classification

Air pressure was analyzed as respiratory cycles, which was defined as an inspiration followed by expiration. The onset of inspiration was identified as subambient air pressurization and the return to ambient pressure following the expiratory phase of the cycle. The cycle duration (s), duty cycle (% time spent in the expiratory phase of respiration), and average rectified amplitude (a.u.) was calculated for each cycle. Song respiration was analyzed prior to song onset and following song termination. Song onset was defined as the inspiration preceding the first introductory note; using this marker, the onset time for each respiratory cycle in the pre-song recording period was determined. The conclusion of song was defined as the termination of the expiration generating the last song syllable in the bird's song bout. The timing of the respiratory cycles following song were identified relative to the song termination marker.

Statistical analyses of respiratory data

For statistical analyses of the respiratory data, each bird contributed a single average value for each measured parameter (cycle duration, duty cycle, average amplitude). A repeated measures ANOVA was used to determine how respiration changes prior to and following song. For each bird, ten to twenty songs were identified for the statistical analysis (see above for criteria). The average for the pre- and post-song (3-5s) for each measured parameter for each bird was calculated. To evaluate the time course of change in respiratory patterns preceding and following song, the average for one second bins for each bird were used in the repeated measures ANOVA. In cases where the assumption of sphericity was violated, the Greenhouse-Geisser correction for the *degrees of freedom* was used. All *p* values reported are based on this correction. An *a priori* alpha level of .05 was used for determining statistical significance.

CHAPTER 4

Discussion

Previous studies suggested that the HVC_{RA} network functions exclusively as a timekeeper, encoding motif-level temporal representations of song via propagation of precisely timed neural sequences (Hahnloser et al 2002, Kozhevnikov & Fee 2007, Long & Fee 2008, Long et al 2010, Lynch et al 2016, Markowitz et al 2015, Picardo et al 2016). Central to this view is that HVC_{RA} neurons are active only during singing and hence behave in primarily two modes, inactive or propagating neural sequences. Our principal result is that neural sequences among HVC_{RA} neurons emerge as part of orchestrated population activity across a larger network of HVC_{RA} neurons. This activity can be correlated with motor planning and preparation prior to song initiation. Peri-song and pan-song HVC_{RA} neurons forecast the start of singing. Peri-song HVC_{RA} neurons are inactive during song, whereas pan-song neurons become heterogeneously active prior to time-locked sequential activity during song performances (**Figures 2 & 3**). Moreover, we find that preparatory activity in HVC_{RA} neurons precedes the pre-bout activity described in other classes of HVC neurons and other portions of the song system previously described in zebra finches (Danish et al 2017, Goldberg et al 2010, Goldberg & Fee 2012, Kao et al 2008, Rajan 2018, Roberts et al 2017, Vyssotski et al 2016, Williams & Vicario 1993) and described here in Bengalese finches (**Figure 4**). This suggests that HVC_{RA} neurons may seed network wide changes among other classes of HVC neurons and the song system more generally.

Indeed, the rigid stereotypy of singing behavior enables comparisons from different levels of the nervous system and periphery. We find that preparatory activity in HVC_{RA}

neurons drives descending motor commands via RA and motor movements that set the stage for producing song (**Figures 5 & 6**). Because song is a self-initiated, volitional behavior, our findings further indicate that the HVC_{RA} network either functions as a sensitive read-out of the decision to sing or as an integral factor in the decision itself. Finally, previous studies have shown that about half of HVC_{RA} neurons are inactive during song (Hahnloser et al 2002, Hamaguchi et al 2016, Kozhevnikov & Fee 2007, Long et al 2010). We find that approximately half of the HVC_{RA} neuronal network is active at peri-song intervals, perhaps accounting for previous recordings from neurons that are inactive during singing. We therefore propose that one important function of HVC_{RA} neurons is to plan and prepare for the upcoming song performance.

Together, these findings support a simple model for song and neural sequence initiation. Preparatory activity in populations of HVC_{RA} neurons drives descending motor commands via RA and its connections to the ventral respiratory group and syringeal motoneurons in the medulla (Andalman et al 2011, Goller & Cooper 2004, Roberts et al 2008, Sturdy et al 2003, Suthers et al 1999, Wild 1993). Given the sparsity of HVC_{RA} neuron activity and the convergence of HVC_{RA} input to RA, it is likely that only population activity, like that described here, is sufficient to drive bursting in RA. These motor signals increase respiratory rate, bringing it closer to the high rate needed to coordinate production of song syllables. Because the initiation of singing requires precise coordination between respiratory states and descending motor commands, we hypothesize that recurrent projections from the brainstem update activity in HVC and trigger the initiation of neural sequences once the periphery is readied for the first respiratory cycle for song (Ashmore et

al 2005, Hamaguchi et al 2016, Schmidt et al 2012). Circuitry related to recurrent projections into HVC increase their activity tens of milliseconds prior to song onset (Danish et al 2017, Vyssotski et al 2016, Williams & Vicario 1993) and thus may provide final inputs that help mediate the transition from heterogeneous preparatory activity to the precisely sequenced activity that underlies song.

Absent from this model is how activity in peri-song and pan-song neurons is first initiated seconds before song onset. HVC receives input from cholinergic neurons in the basal forebrain(Li & Sakaguchi 1997, Shea et al 2010, Shea & Margoliash 2003), noradrenergic neurons in the locus coeruleus (Appeltants et al 2000), and dopaminergic neurons in the midbrain (Hamaguchi & Mooney 2012, Tanaka et al 2018), any or all of which could play potent roles in shifting the excitability of subsets of HVC_{RA} involved in song preparation and initiation. Neuromodulatory inputs may also play a role in shifting the excitability of the entire song system as birds prepare to sing. Further studies will be needed to understand the function of neuromodulatory inputs to HVC_{RA} neurons and the rest of the song circuitry in song initiation. Also absent from our model are specific predictions about the role peri-song neurons and pan-song neurons may play in motor planning. Although it is not yet known whether activity occurring among peri-song and pan-song HVC_{RA} neurons prior to song onset is necessary for song initiation or production, previous studies have identified pyramidal tract neurons (PT_{upper}) in the anterior lateral motor cortex that play a specific role in motor planning (Economo et al 2018). These neurons are active prior to movement onset and show decreased activity during movement, similar to the activity of HVC_{RA} peri-song neurons described here. PT_{upper}

neurons innervate the thalamus rather than medulla and are hypothesized to encode cognitive signals related to motor planning(Economo et al 2018). Likewise, RA provides inputs to the medulla and the thalamus(Goldberg & Fee 2012, Roberts et al 2008, Vates et al 1997, Wild 1993). However, it is currently not known if subpopulations of RA neurons project exclusively to the thalamus or if peri-song and pan-song HVC_{RA} neurons have unique downstream targets within RA. Future experiments, requiring novel closed-loop manipulations to exclusively disrupt the activity of functionally identified peri-song or pan-song neurons, independent of activity associated with the motif-level temporal representations of song, and detailed circuit mapping studies will be needed to dissect the function of these newly identified subpopulations of HVC_{RA} neurons. When possible, such experiments will undoubtedly lend insights into whether subpopulations of HVC_{RA} neurons are involved in aspects of motor planning independent of motor preparation or song performance.

Neural activity associated with motor planning and preparation has been observed in motor and premotor cortices for a variety of different motor tasks in rodents and primates (Chen et al 2017, Churchland et al 2010, Churchland et al 2006a, Churchland et al 2006b, Economo et al 2018, Inagaki et al 2019, Kaufman et al 2014, Li et al 2015, Li et al 2016, Murakami & Mainen 2015, Murakami et al 2014, Tanji & Evarts 1976), including vocalizations (Gavrilov et al 2017). This activity is thought to reflect the decision to perform movements and is characterized by a high degree of variability from trial to trial. Changes in circuit dynamics function to shift the initial state of a network to levels that enable efficient and accurate motor performances and this activity can start to unfold

seconds prior to movement initiation (Churchland et al 2010, Inagaki et al 2019, Murakami & Mainen 2015, Svoboda & Li 2017). HVC is proposed to be analogous to the mammalian motor cortex (layer III neurons of the primary motor cortex) (Pfenning et al 2014), or premotor cortex (Bolhuis et al 2010). Our observation of preparatory activity seconds before the onset of courtship song in two different songbird species suggests that pre-movement activity is a common mechanism for ensuring the accurate production of volitional behaviors. In line with recordings of pre-motor activity in mammals, individual HVC_{RA} neurons exhibit a high degree of trial-to-trial variability. Although zebra finch courtship song is famously stereotyped, there is a measurable degree of variability in the structure and duration of song motifs, bouts and phrases from trial to trial. Recording of preparatory activity across larger populations of HVC_{RA} neurons may be useful for decoding this trial to trial variability in song structure, ultimately providing a predictive readout of impending behaviors.

Sequential activation of neurons is thought to provide computational advantages for encoding temporal information associated with episodic memories or behavioral sequences (Fiete et al 2004, Kumar et al 2010, Rajan et al 2016). Neural sequences in HVC provide one of the cleanest examples linking brain activity with a naturally learned and volitionally produced skilled motor behavior (Fee et al 2004). Our study provides a glimpse of how these sequences emerge through temporally coordinated transitions within a potentially hierarchically organized network and suggests a general framework for initiating the production of skilled motor behaviors.

Future Experiments

The results presented in this thesis, along with evidence in mammalian species, suggest the presence of more complex network level dynamics underlying the production of song and the production of temporally structured motor behavior, in general. Further experiments will be required to better understand how initial network states contribute to synchronous activity, how different populations of neurons (i.e. peri-song, pan-song, song neurons) interact to create representations of the motor program, and the exact relationship between preparatory activity and motor periphery.

Currently little is known about the conditions of network states that enable robust transmission of neural activity through interconnected circuits (Kumar et al 2010). Dimensionality reduction techniques suggest that preparatory activity is guiding the network to some attractor in low dimensional space, but these are not necessarily intuitive ideas and are difficult to understand in the context of biological processes (Churchland et al 2010, Inagaki et al 2019, Svoboda & Li 2017). Preparatory activity is likely to be an emergent phenomenon of complex neural networks rather than a reflection of any specific cell-type, although the activity might be more acutely represented in some populations of neurons (i.e. peri-song and pan-song neurons, (Chen et al 2017, Li et al 2015)). However, what we already know about preparatory activity provides a guide for better understanding the underlying network characteristics. By definition, preparatory activity is present before all successful trials of motor movement (or is impaired prior to incorrect trials), and exhibits a large degree of variability from trial to trial. Moreover, experiments covering a wide range of species and motor behaviors suggest that preparatory activity is highly conserved. Our experiments in zebra finches and Bengalese finches indicate that comparable motor tasks in different species may exhibit similar preparatory activity

timing. Based on this information, what are the network characteristics that determine the range of preparatory activity that is sufficient to drive synchronous activity? One theory, based on evidence for neural avalanches in neocortical circuits, suggests that levels of excitatory connections, inhibitory connections, the degree of excitatory branching, the degree of inhibitory branching, and the adaptation through the neural circuitry could predict the range of preparatory activity seen during behavior (Beggs & Plenz 2003). However, it's unclear how much of these parameters need to be quantified and how well they can predict the trajectory of preparatory activity or if they are even sufficient to capture the dynamics. Alternatively, and likely related to the network parameters listed above, empirical and theoretical studies provide evidence that the brain operates at criticality – a concept in dynamical systems theory for how unexpected patterns emerge from complex systems(Chialvo 2010). This approach would require a better understanding of the underlying nonlinear elements (in this case, neurons) and how they as a population contribute to emergent properties of a network(Chialvo 2010). Regardless, better understanding how preparatory activity is generated and how it enables transitions to rhythmic activity has the potential to address fundamental questions about how complex networks operate.

Technical advances in recording from large populations of neurons, combined with cell-type specific manipulations in HVC and in other regions of the brain are likely to be essential for systematically addressing different network states. In this thesis, we have identified two new functional pools of neurons within HVC (peri-song and pan-song neurons), future experiments would attempt to characterize the functional connectivity rules that govern the interactions between these neurons, the transition to rhythmic

activity (by examining pan-song and song neurons), and the contribution of local inhibitory circuits. Near the end of my dissertation work, I became interested in the prospect of using image guided two-photon patching and holographic masks for optogenetic manipulation of identified cells within the HVC circuitry. These experiments would involve functional imaging of populations of HVC-RA neurons during singing behavior followed by *in vivo* circuit dissection of identified peri-song, pan-song, song neurons. I'm curious as to whether, for example, peri-song and pan-song neurons, have distinguishing intrinsic physiological characteristics. It may be possible that peri-song neurons receive larger inhibitory inputs or are more sensitive to external neuromodulatory tone than the other pools of neurons. Perhaps, this may explain why peri-song neuronal activity seems left shifted relative to pan-song neurons. How do pan-song neurons shift from sparse heterogeneous activity prior to song to rhythmic activity during motifs? Are these transitions evident at the single neuron level (in terms of physiology) or are these a product of network interactions as speculated above? Regardless, our understanding of preparatory activity in songbirds would benefit from the ability to exclusively label and manipulate the different functional classes of HVC-RA neurons described in this thesis.

Lastly, we identified correlations between the timing of preparatory activity in HVC and the timing of respiratory changes prior to song onset. Its unclear whether preparatory activity carries information about motor parameters relevant for accurate production of subsequent motor movement. In addition, more information is required about how variations in preparatory activity from trial-to-trial reflect respiratory changes prior to song onset. Future experiments would involve simultaneous respiratory recordings with functional imaging to show more direct relationships. Recent advances in flexible electrode

arrays could enable recordings of syringeal muscle groups; our data indicates that we should expect to see changes in muscle activity prior to song onset particularly if preparatory activity is priming the periphery for song vocalization. A somewhat easier experiment that can be more readily conducted in the lab would involve closed-loop experiments inhibiting preparatory activity. Our nVoke (Inscopix) system is a miniscope with dual paths, one for imaging and another for optogenetic manipulation of the entire field of view. Optogenetically inhibiting the preparatory activity might decrease the probability of song vocalization and changes in the periphery.

References

Abeles M. 1982. *Local cortical circuits: An electrophysiological study*. Springer Science & Business Media.

Abeles M. 1991. *Corticonics: Neural circuits of the cerebral cortex*. Cambridge University Press.

Akutagawa E, Konishi M. 2010. New brain pathways found in the vocal control system of a songbird. *Journal of Comparative Neurology* 518: 3086-100

Amador A, Perl YS, Mindlin GB, Margoliash D. 2013. Elemental gesture dynamics are encoded by song premotor cortical neurons. *Nature* 495: 59-64

Andalman AS, Foerster JN, Fee MS. 2011. Control of vocal and respiratory patterns in birdsong: dissection of forebrain and brainstem mechanisms using temperature. *PLoS One* 6: e25461

Appeltants D, Absil P, Balthazart J, Ball GF. 2000. Identification of the origin of catecholaminergic inputs to HVc in canaries by retrograde tract tracing combined with tyrosine hydroxylase immunocytochemistry. *J Chem Neuroanat* 18: 117-33

Ashmore RC, Wild JM, Schmidt MF. 2005. Brainstem and forebrain contributions to the generation of learned motor behaviors for song. *J Neurosci* 25: 8543-54

Barnes TD, Kubota Y, Hu D, Jin DZ, Graybiel AM. 2005. Activity of striatal neurons reflects dynamic encoding and recoding of procedural memories. *Nature* 437: 1158-61

Beggs JM, Plenz D. 2003. Neuronal Avalanches in Neocortical Circuits. *The Journal of Neuroscience* 23: 11167-77

Bolhuis JJ, Okanoya K, Scharff C. 2010. Twitter evolution: converging mechanisms in birdsong and human speech. *Nat Rev Neurosci* 11: 747-59

Cannon J, Kopell N, Gardner T, Markowitz J. 2015. Neural Sequence Generation Using Spatiotemporal Patterns of Inhibition. *PLoS Comput Biol* 11: e1004581

Chen TW, Li N, Daie K, Svoboda K. 2017. A Map of Anticipatory Activity in Mouse Motor Cortex. *Neuron* 94: 866-79 e4

Chen TW, Wardill TJ, Sun Y, Pulver SR, Renninger SL, et al. 2013. Ultrasensitive fluorescent proteins for imaging neuronal activity. *Nature* 499: 295-300

Chialvo DR. 2010. Emergent complex neural dynamics. *Nature Physics* 6: 744

Churchland MM, Cunningham JP, Kaufman MT, Ryu SI, Shenoy KV. 2010. Cortical preparatory activity: representation of movement or first cog in a dynamical machine? *Neuron* 68: 387-400

Churchland MM, Santhanam G, Shenoy KV. 2006a. Preparatory activity in premotor and motor cortex reflects the speed of the upcoming reach. *J Neurophysiol* 96: 3130-46

Churchland MM, Yu BM, Ryu SI, Santhanam G, Shenoy KV. 2006b. Neural variability in premotor cortex provides a signature of motor preparation. *J Neurosci* 26: 3697-712

Cooper BG, Goller F. 2006. Physiological insights into the social-context-dependent changes in the rhythm of the song motor program. *J Neurophysiol* 95: 3798-809

Crandall SR, Aoki N, Nick TA. 2007. Developmental modulation of the temporal relationship between brain and behavior. *J Neurophysiol* 97: 806-16

Danish HH, Aronov D, Fee MS. 2017. Rhythmic syllable-related activity in a songbird motor thalamic nucleus necessary for learned vocalizations. *PLoS One* 12: e0169568

Day NF, Kinnischtzke AK, Adam M, Nick TA. 2009. Daily and developmental modulation of "premotor" activity in the birdsong system. *Dev Neurobiol* 69: 796-810

Dragoi G, Buzsaki G. 2006. Temporal encoding of place sequences by hippocampal cell assemblies. *Neuron* 50: 145-57
Economo MN, Viswanathan S, Tasic B, Bas E, Winnubst J, et al. 2018. Distinct descending motor cortex pathways and their roles in movement. *Nature* 563: 79-84
Fee MS, Kozhevnikov AA, Hahnloser RH. 2004. Neural mechanisms of vocal sequence generation in the songbird. *Ann N Y Acad Sci* 1016: 153-70
Fiete IR, Hahnloser RH, Fee MS, Seung HS. 2004. Temporal sparseness of the premotor drive is important for rapid learning in a neural network model of birdsong. *J Neurophysiol* 92: 2274-82
Fiete IR, Senn W, Wang CZ, Hahnloser RH. 2010. Spike-time-dependent plasticity and heterosynaptic competition organize networks to produce long scale-free sequences of neural activity. *Neuron* 65: 563-76
Foster DJ, Wilson MA. 2006. Reverse replay of behavioural sequences in hippocampal place cells during the awake state. *Nature* 440: 680-3
Franz M, Goller F. 2003. Respiratory patterns and oxygen consumption in singing zebra finches. *J Exp Biol* 206: 967-78
Friedrich J, Zhou P, Paninski L. 2017. Fast online deconvolution of calcium imaging data. *PLOS Computational Biology* 13: e1005423
Gavrilov N, Hage SR, Nieder A. 2017. Functional Specialization of the Primate Frontal Lobe during Cognitive Control of Vocalizations. *Cell Rep* 21: 2393-406
Ghosh KK, Burns LD, Cocker ED, Nimmerjahn A, Ziv Y, et al. 2011. Miniaturized integration of a fluorescence microscope. *Nat Methods* 8: 871-8
Goldberg JH, Adler A, Bergman H, Fee MS. 2010. Singing-related neural activity distinguishes two putative pallidal cell types in the songbird basal ganglia: comparison to the primate internal and external pallidal segments. *J Neurosci* 30: 7088-98
Goldberg JH, Fee MS. 2012. A cortical motor nucleus drives the basal ganglia-recipient thalamus in singing birds. *Nat Neurosci* 15: 620-7
Goller F, Cooper BG. 2004. Peripheral motor dynamics of song production in the zebra finch. *Ann N Y Acad Sci* 1016: 130-52
Haga T, Fukai T. 2018. Recurrent network model for learning goal-directed sequences through reverse replay. *Elife* 7
Hahnloser R, Kozhevnikov A, Fee M. 2002. An ultra-sparse code underlies the generation of neural sequences in a songbird. *Nature* 419: 65-70
Hamaguchi K, Mooney R. 2012. Recurrent interactions between the input and output of a songbird cortico-basal ganglia pathway are implicated in vocal sequence variability. *J Neurosci* 32: 11671-87
Hamaguchi K, Tanaka M, Mooney R. 2016. A Distributed Recurrent Network Contributes to Temporally Precise Vocalizations. *Neuron* 91: 680-93
Hartley RS, Suthers RA. 1989. Airflow and pressure during canary song: direct evidence for mini-breaths. *Journal of Comparative Physiology A* 165: 15-26
Harvey CD, Coen P, Tank DW. 2012. Choice-specific sequences in parietal cortex during a virtual-navigation decision task. *Nature* 484: 62-8
Ikegaya Y, Aaron G, Cossart R, Aronov D, Lampl I, et al. 2004. Synfire chains and cortical songs: temporal modules of cortical activity. *Science* 304: 559-64

Inagaki HK, Fontolan L, Romani S, Svoboda K. 2019. Discrete attractor dynamics underlies persistent activity in the frontal cortex. *Nature* 566: 212-17
Jin DZ, Fujii N, Graybiel AM. 2009. Neural representation of time in cortico-basal ganglia circuits. *Proc Natl Acad Sci U S A* 106: 19156-61
Jog MS, Kubota Y, Connolly CI, Hillegaart V, Graybiel AM. 1999. Building neural representations of habits. *Science* 286: 1745-49
Kao MH, Wright BD, Doupe AJ. 2008. Neurons in a forebrain nucleus required for vocal plasticity rapidly switch between precise firing and variable bursting depending on social context. *J Neurosci* 28: 13232-47
Katlowitz KA, Picardo MA, Long MA. 2018. Stable Sequential Activity Underlying the Maintenance of a Precisely Executed Skilled Behavior. *Neuron* 98: 1133-40 e3
Kaufman MT, Churchland MM, Ryu SI, Shenoy KV. 2014. Cortical activity in the null space: permitting preparation without movement. *Nat Neurosci* 17: 440-8
Keller GB, Hahnloser RH. 2009. Neural processing of auditory feedback during vocal practice in a songbird. *Nature* 457: 187-90
Kornhuber HH, Deecke L. 2016. Brain potential changes in voluntary and passive movements in humans: readiness potential and reafferent potentials. *Pflügers Archiv - European Journal of Physiology* 468: 1115-24
Kosche G, Vallentin D, Long MA. 2015. Interplay of inhibition and excitation shapes a premotor neural sequence. *J Neurosci* 35: 1217-27
Kozhevnikov AA, Fee MS. 2007. Singing-related activity of identified HVC neurons in the zebra finch. *J Neurophysiol* 97: 4271-83
Kumar A, Rotter S, Aertsen A. 2010. Spiking activity propagation in neuronal networks: reconciling different perspectives on neural coding. *Nat Rev Neurosci* 11: 615-27
Lashley KS. 1951. The problem of serial order in behavior In *Cerebral mechanisms in behavior; the Hixon Symposium.*, pp. 112-46. Oxford, England: Wiley
Leonardo A, Fee MS. 2005. Ensemble coding of vocal control in birdsong. *J Neurosci* 25: 652-61
Li N, Chen TW, Guo ZV, Gerfen CR, Svoboda K. 2015. A motor cortex circuit for motor planning and movement. *Nature* 519: 51-6
Li N, Daie K, Svoboda K, Druckmann S. 2016. Robust neuronal dynamics in premotor cortex during motor planning. *Nature* 532: 459-64
Li R, Sakaguchi H. 1997. Cholinergic innervation of the song control nuclei by the ventral paleostriatum in the zebra finch: a double-labeling study with retrograde fluorescent tracers and choline acetyltransferase immunohistochemistry. *Brain Res* 763: 239-46
Liberti WA, 3rd, Markowitz JE, Perkins LN, Liberti DC, Leman DP, et al. 2016. Unstable neurons underlie a stable learned behavior. *Nat Neurosci* 19: 1665-71
Long MA, Fee MS. 2008. Using temperature to analyse temporal dynamics in the songbird motor pathway. *Nature* 456: 189-94
Long MA, Jin DZ, Fee MS. 2010. Support for a synaptic chain model of neuronal sequence generation. *Nature* 468: 394-9
Luczak A, Bartho P, Marguet SL, Buzsaki G, Harris KD. 2007. Sequential structure of neocortical spontaneous activity in vivo. *Proc Natl Acad Sci U S A* 104: 347-52
Lynch GF, Okubo TS, Hanuschkin A, Hahnloser RH, Fee MS. 2016. Rhythmic Continuous-Time Coding in the Songbird Analog of Vocal Motor Cortex. *Neuron* 90: 877-92

Markowitz JE, Liberti WA, 3rd, Guitchounts G, Velho T, Lois C, Gardner TJ. 2015. Mesoscopic patterns of neural activity support songbird cortical sequences. *PLoS Biol* 13: e1002158
Mauk MD, Buonomano DV. 2004. The neural basis of temporal processing. *Annu Rev Neurosci* 27: 307-40
McCasland JS. 1987. Neuronal control of birdsong production. *Journal of Neuroscience* 7: 23-39
Mooney R. 1992. Synaptic basis for developmental plasticity in a birdsong nucleus. *Journal of Neuroscience* 12: 2464-77
Mooney R, Prather JF. 2005. The HVC microcircuit: the synaptic basis for interactions between song motor and vocal plasticity pathways. *J Neurosci* 25: 1952-64
Murakami M, Mainen ZF. 2015. Preparing and selecting actions with neural populations: toward cortical circuit mechanisms. *Curr Opin Neurobiol* 33: 40-6
Murakami M, Vicente MI, Costa GM, Mainen ZF. 2014. Neural antecedents of self-initiated actions in secondary motor cortex. *Nat Neurosci* 17: 1574-82
Nottebohm F, Stokes TM, Leonard CM. 1976. Central control of song in the canary, *Serinus canarius*. *Journal of Comparative Neurology* 165: 457-86
Okanoya K. 2004. The Bengalese finch: a window on the behavioral neurobiology of birdsong syntax. *Ann N Y Acad Sci* 1016: 724-35
Okubo TS, Mackevicius EL, Payne HL, Lynch GF, Fee MS. 2015. Growth and splitting of neural sequences in songbird vocal development. *Nature* 528: 352-7
Peters AJ, Chen SX, Komiyama T. 2014. Emergence of reproducible spatiotemporal activity during motor learning. *Nature* 510: 263-7
Pfeiffer BE, Foster DJ. 2013. Hippocampal place-cell sequences depict future paths to remembered goals. *Nature* 497: 74-9
Pfeiffer BE, Foster DJ. 2015. PLACE CELLS. Autoassociative dynamics in the generation of sequences of hippocampal place cells. *Science* 349: 180-3
Pfenning AR, Hara E, Whitney O, Rivas MV, Wang R, et al. 2014. Convergent transcriptional specializations in the brains of humans and song-learning birds. *Science* 346: 1256846
Picardo MA, Merel J, Katlowitz KA, Vallentin D, Okobi DE, et al. 2016. Population-Level Representation of a Temporal Sequence Underlying Song Production in the Zebra Finch. *Neuron* 90: 866-76
Pnevmatikakis Eftychios A, Soudry D, Gao Y, Machado TA, Merel J, et al. 2016. Simultaneous Denoising, Deconvolution, and Demixing of Calcium Imaging Data. *Neuron* 89: 285-99
Prather JF, Mooney R. *Society for Neuroscience Abstracts2003*: 294.11.
Rajan K, Harvey CD, Tank DW. 2016. Recurrent Network Models of Sequence Generation and Memory. *Neuron* 90: 128-42
Rajan R. 2018. Pre-Bout Neural Activity Changes in Premotor Nucleus HVC Correlate with Successful Initiation of Learned Song Sequence. *The Journal of Neuroscience* 38: 5925-38
Rajan R, Doupe AJ. 2013. Behavioral and neural signatures of readiness to initiate a learned motor sequence. *Curr Biol* 23: 87-93
Roberts TF, Hisey E, Tanaka M, Kearney MG, Chattree G, et al. 2017. Identification of a motor-to-auditory pathway important for vocal learning. *Nat Neurosci* 20: 978-86

Roberts TF, Klein ME, Kubke MF, Wild JM, Mooney R. 2008. Telencephalic neurons monosynaptically link brainstem and forebrain premotor networks necessary for song. *J Neurosci* 28: 3479-89
Scharff C, Kirn JR, Grossman M, Macklis JD, Nottebohm F. 2000. Targeted neuronal death affects neuronal replacement and vocal behavior in adult songbirds. *Neuron* 25: 481-92
Schmidt MF, Goller F. 2016. Breathtaking Songs: Coordinating the Neural Circuits for Breathing and Singing. *Physiology (Bethesda)* 31: 442-51
Schmidt MF, McLean J, Goller F. 2012. Breathing and vocal control: the respiratory system as both a driver and a target of telencephalic vocal motor circuits in songbirds. *Exp Physiol* 97: 455-61
Schwartz AB, Moran DW. 1999. Motor cortical activity during drawing movements: population representation during lemniscate tracing. *J Neurophysiol* 82: 2705-18
Secora KR, Peterson JR, Urbano CM, Chung B, Okanoya K, Cooper BG. 2012. Syringeal specialization of frequency control during song production in the Bengalese finch (Lonchura striata domestica). *PLoS One* 7: e34135
Shea SD, Koch H, Baleckaitis D, Ramirez JM, Margoliash D. 2010. Neuron-specific cholinergic modulation of a forebrain song control nucleus. *J Neurophysiol* 103: 733-45
Shea SD, Margoliash D. 2003. Basal forebrain cholinergic modulation of auditory activity in the zebra finch song system. *Neuron* 40: 1213-26
Shenoy KV, Sahani M, Churchland MM. 2013. Cortical control of arm movements: a dynamical systems perspective. *Annu Rev Neurosci* 36: 337-59
Sober SJ, Wohlgemuth MJ, Brainard MS. 2008. Central contributions to acoustic variation in birdsong. *Journal of Neuroscience* 28: 10370-9
Spiro J, Dalva M, Mooney R. 1999. Long-range inhibition within the zebra finch song nucleus RA can coordinate the firing of multiple projection neurons. *Journal of Neurophysiology* 81: 3007-20
Sturdy CB, Wild JM, Mooney R. 2003. Respiratory and telencephalic modulation of vocal motor neurons in the zebra finch. *J Neurosci* 23: 1072-86
Suthers RA, Goller F, Pytte C. 1999. The neuromuscular control of birdsong. *Philos Trans R Soc Lond B Biol Sci* 354: 927-39
Svoboda K, Li N. 2017. Neural mechanisms of movement planning: motor cortex and beyond. *Curr Opin Neurobiol* 49: 33-41
Tanaka M, Sun F, Li Y, Mooney R. 2018. A mesocortical dopamine circuit enables the cultural transmission of vocal behaviour. *Nature* 563: 117-20
Tang C, Chehayeb D, Srivastava K, Nemenman I, Sober SJ. 2014. Millisecond-scale motor encoding in a cortical vocal area. *PLoS Biol* 12: e1002018
Tanji J. 2001. Sequential organization of multiple movements: involvement of cortical motor areas. *Annu Rev Neurosci* 24: 631-51
Tanji J, Evarts EV. 1976. Anticipatory activity of motor cortex neurons in relation to direction of an intended movement. *J Neurophysiol* 39: 1062-8
Vates GE, Vicario DS, Nottebohm F. 1997. Reafferent thalamo- "cortical" loops in the song system of oscine songbirds. *Journal of Comparative Neurology* 380: 275-90

Vyssotski AL, Stepien AE, Keller GB, Hahnloser RH. 2016. A Neural Code That Is Isometric to Vocal Output and Correlates with Its Sensory Consequences. *PLoS Biol* 14: e2000317
Wild JM. 1993. Descending projections of the songbird nucleus robustus archistriatalis. *Journal of Comparative Neurology* 338: 225-41
Williams H. 2004. Birdsong and singing behavior. *Ann N Y Acad Sci* 1016: 1-30
Williams H, Vicario DS. 1993. Temporal patterning of song production: participation of nucleus uvaeformis of the thalamus. *Journal of Neurobiology* 24: 903-12
Yu AC, Margoliash D. 1996. Temporal hierarchical control of singing in birds. *Science* 273: 1871-75